IMPACTS OF CLIMATE CHANGE AND HYDROPOWER DAMS ON FLOW REGIMES AND FLOOD INUNDATION IN THE MEKONG RIVER BASIN

STEVEN LY

2022

IMPACTS OF CLIMATE CHANGE AND HYDROPOWER DAMS ON FLOW REGIMES AND FLOOD INUNDATION IN THE MEKONG RIVER BASIN

(メコン川流域の流況と洪水氾濫に及ぼす気候変動および水力発電ダムの影響)

by

STEVEN LY

A Dissertation

Submitted in partial fulfillment of

the requirement for the Degree of

Doctor of Engineering

Department of Civil and Earth Resources Engineering

Graduate School of Engineering

Kyoto University

September 2022

ACKNOWLEDGEMENT

This doctoral dissertation is the result of three-year works during the year 2019–2022 under the Human Security Engineering Education Program (HSE) of the Graduate School of Engineering, Kyoto University. This research would hardly have been accomplished without the continuous support and tremendous contributions of many people.

First and foremost, I am extremely grateful to Professor Kaoru Takara for accepting me to be his student in 2017 when I started my master's degree. His immense knowledge, leadership, and plentiful experiences have inspired me all the time during my academic research and daily life in Japan. Although Professor Takara has already retired from academic research, his achievements and contributions to the scientific community keep inspiring me every day.

I would like to express my sincere gratitude to my supervisor, Associate Professor Takahiro Sayama, for his supervision and guidance on my research work throughout these years. Without his enormous support, advice, and encouragement, this research work would have not been completed. His insightful suggestions and technical support have always guided me throughout this research.

I would like to extend my sincere thanks to Associate Professor Florence Lahourant, who is also my mentor in the GSS Program, for her kindness and thoughtful advice on my Ph.D. research as well as daily life in Japan.

I would like to offer my special thanks to the co-chair of my dissertation committees, Professor Yasuto Tachikawa and Professor Tetsuya Sumi, for their invaluable comments and feedback during my defense which broaden my perspective and improve my research work. I also would like to thank them for taking time from their tight schedule to be the committees for my defense.

I convey special acknowledgment to Dr. Chantha Oeurng, my undergraduate supervisor, Dr. Sokchhay Heng, and Dr. Sophal Try for their advice, suggestions, and support with some important datasets used in this research. Their extensive knowledge of the hydrology of the Mekong River Basin and water resources in Cambodia hugely contribute to this dissertation.

I wish to thank the secretaries in Sayama-lab (formerly known as Takara-lab), Ms. Sono Inoue and Ms. Kaori Saidera, for their continuous support in paper works and administrative tasks during my study at Kyoto University.

I also thank my fellow lab members, Dr. Netrananda Sahu, Dr. Masafumi Yamada, Dr. Eva Mia Siska Yamamoto, Dr. Kodai Yamamoto, Dr. Karlina, Dr. Yongxue Shi, Dr. Nguyen Duc Ha, Dr. Van Tien Pham, Dr. Yoshito Sugawara, Dr. Muhammad Sohaib Baig, Mr. Tomo Stoyanov, Mr. Adnan Arutyunov, Mr. Djamres Eilif, Mr. Ryosuke Kobayashi, Mr. Koji Matsumoto, Mr. Shinntairo Miyake, Ms. Jamila Rajabi, Ms. Saeka Togashi, Ms. Ryoko Araki, Mr. Sosuke Ichihashi, Mr. Ayato Yamakita, Mr. Syoto Tanioka, and Mr. Shuangtao Wang, for their support, discussions, and all joyful moments we shared during the past years in this laboratory.

I am deeply grateful to the Ministry of Education, Culture, Sports, Science and Technology of Japan (MEXT) for financially supporting my study at Kyoto University for the past five years. My study in Japan would not be possible without their support.

Finally, but most importantly, I would like to express my deepest gratitude to my parents for their unwavering support and belief in me. Without their unconditional support, patience, encouragement, and tremendous understanding in the past few years, I would not be here today. I am thankful to all my relatives and friends for their supportive advice towards my study in Japan.

Steven Ly

Kyoto, June 2022

ABSTRACT

Changes in global surface temperature and precipitation patterns induced by climate change have threatened the water resources and natural ecosystem worldwide. As reported by the Intergovernmental Panel on Climate Change in the Sixth Assessment Report, the average global surface temperature is projected to rise by up to 4.4°C under a high emission scenario by the end of the 21st century. Spatiotemporal patterns of the precipitation will be altered, thus affecting the river flow regime and flood characteristics. Dams have been constructed to mitigate flood risks in many river basins. The dams modify the natural flow regime and contribute to reducing flood frequency and intensity induced by climate change. In addition to flood mitigation, the dam can provide additional water for irrigation during the dry season, navigation system, and energy supply (hydroelectric dam). Known as the largest transboundary river basin in Southeast Asia, the Mekong River Basin (MRB) is the most productive ecosystem in the world, supporting more than 70 million inhabitants. Given the population growth and rapid development, the basin is facing two major problems, namely climate change and large hydropower development. Changes in basin characteristics, including flow regime and flood characteristics, will significantly impact the natural ecosystem, biodiversity, and people's livelihood.

This dissertation aims to investigate the changes in river flow and flood characteristics under the future climate projections and the effects of hydropower dams in the MRB. The Rainfall-Runoff-Inundation (RRI) model is used as the main hydrologic tool to simulate the river discharge and flood inundation. The most recent General Circulation Models (GCM) from the Coupled Model Intercomparison Project Phase 6 (CMIP6) are adopted in the study for the future climate change assessment.

First of all, a simple storage model for reservoir operation is developed following a non-linear optimization method, aiming to maximize hydropower production. Then, river discharge under the reservoir operation was simulated by the Rainfall-Runoff-Inundation (RRI) model coupled with the simple storage model. Compared to the observed data, the model is able to reproduce the river discharge with the $NSE > 0.8$. The findings show that monthly and seasonal discharge have been altered by the reservoir operations during the study period of 2010–2016. At the downstream hydrological station, Kratie, relative changes in monthly discharge vary from -16% to +100%, and dry season discharge is increased by over 40% while wet season discharge is decreased by

about 15%. On the other hand, future hydropower operation is expected to reduce the annual peak discharge.

The study further examines the changes in flow regimes and flood characteristics under the future climate projections using eight GCMs from the CMIP6, along with reservoir operations. Two Share Socioeconomic Pathways (SSP) scenarios, SSP2-4.5 and SSP5-8.5, are adopted in the study. Daily discharge is simulated using the RRI model for the present (1980–2014) and the future climate (2026–2100). Results indicate significant changes in seasonal discharge, particularly in the far-future period (2076–2100), and highlight the important role of hydropower in reducing peak discharge, thus mitigating flood risk in the Lower Mekong Basin (LMB). Flow alteration is detected from the upstream station at Chiang Saen to the downstream station at Kratie. Under climate change (SSP5-8.5), without the dam operation, discharge at Kratie is increased by up to 27% and 33% in the dry season and wet season, respectively. Peak discharge also shows an increasing trend in the future climate projections. Nonetheless, hydropower operations can reduce the effect of climate change on wet seasonal discharge and peak discharge as well as flood extend. In the wet season, the relative flow changes decreased from 33% (climate change only) to 19% under cumulative impacts (climate change and reservoir operations). Hydropower operations, on the other hand, potentially decrease peak discharge, thus reducing relative changes in flood extend in the LMB from 33% (climate change only) to 27% (climate change and reservoir operations). A statistical Kolmogorov-Smirnov test is performed to evaluate the significance of flood risk in the LMB. As a result, changes in inundated areas are found to be significant in most scenarios. Despite the effect of hydropower operations, climate change remains the key contributor to hydrological changes in the MRB.

Given an increase in energy consumption in the MRB, the study also analyzes the changes in energy production from hydropower under the future climate projections. Results from the RRI simulations show that annual discharge and total inflow will be increased in the future under all scenarios, indicating an increase in hydropower production. However, due to the limited turbine capacity, future hydropower production is expected to increase by only 5% although there is a 22% increase in the future total inflow. The study further characterizes and classifies the future hydropower dams to investigate their potential for future development. According to the classification, type-A dam, a dam with large turbine capacity compared to the inflow, is the most common type in the MRB, while type C dam (dam with small turbine capacity compared to the inflow) has the most potential for future hydropower production. To increase future energy production, the study examines a strategy by enlarging the turbine capacity. The results reveal

that hydropower can generate up to 10% additional energy with a 50% increase in turbine capacity. Moreover, the hydropower in the Mekong mainstream is found to get the most benefit from the turbine capacity increase in terms of energy production. Therefore, stakeholders should consider prioritizing these regions for future hydropower development.

CONTENTS

LIST OF TABLES

LIST OF FIGURES

LIST OF ABBREVIATIONS

3S	Sesan, Sre Pek, and Sekong
ACC	Flow Accumulation
ADB	Asian Development Bank
AGCM	Atmospheric General Circulation Model
AR5	The Fifth Assessment Report
AR6	The Sixth Assessment Report
CMIP5	Coupled Model Intercomparison Project Phase 5
CMIP6	Coupled Model Intercomparison Project Phase 6
d4PDF	Database for Policy Decision making for Future climate change
DEM	Digital Elevation Model
DIR	Flow Direction
ECS	Equilibrium Climate Sensitivity
FDC	Flow Duration Curve
GCM	General Circulation Model
GHG	Greenhouse Gas
GPCC	Global Precipitation Climatology Centre
IPCC	Intergovernmental Panel on Climate Change
JRA-55	Japanese 55-year Reanalysis dataset
K-S	Kolmogorov-Smirnov
kWh	Kilowatt hour
LMB	Lower Mekong Basin
MCM	Million cubic meter
MERIT	Multi-Error-Removed-Improved-Terrain
MODIS	Moderate Resolution Imaging Spectroradiometer
MRB	Mekong River Basin
MRC	Mekong River Commission
MW	Megawatt

NSE	Nash-Sutcliffe model Efficiency
R2	Coefficient of Determination
RCM	Regional Climate Model
RCP	Representative Concentration Pathway
RMSE	Root Mean Square Error
RRI	Rainfall-Runoff-Inundation model
SCE-UA	Shuffled Complex Evolution
SSP	Shared Socioeconomic Pathway
SWAT	Soil and Water Assessment Tool
TSLB	Tonle Sap Lake Basin
TSR	Tonle Sap River
UMB	Upper Mekong Basin
WCRP	World Climate Research Program

CHAPTER 1 General Introduction

1.1 Research Background

Climate change is one of the most critical threats to water resources and other natural ecosystems. Surface water temperature, evaporation and water level are very sensitive to changing climate (Woolway et al., 2020). Global surface temperature is getting warmer than ever since 1970. Many kinds of weather and climate extremes are already being affected by climate change in every region of the world. Since the Fifth Assessment Report (AR5) of the Intergovernmental Panel on Climate Change (IPCC), evidence of observed changes in extremes like heatwaves, heavy precipitation, droughts, and tropical cyclones, has become stronger (IPCC, 2014). According to the AR6, the average changes in global surface temperature at the end of the 21st century compared to the historical period of 1850–1900 is 1.4°C for the Shared Socioeconomic Pathway (SSP1-1.9) and 4.4°C for the SSP5-8.5 (IPCC, 2021). Projected changes in global surface temperature under different scenarios in the AR6 are listed in **Table 1.1**. Temperature rise significantly affects the global rainfall pattern and evapotranspiration, thus changing the river flow region and flood characteristics (Wang et al., 2019). Moreover, future climate projections are expected to increase the frequency and intensity of global precipitation, causing extreme flooding and drought **(Figure 1.1)**.

Table 1.1 Projected changes in global surface temperature compared to the baseline of 1850–1900 in the AR6 (IPCC, 2021)

Scenario	Near-term 2021–2040		Mid-term 2041–2060		Long-term 2081–2100	
	Mean (°C)	Range (°C)	Mean (°C)	Range (°C)	Mean (°C)	Range (°C)
SSP1-1.9	1.5	1.2–1.7	1.6	1.2–2.0	1.4	1.0–1.8
SSP1-2.6	1.5	1.2–1.8	1.7	1.3–2.2	1.8	1.3–2.4
SSP2-4.5	1.5	1.2–1.8	2.0	1.6–2.5	2.7	2.1–3.5
SSP3-7.0	1.5	1.2–1.8	2.1	1.7–2.6	3.6	2.8–4.6
SSP5-8.5	1.6	1.3–1.9	2.4	1.9–3.0	4.4	3.3–5.7

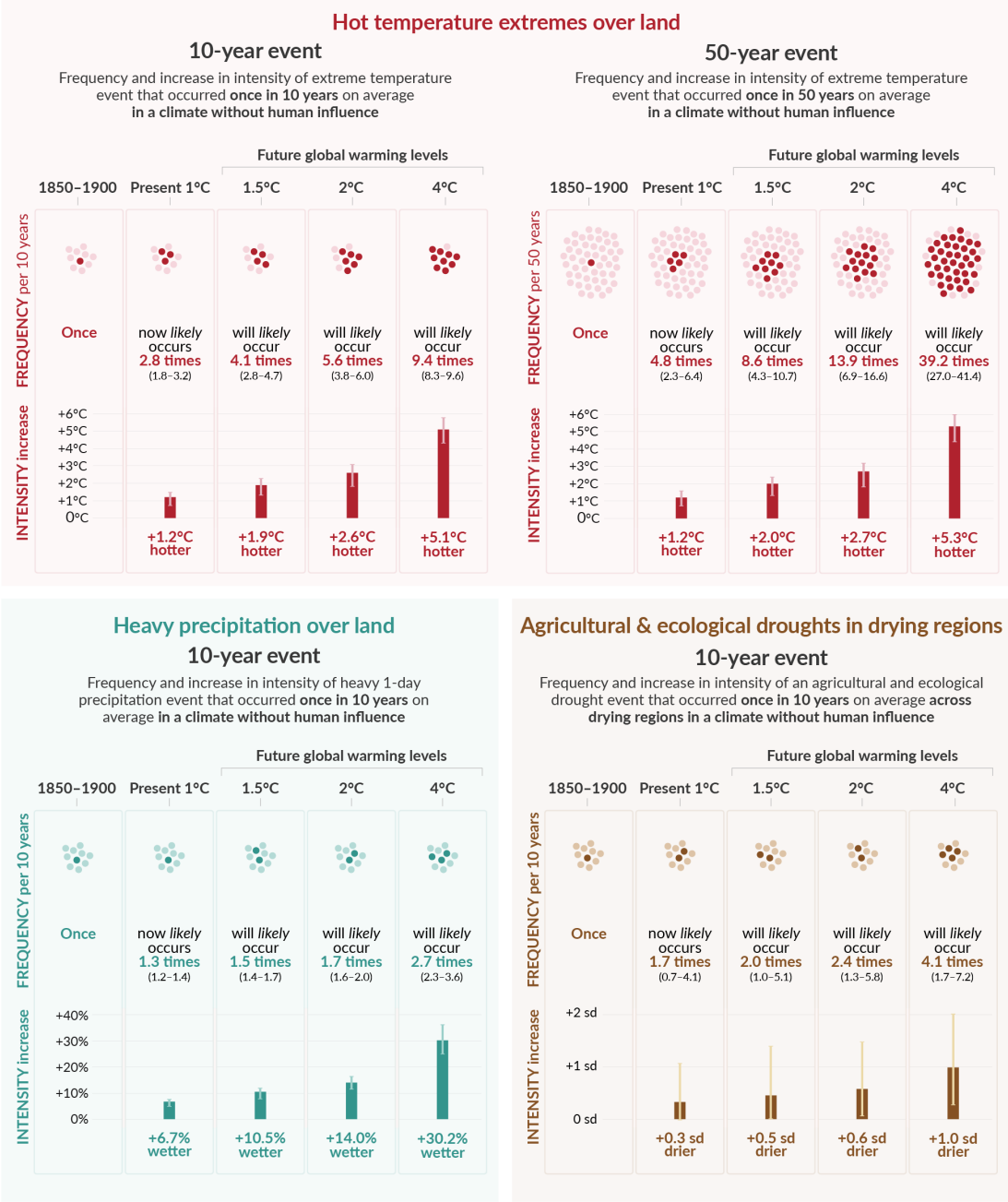

Figure 1.1 Projected changes in the intensity and frequency of extremes events (IPCC, 2021)

The increase in flood frequency and magnitude, due to changes in future precipitation and extreme events, has become a global concern (Shrestha et al., 2019). Flood disasters can potentially cause severe damage to society such as loss of lives and destruction of important infrastructures. The cost of annual flood damage in the Lower Mekong Basin (LMB) is estimated at up to 70 million USD (MRC, 2010). To mitigate flood risks and improve water supply for human consumption, approximate 2.8 million dams have been constructed globally, with total reservoir storage of up

to 10,000 km^3 (Grill et al., 2019; Yun et al., 2021). Although dam generally alters the flow regime by regulating the natural river flow, it has played an important role in reducing flood exposure under climate change in many river basins by decreasing both frequency and intensity (Boulange et al., 2021). On top of flood mitigation, the dam can potentially provide energy supply (hydroelectric dam), additional water for irrigation during the dry season, and navigation system (Intralawan et al., 2019). Therefore, it is important to evaluate the possible effect of climate change on the global water resources and understand the role of the dam in the river basin. Such information could be beneficial for stakeholders and river basin managers in terms of climate change adaptation and risk reduction.

1.2 Objectives

This dissertation aims to understand the effect of the future climate change on river flow regime and flood characteristics and the role of hydropower in the Mekong River Basin (MRB). In particular, the specific objectives of the study are as follows:

- To develop a simple storage model for defining the reservoir operation in the MRB
- To analyze the changes in flow regimes under future hydropower development in the MRB
- To assess the cumulative impacts of climate change and reservoir operations on river flow and flood characteristics in the MRB
- To understand the role of hydropower in reducing flood exposure under the future climate projections in the LMB
- To evaluate the changes in hydropower production under the future climate projections in the MRB

1.3 Dissertation Structure

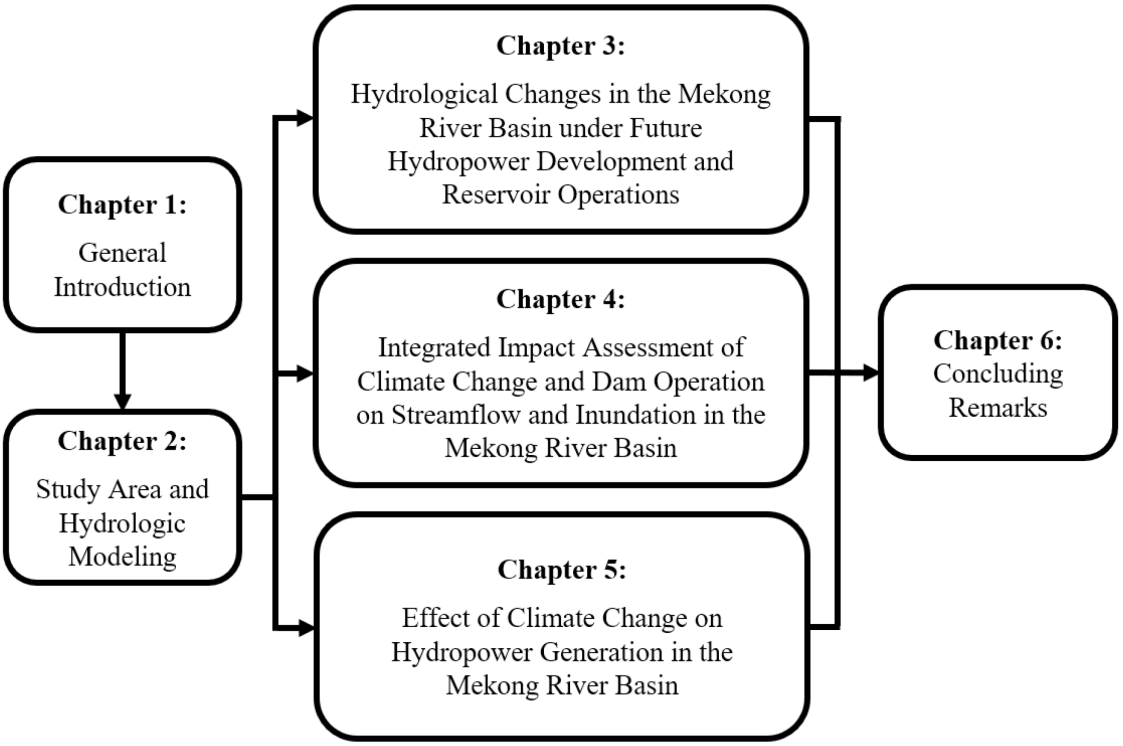

Figure 1.2 Flowchart and contents of each chapter in this dissertation

This dissertation consists of six main chapters. Details of each chapter are briefly described below:

Chapter 1 introduces the general knowledge of global climate change, flood risk, and the general role of the dam. The main purpose, specific objectives, and key contents of this dissertation are also described in this chapter.

Chapter 2 describes key information of the study area of the MRB such as geographical information, climate conditions, and hydropower development situation in the basin. The main hydrological model, Rainfall-Runoff-Inundation (RRI) model, is also briefly explained here.

Chapter 3 presents the development of a simple storage model for the reservoir operation in the MRB. In addition, this chapter applied the RRI coupled with the simple storage model to evaluate the changes in river flow under the future hydropower development.

Chapter 4 analyzes the changes in seasonal discharge in the MRB under the reservoir operations during the historical period from 1982 to 2016. Then, this chapter adopted CMIP6 climate projections to estimate the changes in river flow regime and flood characteristics under climate change scenarios along with reservoir operations from 2026 to 2100. Lastly, the role of hydropower in reducing flood exposure under the changing climate is discussed.

Chapter 5 estimates the energy generation from hydropower in the MRB under the future climate scenarios. Hydropower characterization and classification are also performed to define the potential hydropower regions for future development. Moreover, strategies for increasing hydropower production are also discussed.

Chapter 6 summarizes the findings and gives the overall conclusion to this dissertation.

References

Boulange, J., Hanasaki, N., Yamazaki, D., & Pokhrel, Y. (2021). Role of Dams in Reducing Global Flood Exposure under Climate Change. *Nature Communications*, *12*(1), 1–7. https://doi.org/10.1038/s41467-020-20704-0

Grill, G., Lehner, B., Thieme, M., Geenen, B., Tickner, D., Antonelli, F., Babu, S., Borrelli, P., Cheng, L., Crochetiere, H., Ehalt Macedo, H., Filgueiras, R., Goichot, M., Higgins, J., Hogan, Z., Lip, B., McClain, M. E., Meng, J., Mulligan, M., … Zarfl, C. (2019). Mapping the World's Free-flowing Rivers. *Nature*, *569*(7755), 215–221. https://doi.org/10.1038/s41586-019-1111-9

Intralawan, A., Smajgl, A., McConnell, W., Ahlquist, D. B., Ward, J., & Kramer, D. B. (2019). Reviewing Benefits and Costs of Hydropower Development Evidence From the Lower Mekong River Basin. *WIREs Water*, *6*(4), e1347. https://doi.org/10.1002/WAT2.1347

IPCC. (2014). *Synthesis Report: Contribution of Working Group I, II, and III to the Fifth Assessment Report of the Intergovernmental Panel on Climate Change*. IPCC.

IPCC. (2021). *The Physical Science Basis - Summary for Policymakers: Working Group I Contribution to the Sixth Assessment Report of the Intergovernmental Panel on Climate Change*. IPCC.

MRC. (2010). *State of Basin Report 2010*. Mekong River Commission.

Shrestha, B. B., Perera, E. D. P., Kudo, S., Miyamoto, M., Yamazaki, Y., Kuribayashi, D., Sawano, H., Sayama, T., Magome, J., Hasegawa, A., Ushiyama, T., Iwami, Y., & Tokunaga, Y. (2019). Assessing Flood Disaster Impacts in Agriculture under Climate Change in the River Basins of Southeast Asia. *Natural Hazards*, *97*(1), 157–192. https://doi.org/10.1007/S11069-019-03632-1/FIGURES/26

Wang, H., Xiao, W., Wang, Y., Zhao, Y., Lu, F., Yang, M., Hou, B., & Yang, H. (2019). Assessment of the Impact of Climate Change on Hydropower Potential in the Nanliujiang River Basin of China. *Energy*, *167*, 950–959. https://doi.org/10.1016/J.ENERGY.2018.10.159

Woolway, R. I., Kraemer, B. M., Lenters, J. D., Merchant, C. J., O'Reilly, C. M., & Sharma, S. (2020). Global Lake Responses to Climate Change. *Nature Reviews Earth & Environment*,

1(8), 388–403. https://doi.org/10.1038/s43017-020-0067-5

Yun, X., Tang, Q., Sun, S., & Wang, J. (2021). Reducing Climate Change Induced Flood at the Cost of Hydropower in the Lancang-Mekong River Basin. *Geophysical Research Letters*, *48*(20), e2021GL094243. https://doi.org/10.1029/2021GL094243

CHAPTER 2 Study Area and Hydrologic Model

2.1 The Study Area

2.1.1 The Mekong River Basin

The Mekong River Basin is the most productive ecosystem in the world and the largest transboundary river in Southeast Asia. Originating from the Tibetan highlands in China, the Mekong River travels across six countries: China, Myanmar, Laos, Thailand, Cambodia, and Vietnam **(Figure 2.1)**. The basin covers a catchment area of 795,000 km^2 with an annual mean discharge of 14,500 m^3/s (MRC, 2005). Its river system is the livelihood of more than 70 million inhabitants, where fishery and agriculture are the main sources of income (Varis et al., 2012). Flood inundation is one of the most important characteristics of the basin because it creates remarkable biodiversity, particularly in the Tonle Sap floodplain and the Mekong Delta (Arias et al., 2012; Hoang et al., 2019; Lamberts, 2006; Try et al., 2020b). Its extensive wetlands and floodplains provide the most inland fisheries of 2.6 million tons annually, and other animals are valued at up to 7 million USD (Hortle, 2007). On the other hand, the annual flood pulse transports sediments across the LMB floodplain, functioning as the natural soil fertilizer for agriculture. Annual flooding also plays a significant role in replenishing the groundwater table and preserving the river morphology of the basin.

The MRB consists of two major parts: the Upper Mekong Basin (UMB) in China (so-called Lancang Jiang), and the Lower Mekong Basin (LMB) from Yunnan downstream in China to the South China Sea. The upper basin covers up to 24 percent of the total area and contributes about 16 percent to the total annual flow, whereas the left bank tributaries in Laos along with the Se Kong, Se San, and Sre Pok (3S) river system (Vietnam central highlands, Laos, and Cambodia) contributes up to 55 percent. Snowmelt from China, on the other hand, contributes about 24 percent to the total flows from the UMB during the dry season (MRC, 2019). In an average year, the river catchment in Laos has the largest basin annual flow (i.e., 35 percent), followed by Thailand, Cambodia, China, and Vietnam at about 18, 18, 16, and 11 percent, respectively **(Table 2.1)**.

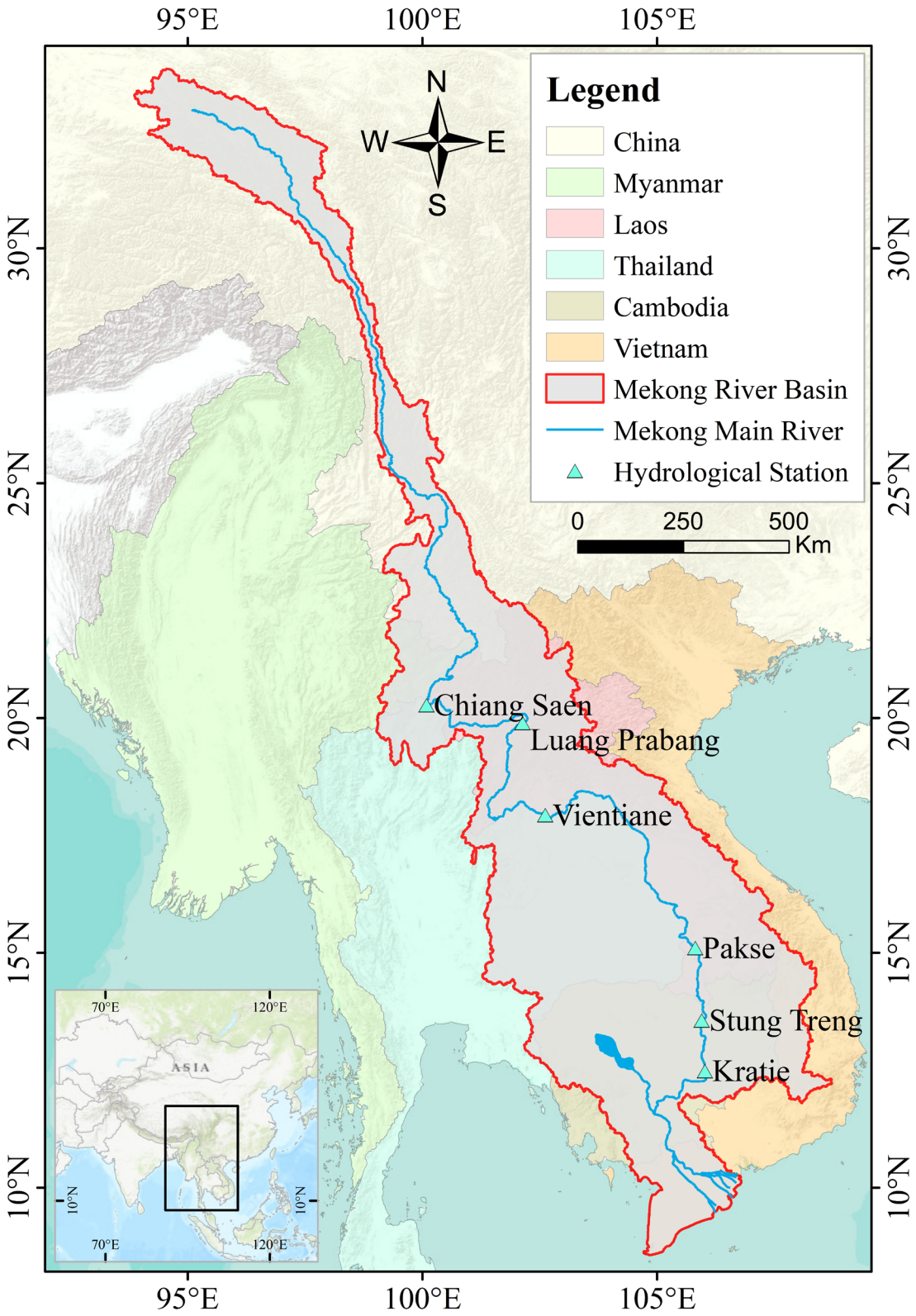

Figure 2.1 Map of the Mekong River Basin and location of the hydrological stations

Table 2.1 Distribution of the catchment area and flow contribution in the Mekong River Basin

Description	China	Myanmar	Laos	Thailand	Cambodia	Vietnam	Total
Area ($\times 10^3$ km^2)	165	24	202	184	155	65	795
Area as of MRB (%)	21	3	25	23	20	8	100
Flow as of MRB (%)	16	2	35	18	18	11	100

2.1.2 The Tonle Sap Lake Basin

Located in the central plain of Cambodia, the Tonle Sap Lake Basin (TSLB) is the largest freshwater body in Southeast Asia and is regarded as the heart of the Mekong River system (Lamberts, 2006). The major parts of the basin are lowlands with elevation less than 100 m above mean sea level with a gentle slope. It shares the border with the Cardamom Mountains in the west and south, and the Dangrek Mountains in the north, separating the basin from the Khorat Plateau of Thailand (Oeurng et al., 2019). The elevation rises in the southwest in the Cardamom Mountains to over 1,700 m, while the steep escapement of the Dangrek Mountains reaches an average of 500 m in the north. The TSLB covers a catchment area of 86,000 km^2, with five percent of its area located in Thailand territory.

The TSLB consists of twelve sub-basins and the Tonle Sap Lake known as the Great Lake **(Figure 2.2)**. The lake covers an area of 2,500 to 3,000 km^2 during the dry season. In the wet season, it expands its water body four to six times covering an area between 10,000 to 16,000 km^2. The climate of the basin is controlled by the monsoon, giving a wet season (May–October) and a dry season (November–April). The average annual precipitation varies from 1,000 to 1,700 mm, increasing in an easterly direction. Each year, there are two noticeable peaks of rainfall. The first peak occurs at the beginning of the wet season as the monsoon rain moves north, while the second peak occurs between August and October as the monsoon rain moves south (ADB, 2006).

The Tonle Sap River (TSR) connects the Great Lake to the Mekong River. This connection allows floodwaters, sediments, fishes, and other biodiversity to transport between the basins. The hydrology of the TSR is governed by the monsoonal flood regime of the Mekong system, creating a unique hydrological system of two-directional flows. Almost half of the Tonle Sap sub-basins are affected by the backwater from the Mekong River due to the seasonal bi-directional flow. During the dry season, the TSR flows south from the Great Lake into the Mekong River at the

Chaktomuk confluence in Phnom Penh. During the rainy season, flooding and associated water level in the Mekong River reverse the TSR's direction to flow back into the lake. At this point, the lake is well-known for its important roles in flood control, acting as a flood buffer in the Mekong River system, and providing beneficial dry seasonal flows (ADB, 2014).

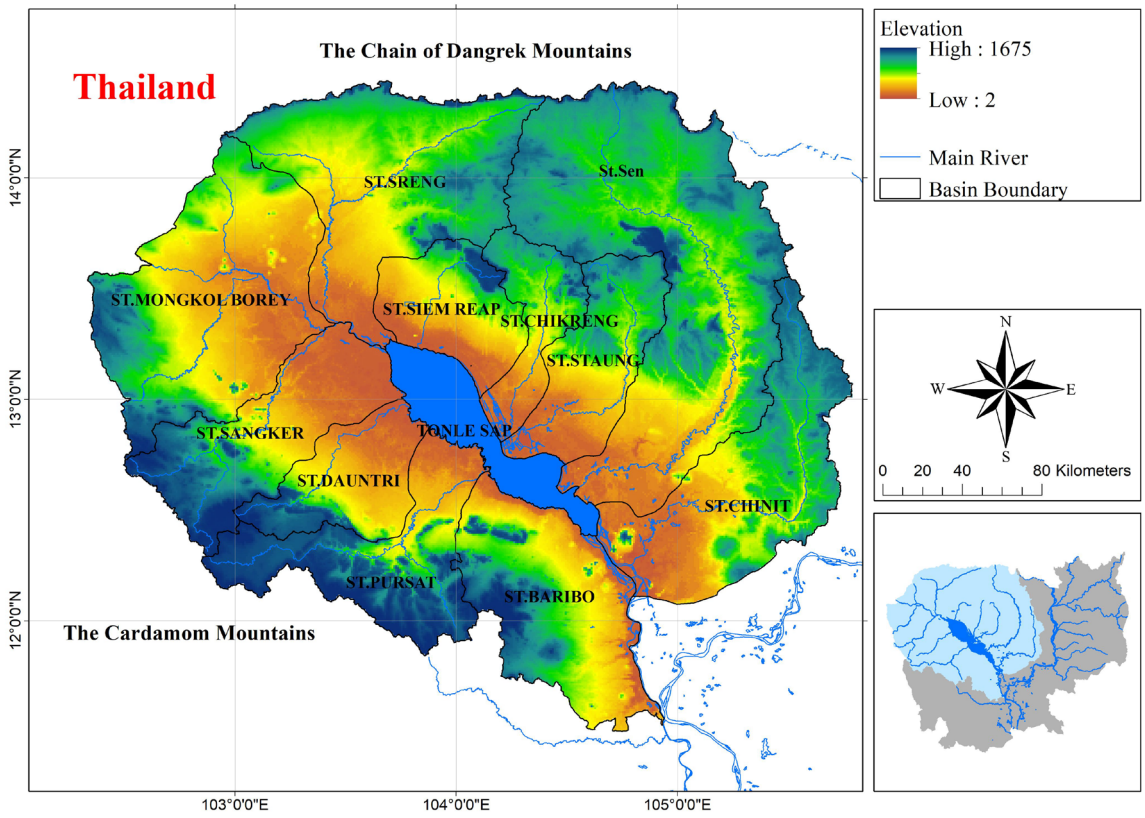

Figure 2.2 Map of the Tonle Sap Lake Basin and its sub-basins

2.1.3 Climate Conditions of the Mekong River Basin

The climate of the MRB is governed by the Asian monsoon, which results in two distinct seasons: a wet season and a dry season **(Table 2.2)**. From mid-May to early October, the southwest monsoon brings heavy rainfall and high humidity, while the northeast monsoon brings drier and cooler air (lower temperature) from early November to March. Tropical cyclones affect most of the region, making August and September, and sometimes October (in the delta) the wettest months of the year. On the other hand, Yunnan province in the upper basin shares a similar monsoon climate, although there is significant variation due to local topography. As the elevation rises to 4,000 m above sea level in the Tibetan Plateau, the climate shifts from tropical and subtropical monsoons in the south of Yunnan to temperate monsoons in the north. In general, the lower basin receives more rainfall than the upper basin. During an average year, the annual

Table 2.2 Seasonality of climate conditions in the Mekong River Basin

Cool/Cold			Hot/Dry		Wet						Cool/Cold
Jan	Feb	Mar	Apr	May	Jun	Jul	Aug	Sep	Oct	Nov	Dec
NE Monsoon			Transition		SW Monsoon						NE Monsoon

precipitation for the whole basin is approximately 1,500 mm (MRC, 2005).

The seasonal variation of mean temperature in the lower basin's lowland and river valleys is not large. However, there are significant changes at higher altitudes and in the more temperate climate. The lower basins share similar mean summer temperatures from March to October, ranging from 28–30 degree Celsius in Phnom Penh (Cambodia) to 26–28 degree Celsius in Luang Prabang (Laos), and 26–29 degree Celsius in Chiang Rai (Thailand). However, mean winter temperatures drop significantly from south to north, from 26–27 degree Celsius in Phnom Penh to 21–23 degree Celsius in Chiang Rai. In addition, it is much cooler in the upper basin in Yunnan province. There is a low fluctuation in annual evapotranspiration in the MRB, with an annual rate between 1,000 to 2,000 mm. The annual evapotranspiration rate in the lower basin is higher than in the upper basin, ranging from 1,500 to 1,700 mm in Cambodia and Vietnam (MRC, 2005).

2.1.4 Hydropower Development in the Mekong River Basin

As the population increases, the LMB's energy demand is expected to grow at 6–7 percent annually. In response, riparian countries are capitalizing on hydropower potential. Obviously, hydropower is widely acknowledged as a significant development opportunity for the MRB and its people (MRC, 2019). To some LMB countries, hydropower development is a national development strategy aiming to increase foreign direct investment and revenue from electricity generation, expand irrigated areas, improve navigation, and reduce flooding and drought. For instance, with current hydropower development, Laos has been recognized as the "Battery of Asia" with revenue from electricity exports used for national economic development (Intralawan et al., 2019).

Hydropower development in the MRB has started over half a century ago. However, the development rate in the LMB has accelerated in the last decades, accompanied by growing private sector investment in power infrastructure (Soukhaphon et al., 2021). Hydropower development mainly occurred in three different regions. The first region is the Lancang-Jiang cascade in the

UMB in China (Arias et al., 2014). The second focus of development is a series of 11 dams along the mainstream channel in the LMB, with 7 in Laos, 2 in Cambodia, and 2 across the Laos-Thai border. Of those, 2 hydropower dams, Xaiyaburi and Don Sahong have started their operation while another 4 are under consultation process. The third region of development takes place in the Mekong tributaries, in particular the 3S (Sesan, Sre Pok, and Sekong) river system, where 42 dams are being under construction and planned. As of 2019, there are 89 hydropower projects in the lower basin, with a total installed capacity of 12,285 megawatts (MW) **(Figure 2.3)**. Of those, 2 are in Cambodia (401 MW installed capacity), 65 in Laos (8,033 MW), 7 in Thailand (1,245 MW), and 14 in Vietnam (2,607 MW). Hydropower is expected to generate more than 30,000 MW by 2040 (Hecht et al., 2019). **Table 2.3** presents the hydropower projects in the MRB and their technical specifications.

The development of hydropower has both advantages and disadvantages for the river basin. Full hydropower development could generate more than 160 billion USD in economic growth. However, there are potential trade-offs such as declines in fisheries, loss of forests, wetlands and mangroves, and reduction of sediment transport. Many studies (Arias et al., 2014; Cochrane et al., 2014; Hoang et al., 2019; Lauri et al., 2012; Räsänen et al., 2012) have investigated the impact of

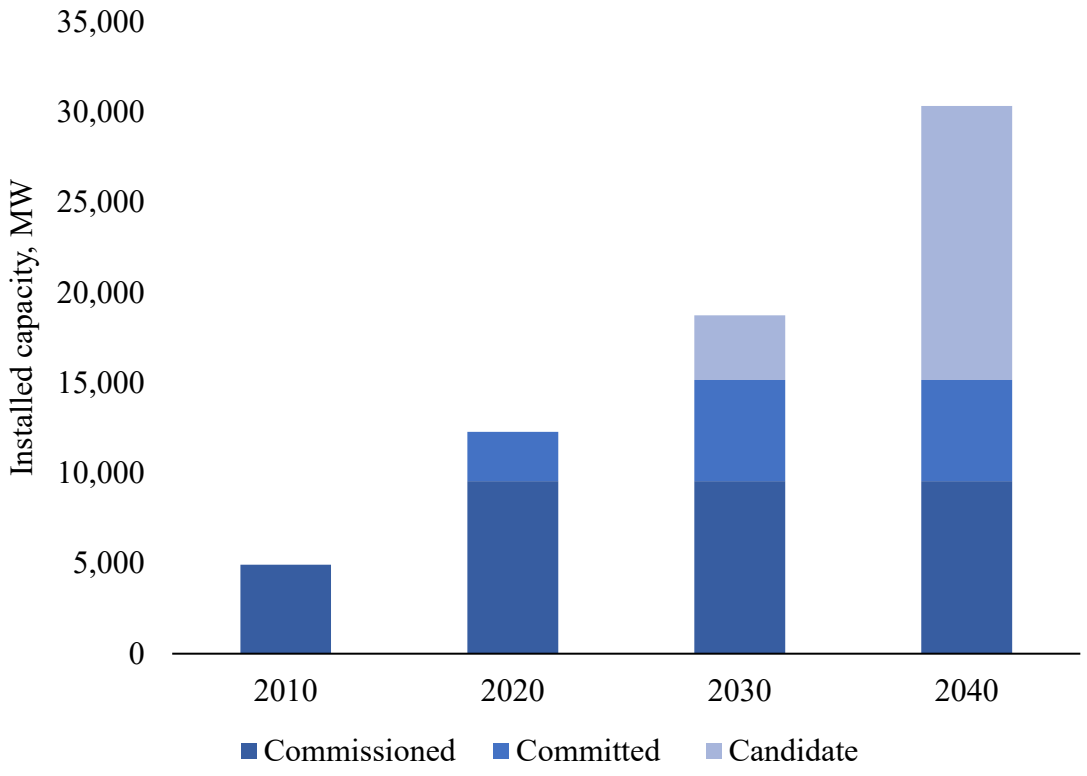

Figure 2.3 Potential of hydropower development in the Mekong River Basin

hydropower development on river flow in the MRB. Hydropower operation is expected to significantly increase dry season flows, decrease wet season flow, and reduce sediment budget. Therefore, good practices in managing water resources and adaptive reservoir operations can help balance upstream and downstream flow regimes (MRC, 2019).

Table 2.3 List of hydropower projects in the Mekong River Basin

Project Name	Country	Purpose	Installed Capacity (MW)
Battambang 1	Cambodia	Multi-purpose	24.00
Battambang 2	Cambodia	Multi-purpose	22.00
Lower Se San 2 & Lower Sre Pok 2	Cambodia	Hydropower	480.00
Lower Se San 3	Cambodia	Hydropower	243.00
Lower Sre Pok 3	Cambodia	Hydropower	204.00
Lower Sre Pok 4	Cambodia	Hydropower	143.00
Prek Liang 1	Cambodia	Hydropower	35.00
Prek Liang 2	Cambodia	Hydropower	25.00
Pursat 1	Cambodia	Hydropower	100.00
Pursat 2	Cambodia	Hydropower	10.00
Sambor	Cambodia	Hydropower	3,300.00
Stung Sen	Cambodia	Hydropower	23.00
Stung Treng	Cambodia	Hydropower	980.00
Dachaoshan	China	Hydropower	1,350.00
Dahuaqiao	China	Hydropower	920.00
Gongguoqiao	China	Hydropower	900.00
Huangdeng	China	Hydropower	1,900.00
Jinghong	China	Hydropower	1,750.00
Lidi	China	Hydropower	420.00
Manwan	China	Hydropower	1,550.00
Miaowei	China	Hydropower	1,400.00
Nuozhadu	China	Hydropower	5,850.00

Tuoba	China	Hydropower	1,400.00
Wunonglong	China	Hydropower	990.00
Xiaowan	China	Hydropower	4,200.00
Dak E Mule	Laos	Hydropower	105.00
Houay Lamphan	Laos	Hydropower	60.00
Houayho	Laos	Hydropower	150.00
Nam Beng	Laos	Hydropower	30.00
Nam Chian	Laos	Hydropower	148.00
Nam Feuang 1	Laos	Hydropower	28.00
Nam Feuang 2	Laos	Hydropower	25.00
Nam Feuang 3	Laos	Hydropower	20.00
Nam Hinboun 1	Laos	Hydropower	45.00
Nam Hinboun 2	Laos	Hydropower	13.00
Nam Khan 1	Laos	Hydropower	101.77
Nam Khan 2	Laos	Hydropower	140.00
Nam Khan 3	Laos	Hydropower	47.00
Nam Kong 1	Laos	Hydropower	75.00
Nam Kong 2	Laos	Hydropower	74.00
Nam Leuk	Laos	Hydropower	60.00
Nam Lik 1	Laos	Hydropower	54.00
Nam Lik 2	Laos	Hydropower	100.00
Nam Mang 1	Laos	Hydropower	51.00
Nam Mang 3	Laos	Hydropower	40.00
Nam Mouan	Laos	Hydropower	110.00
Nam Nga	Laos	Hydropower	97.84
Nam Ngao	Laos	Hydropower	20.00
Nam Ngiep 1	Laos	Hydropower	260.00

Nam Ngiep-regulating dam	Laos	Hydropower	16.80
Nam Ngieu	Laos	Hydropower	30.40
Nam Ngum 1	Laos	Multi-purpose	148.70
Nam Ngum 2	Laos	Hydropower	615.00
Nam Ngum 3	Laos	Hydropower	440.00
Nam Ngum 4A	Laos	Hydropower	54.00
Nam Ngum 5	Laos	Hydropower	120.00
Nam Ngum-Lower dam	Laos	Hydropower	90.00
Nam Ou 1	Laos	Hydropower	180.00
Nam Ou 2	Laos	Hydropower	90.00
Nam Ou 3	Laos	Hydropower	300.00
Nam Ou 4	Laos	Hydropower	75.00
Nam Ou 5	Laos	Hydropower	108.00
Nam Ou 6	Laos	Hydropower	210.00
Nam Ou 7	Laos	Hydropower	180.00
Nam Pay	Laos	Hydropower	62.00
Nam Pha	Laos	Hydropower	147.20
Nam Phak	Laos	Hydropower	75.00
Nam Pok	Laos	Hydropower	2.60
Nam Pot	Laos	Irrigation	22.00
Nam Poun	Laos	Hydropower	84.87
Nam Pouy	Laos	Hydropower	43.73
Nam San 2	Laos	Hydropower	60.00
Nam San 3	Laos	Hydropower	48.00
Nam San 3B	Laos	Hydropower	38.00
Nam Suang 1	Laos	Hydropower	40.00
Nam Suang 2	Laos	Hydropower	134.00

Nam Tha 1	Laos	Hydropower	168.00
Nam Theun 1	Laos	Hydropower	523.00
Nam Theun 2	Laos	Hydropower	1,075.00
Nam Theun 4	Laos	Hydropower	30.00
Theun Hinboun	Laos	Hydropower	430.00
Theun Hinboun-exp NG8	Laos	Hydropower	60.00
Xe Bang Hieng 2	Laos	Hydropower	16.00
Xe Bang Nouan	Laos	Hydropower	18.00
Xe Don 2	Laos	Hydropower	54.00
Xe Kaman 1	Laos	Hydropower	290.00
Xe Kaman 2A	Laos	Hydropower	64.00
Xe Kaman 2B	Laos	Hydropower	100.00
Xe Kaman 3	Laos	Hydropower	250.00
Xe Kaman 4A	Laos	Hydropower	96.00
Xe Kaman 4B	Laos	Hydropower	74.00
Xe Katam	Laos	Hydropower	60.80
Xe Kong 3d	Laos	Hydropower	91.10
Xe Kong 3up	Laos	Hydropower	144.60
Xe Kong 4	Laos	Hydropower	300.00
Xe Kong 5	Laos	Hydropower	248.00
Xe Lanong 1	Laos	Hydropower	30.00
Xe Lanong2	Laos	Hydropower	20.00
Xe Nam Noy 5	Laos	Hydropower	20.00
Xe Neua	Laos	Hydropower	60.00
Xe Pon3	Laos	Hydropower	75.00
Xe Set2	Laos	Hydropower	76.00
Xe Set3	Laos	Hydropower	20.00

Xe Xou	Laos	Hydropower	63.39
Xepian-Xenamnoy	Laos	Hydropower	390.00
Ban Kum	Laos/Thailand	Hydropower	1,872.00
Don Sahong	Laos/Thailand	Hydropower	360.00
Latsua	Laos/Thailand	Hydropower	686.00
Luang Prabang	Laos/Thailand	Hydropower	1,410.00
Pakbeng	Laos/Thailand	Hydropower	1,230.00
Paklay	Laos/Thailand	Hydropower	1,320.00
Sanakham	Laos/Thailand	Hydropower	1,200.00
Sangthong-Pakchom	Laos/Thailand	Hydropower	1,079.00
Xayabuly	Laos/Thailand	Hydropower	1,260.00
Buon Kuop	Vietnam	Hydropower	280.00
Buon TuaSrah	Vietnam	Multi-purpose	86.00
Duc Xuyen	Vietnam	Hydropower	49.00
Plei Krong	Vietnam	Hydropower	100.00
Se San 3	Vietnam	Hydropower	260.00
Se San 3A	Vietnam	Hydropower	96.00
Se San 4	Vietnam	Hydropower	360.00
Se San 4A	Vietnam	Hydropower	63.00
Sre Pok 3	Vietnam	Hydropower	220.00
Sre Pok 4	Vietnam	Hydropower	70.00
Upper Kontum	Vietnam	Hydropower	250.00
Yali	Vietnam	Multi-purpose	720.00

2.2 Rainfall-Runoff-Inundation Model

2.2.1 Model Description

Rainfall-Runoff-Inundation (RRI) model is used to simulate the river discharge and flood inundation in the Mekong River Basin in this whole study. It is a two-dimensional distributed model capable of simulating rainfall-runoff and flood inundation simultaneously (Sayama et al., 2012, 2015). This model has been widely adopted in various studies to assess the flood risk and changes in flow regimes in many different river basins (Bhagabati & Kawasaki, 2017; Kuribayashi et al., 2016; Ly et al., 2021; Perera et al., 2017; Sayama et al., 2015; Try et al., 2020a; Yamamoto et al., 2021).

In the calculation process, slopes and river channels are treated independently in the model **(Figure 2.4)**. The model assumes that both the slope and the river are located within the same grid cell when a river channel is present. The 2D diffusive wave model is used to calculate the flow on the slope grid cells, whereas the 1D diffusive wave model is used to compute the flow in the channel. In addition to surface flow, the model also simulates the lateral subsurface flow and

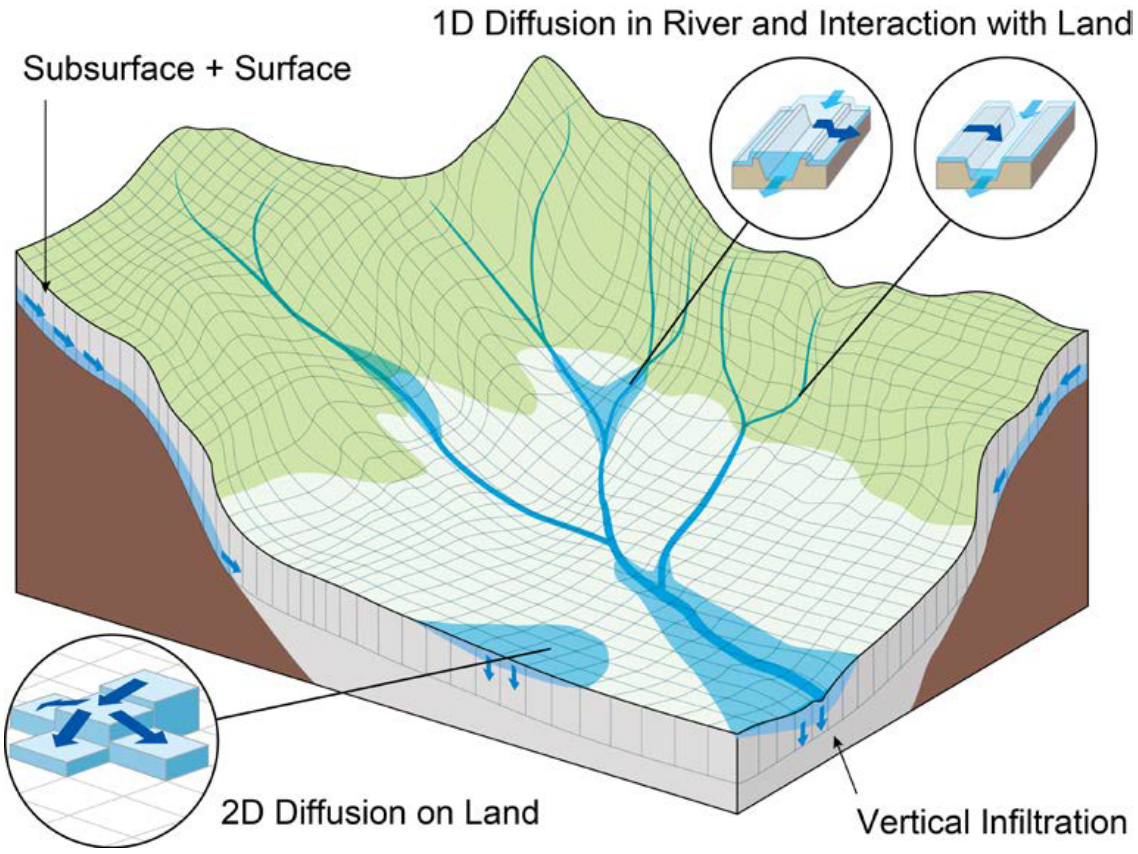

Figure 2.4 Schematic diagram of the RRI model (Sayama et al., 2015)

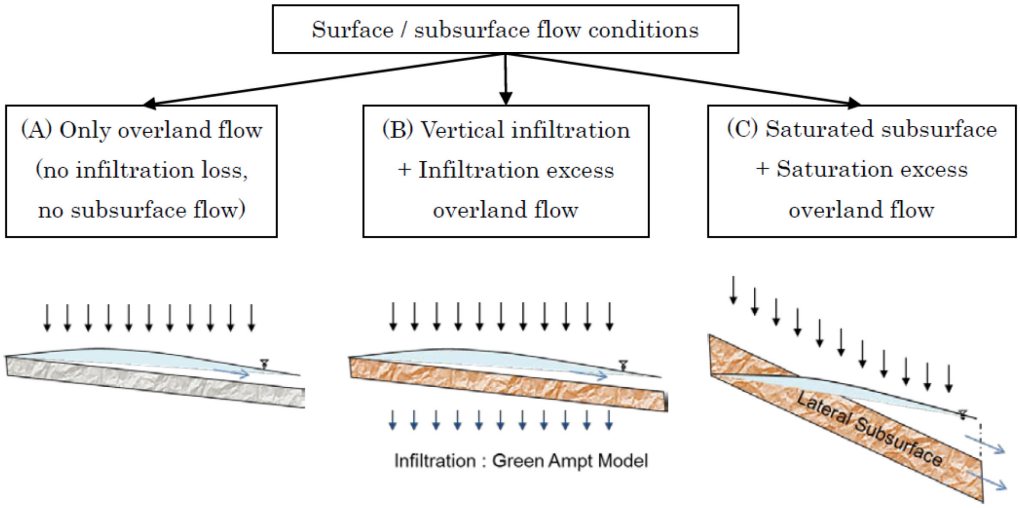

Figure 2.5 Graphical representation of the hydrological process of surface and subsurface flow under different conditions

and vertical infiltration flow. The lateral subsurface flow, typically in the mountainous regions, is calculated by the discharge-hydraulic gradient relationship. The Green-Ampt model, on the other hand, is used to calculate the vertical infiltration flow. **Figure 2.5** illustrates the hydrological process of surface and subsurface flow under different conditions in the model.

Governing Equations of the RRI Model

The governing equations of the RRI model follow the mass balance equation (2.1) and the momentum equation (2.2) and (2.3) for gradually varied unsteady flow.

$$\frac{\partial h}{\partial t} + \frac{\partial q_x}{\partial x} + \frac{\partial q_y}{\partial y} = r - f \tag{2.1}$$

$$\frac{\partial q_x}{\partial t} + \frac{\partial u q_x}{\partial x} + \frac{\partial v q_y}{\partial y} = -gh\frac{\partial H}{\partial x} - \frac{\tau_x}{\rho_w} \tag{2.2}$$

$$\frac{\partial q_y}{\partial t} + \frac{\partial u q_x}{\partial x} + \frac{\partial v q_y}{\partial y} = -gh\frac{\partial H}{\partial y} - \frac{\tau_y}{\rho_w} \tag{2.3}$$

where h is the height of the water from the local surface,

q_x and q_y are the unit width discharges in x and y directions,

u and v are the flow velocities in x and y directions,

r is the rainfall intensity,

f is the infiltration rate,

H is the height of the water from the datum,

ρ_w is the density of water, g is the gravitational acceleration,

τ_x and τ_y are the shear stresses in x and y directions.

The second terms of the right-side of (2.2) and (2.3) are calculated with the Manning's equation.

$$\frac{\tau_x}{\rho_w} = \frac{gn^2 u\sqrt{u^2+v^2}}{h^{1/3}} \tag{2.4}$$

$$\frac{\tau_y}{\rho_w} = \frac{gn^2 v\sqrt{u^2+v^2}}{h^{1/3}} \tag{2.5}$$

where n is the Manning's roughness coefficient.

Inertia terms (i.e., the left-side terms of (2.2) and (2.3)) are ignored under the diffusion wave approximation. By further separating x and y directions while ignoring v and u terms in equations (2.2) and (2.3), we obtain the following equation:

$$q_x = -\frac{1}{n}h^{5/3}\sqrt{\left|\frac{\partial H}{\partial x}\right|}\,\mathrm{sgn}\left(\frac{\partial H}{\partial x}\right) \tag{2.6}$$

$$q_y = -\frac{1}{n}h^{5/3}\sqrt{\left|\frac{\partial H}{\partial y}\right|}\,\mathrm{sgn}\left(\frac{\partial H}{\partial y}\right) \tag{2.7}$$

where sgn is the signum function.

The RRI model spatially discretizes mass balance equation (2.1) as follows:

$$\frac{dh^{i,j}}{dt} + \frac{q_x^{i,j-1} - q_x^{i,j}}{\Delta x} + \frac{q_y^{i-1,j} - q_y^{i,j}}{\Delta y} = r^{i,j} - f^{i,j} \tag{2.8}$$

where $q_x^{i,j}$ and $q_y^{i,j}$ are x and y direction discharges from a grid cell at (i,j).

With the single variable of h, the effect of unsaturated, saturated subsurface flow and surface flow can be calculated through the following equation (Sayama & McDonnell, 2009):

$$q_x = \begin{cases} -k_m d_m \left(\dfrac{h}{d_m}\right)^{\beta} \dfrac{\partial H}{\partial x}, \ \left(h \le d_m\right) \\ -k_a \left(h - d_m\right) \dfrac{\partial H}{\partial x} - k_m d_m \dfrac{\partial H}{\partial x}, \ \left(d_m < h \le d_a\right) \\ -\dfrac{1}{n}\left(h - d_a\right)^{5/3} \sqrt{\left|\dfrac{\partial H}{\partial x}\right|} \operatorname{sgn}\left(\dfrac{\partial H}{\partial x}\right) - k_a \left(h - d_m\right) \dfrac{\partial H}{\partial x} - k_m d_m \dfrac{\partial H}{\partial x}, \ \left(d_a \le h\right) \end{cases} \tag{2.9}$$

$$q_y = \begin{cases} -k_m d_m \left(\dfrac{h}{d_m}\right)^{\beta} \dfrac{\partial H}{\partial y}, \ \left(h \le d_m\right) \\ -k_a \left(h - d_m\right) \dfrac{\partial H}{\partial y} - k_m d_m \dfrac{\partial H}{\partial y}, \ \left(d_m < h \le d_a\right) \\ -\dfrac{1}{n}\left(h - d_a\right)^{5/3} \sqrt{\left|\dfrac{\partial H}{\partial y}\right|} \operatorname{sgn}\left(\dfrac{\partial H}{\partial y}\right) - k_a \left(h - d_m\right) \dfrac{\partial H}{\partial y} - k_m d_m \dfrac{\partial H}{\partial y}, \ \left(d_a \le h\right) \end{cases} \tag{2.10}$$

The infiltration component is calculated using the Green-Ampt infiltration model in the following equation:

$$f = k_v \left[1 + \frac{(\phi - \theta_i) S_f}{F}\right] \tag{2.11}$$

where k_v is the vertical saturated hydraulic conductivity,
ϕ is the soil porosity,
θ_i is the initial water volume content,
S_f is the suction at the vertical wetting front,
F is the cumulative infiltration depth.

One-Dimensional River Routing Model

In river grid cells, a one-dimensional diffusive wave model is adopted. In this model, the river cross-section is assumed to be rectangle with width W, depth D, and embankment height H_e. When precise geometry information is unavailable, the width and depth are estimated by the following function of upstream contributing area A [km^2].

$$W = C_W A^{Sw} \tag{2.12}$$

$$D = C_D A^{S_D} \tag{2.13}$$

where C_W, S_W, C_D and S_D are river geometry parameters [m], and A is the upstream contributing area [km^2].

2.2.2 Model Calibration

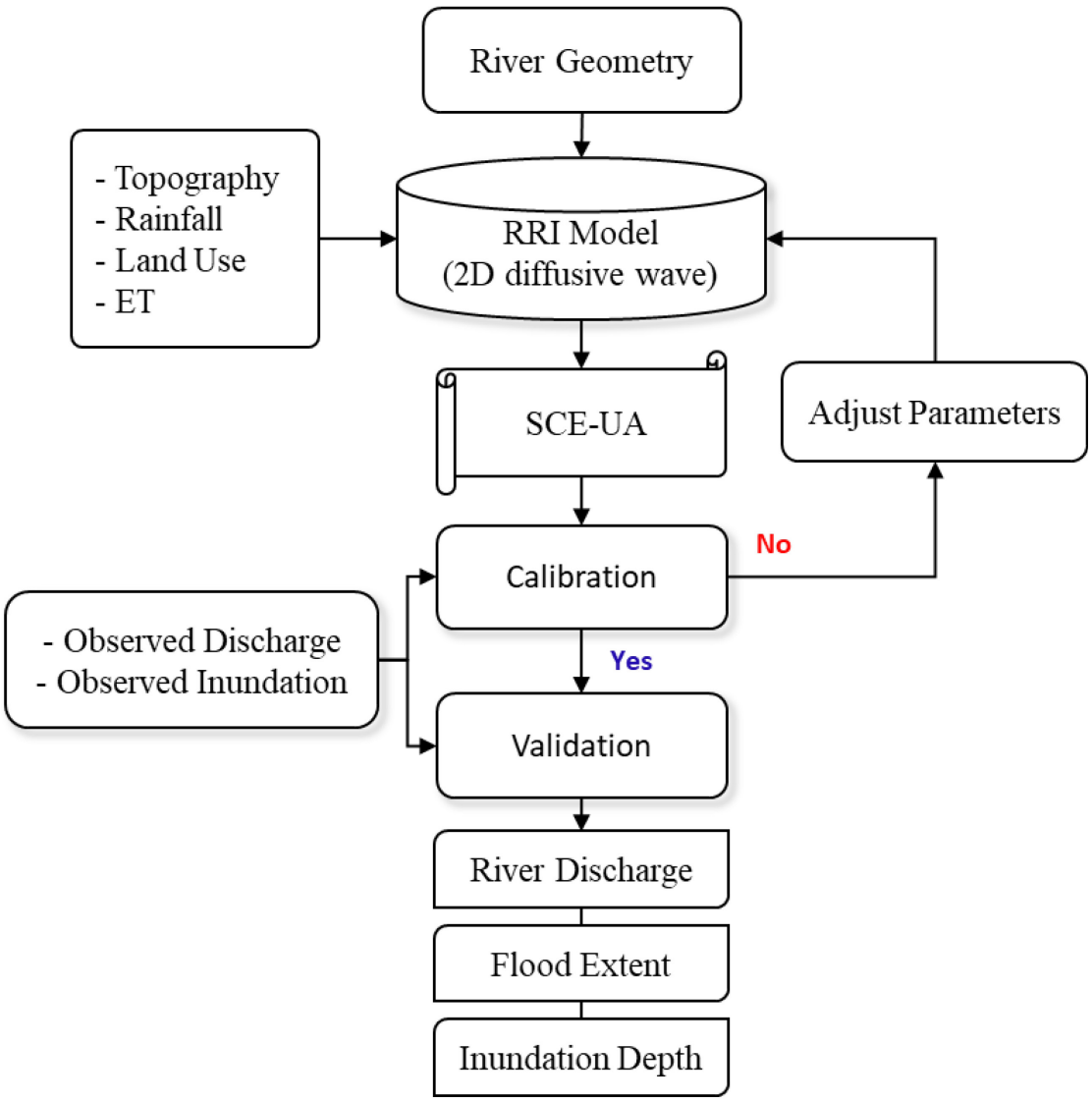

Figure 2.6 Schematic diagram of the RRI model's hydrological process with SCE-UA optimization approach (Try et al., 2018, 2020c)

To obtain the optimum parameters, the RRI model was integrated with a global optimization called the Shuffled Complex Evolution (SCE-UA) (Duan et al., 1994). The optimization method adjusts parameter values until appropriate results are obtained by comparing observed data with simulated data. The goal of this automated calibration is to find the best values for the RRI model's parameters by maximizing the value of the objective function. **Figure 2.6** presents the integration of SCE-UA optimization into the hydrological process of the RRI model. Developed at the University of Arizona, SCE-UA optimization is an effective method for calibrating a non-linear hydrological model. This automatic optimization approach has been widely used in numerous studies (Gan & Biftu, 1996; Kim et al., 2008; Lee et al., 2007; Lee & Kang, 2015; Try et al., 2018, 2020c). The SCE-UA optimization approach follows three steps: (1) the combination of the simplex procedure by applying a controlled random searching approach, (2) competitive evolution, and (3) complex shuffling **(Figure 2.7)**.

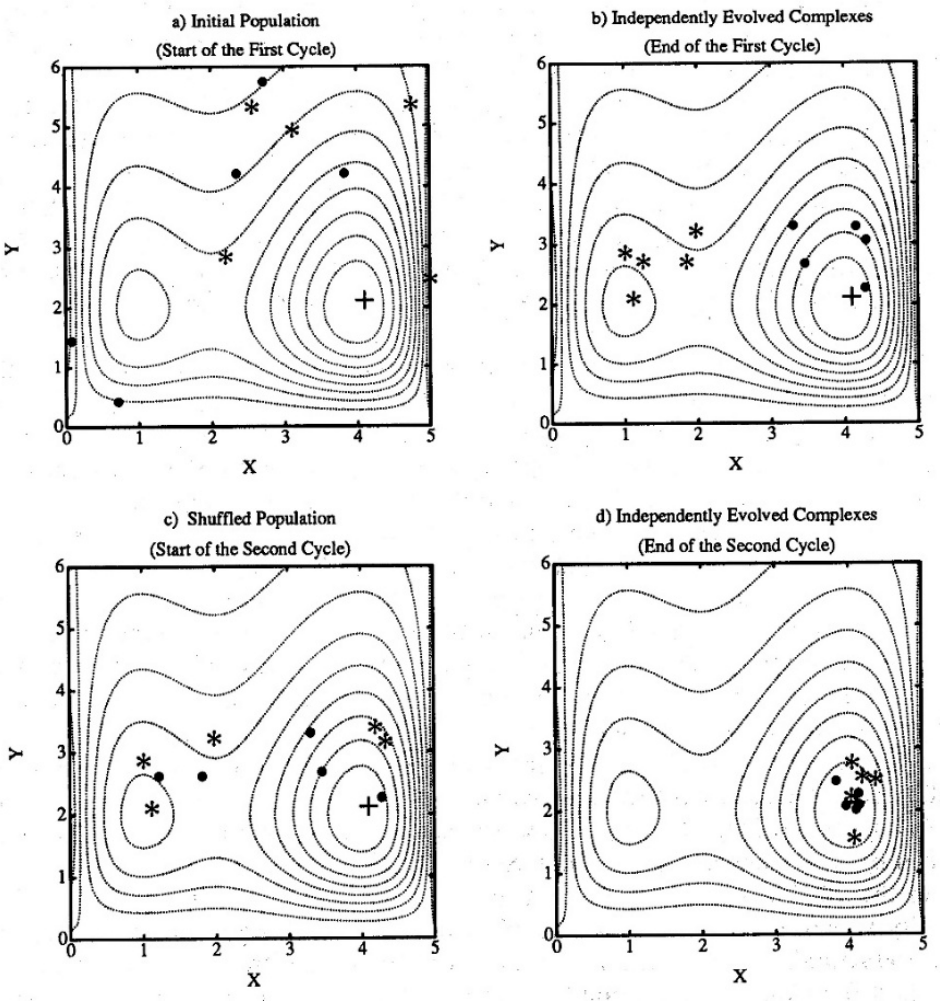

Figure 2.7 Illustration of Shuffled Complex Evolution (SCE-UA) optimization method (Duan et al., 1994)

2.3 Conclusion

This chapter presented detailed information about the study area (i.e., the Mekong River Basin), including the location, hydrological information, and climate condition. Moreover, information on water infrastructure developments (i.e., hydropower) was also introduced. Furthermore, the hydrologic model, Rainfall-Runoff-Inundation (RRI) model, employed throughout the study was thoroughly discussed, including the model calibration procedure. In the following chapter of this dissertation, the RRI model was used as the primary hydrological tool for river discharge and flood inundation simulations. Chapter 3 applied the RRI model with a simple storage model to assess the impact of future hydropower operations on hydrology in the MRB. Chapter 4 used the RRI model and reservoir operation model to investigate the changes in river flow and flood inundation caused by the future climate change and hydropower construction in the MRB. Last but not least, Chapter 5 adopted the RRI model to study the effect of climate change on hydropower generation in the MRB.

References

ADB. (2006). *Report on Water Availability*. Asian Development Bank.

ADB. (2014). *Cambodia Water Resources Profile*. Asian Development Bank.

Arias, M. E., Cochrane, T. A., Piman, T., Kummu, M., Caruso, B. S., & Killeen, T. J. (2012). Quantifying Changes in Flooding and Habitats in the Tonle Sap Lake (Cambodia) Caused by Water Infrastructure Development and Climate Change in the Mekong Basin. *Journal of Environmental Management*, *112*, 53–66. https://doi.org/10.1016/j.jenvman.2012.07.003

Arias, M. E., Piman, T., Lauri, H., Cochrane, T. A., & Kummu, M. (2014). Dams on Mekong Tributaries as Significant Contributors of Hydrological Alterations to the Tonle Sap Floodplain in Cambodia. *Hydrology and Earth System Sciences*, *18*(12), 5303–5315. https://doi.org/10.5194/hess-18-5303-2014

Bhagabati, S. S., & Kawasaki, A. (2017). Consideration of the Rainfall-Runoff-Inundation (RRI) Model for Flood Mapping in a Deltaic Area of Myanmar. *Hydrological Research Letters*, *11*(3), 155–160. https://doi.org/10.3178/HRL.11.155

Cochrane, T. A., Arias, M. E., & Piman, T. (2014). Historical Impact of Water Infrastructure on Water Levels of the Mekong River and the Tonle Sap System. *Hydrology and Earth System Sciences*, *18*(11), 4529–4541. https://doi.org/10.5194/hess-18-4529-2014

Duan, Q., Sorooshian, S., & Gupta, V. K. (1994). Optimal Use of the SCE-UA Global Optimization Method for Calibrating Watershed Models. *Journal of Hydrology*, *158*(3–4), 265–284. https://doi.org/10.1016/0022-1694(94)90057-4

Gan, T. Y., & Biftu, G. F. (1996). Automatic Calibration of Conceptual Rainfall-Runoff Models: Optimization Algorithms, Catchment Conditions, and Model Structure. *Water Resources Research*, *32*(12), 3513–3524. https://doi.org/10.1029/95WR02195

Hecht, J. S., Lacombe, G., Arias, M. E., Dang, T. D., & Piman, T. (2019). Hydropower Dams of the Mekong River Basin: A Review of Their Hydrological Impacts. *Journal of Hydrology*, *568*, 285–300. https://doi.org/10.1016/j.jhydrol.2018.10.045

Hoang, L. P., van Vliet, M. T. H., Kummu, M., Lauri, H., Koponen, J., Supit, I., Leemans, R., Kabat, P., & Ludwig, F. (2019). The Mekong's Future Flows under Multiple Drivers: How

Climate Change, Hydropower Developments and Irrigation Expansions Drive Hydrological Changes. *Science of the Total Environment*, *649*, 601–609. https://doi.org/10.1016/j.scitotenv.2018.08.160

Hortle, K. G. (2007). *Consumption and the Yield of Fish and Other Aquatic Animals from the Lower Mekong Basin. MRC Technical Paper No. 16*. Mekong River Commission.

Intralawan, A., Smajgl, A., McConnell, W., Ahlquist, D. B., Ward, J., & Kramer, D. B. (2019). Reviewing Benefits and Costs of Hydropower Development Evidence From the Lower Mekong River Basin. *WIREs Water*, *6*(4), e1347. https://doi.org/10.1002/WAT2.1347

Kim, S., Tachikawa, Y., Lee, G., & Takara, K. (2008). Prediction of the Largest Ever Flood: Case Study on Typhoon Rusa In 2002 at the Gamcheon Basin, Korea. *Proceedings of Hydraulic Engineering*, *52*, 67–72. https://doi.org/10.2208/PROHE.52.67

Kuribayashi, D., Ohara, M., Sayama, T., Konja, A., & Sawano, H. (2016). Utilization of the Flood Simulation Model for Disaster Management of Local Government. *Journal of Disaster Research*, *11*(6), 1161–1175. https://doi.org/10.20965/JDR.2016.P1161

Lamberts, D. (2006). The Tonle Sap Lake as a Productive Ecosystem. *International Journal of Water Resources Development*, *22*(3), 481–495. https://doi.org/10.1080/07900620500482592

Lauri, H., de Moel, H., Ward, P. J., Räsänen, T. A., Keskinen, M., & Kummu, M. (2012). Future Changes in Mekong River Hydrology: Impact of Climate Change and Reservoir Operation on Discharge. *Hydrology and Earth System Sciences*, *16*(12), 4603–4619. https://doi.org/10.5194/hess-16-4603-2012

Lee, G., Tachikawa, Y., & Takara, K. (2007). Identification of Model Structural Stability Through Comparison of Hydrologic Models. *Proceedings of Hydraulic Engineering*, *51*, 49–54. https://doi.org/10.2208/PROHE.51.49

Lee, S., & Kang, T. (2015). Analysis of Constrained Optimization Problems by the SCE-UA with an Adaptive Penalty Function. *Journal of Computing in Civil Engineering*, *30*(3), 04015035. https://doi.org/10.1061/(ASCE)CP.1943-5487.0000493

Ly, S., Try, S., & Sayama, T. (2021). Hydrological Changes in the Mekong River Basin Under Future Hydropower Developments and Reservoir Operations. *Journal of Japan Society of Civil Engineers, Ser. B1 (Hydraulic Engineering)*, *77*(2), 259–264.

https://doi.org/10.2208/jscejhe.77.2_I_259

MRC. (2005). *Overview of the Hydrology of the Mekong Basin*. The Mekong River Commission.

MRC. (2019). *The MRC Hydropower Mitigation Guidelines Vol. 1*. The Mekong River Commission.

Oeurng, C., Cochrane, T. A., Chung, S., Kondolf, M. G., Piman, T., & Arias, M. E. (2019). Assessing Climate Change Impacts on River Flows in the Tonle Sap Lake Basin, Cambodia. *Water*, *11*(3), 618. https://doi.org/10.3390/W11030618

Perera, E. D. P., Sayama, T., Magome, J., Hasegawa, A., & Iwami, Y. (2017). RCP8.5-Based Future Flood Hazard Analysis for the Lower Mekong River Basin. *Hydrology*, *4*(4), 55. https://doi.org/10.3390/HYDROLOGY4040055

Räsänen, T. A., Koponen, J., Lauri, H., & Kummu, M. (2012). Downstream Hydrological Impacts of Hydropower Development in the Upper Mekong Basin. *Water Resources Management*, *26*(12), 3495–3513. https://doi.org/10.1007/s11269-012-0087-0

Sayama, T., & McDonnell, J. J. (2009). A New Time-Space Accounting Scheme to Predict Stream Water Residence Time and Hydrograph Source Components at the Watershed Scale. *Water Resources Research*, *45*(7), 7401. https://doi.org/10.1029/2008WR007549

Sayama, T., Ozawa, G., Kawakami, T., Nabesaka, S., & Fukami, K. (2012). Rainfall–Runoff–Inundation Analysis of the 2010 Pakistan Flood in the Kabul River Basin. *Hydrological Sciences Journal*, *57*(2), 298–312. https://doi.org/10.1080/02626667.2011.644245

Sayama, T., Tatebe, Y., Iwami, Y., & Tanaka, S. (2015). Hydrologic Sensitivity of Flood Runoff and Inundation: 2011 Thailand Floods in the Chao Phraya River Basin. *Natural Hazards and Earth System Sciences*, *15*(7), 1617–1630. https://doi.org/10.5194/NHESS-15-1617-2015

Soukhaphon, A., Baird, I. G., & Hogan, Z. S. (2021). The Impacts of Hydropower Dams in the Mekong River Basin: A Review. *Water*, *13*(3), 265. https://doi.org/10.3390/W13030265

Try, S., Lee, G., Yu, W., Oeurng, C., & Jang, C. (2018). Large-Scale Flood-Inundation Modeling in the Mekong River Basin. *Journal of Hydrologic Engineering*, *23*(7), 05018011. https://doi.org/10.1061/(ASCE)HE.1943-5584.0001664

Try, S., Tanaka, S., Tanaka, K., Sayama, T., Hu, M., Sok, T., & Oeurng, C. (2020a). Projection of Extreme Flood Inundation in the Mekong River Basin under 4K Increasing Scenario using Large Ensemble Climate Data. *Hydrological Processes*, *34*(22), 4350–4364. https://doi.org/10.1002/hyp.13859

Try, S., Tanaka, S., Tanaka, K., Sayama, T., Lee, G., & Oeurng, C. (2020b). Assessing the Effects of Climate Change on Flood Inundation in the Lower Mekong Basin using High-Resolution AGCM Outputs. *Progress in Earth and Planetary Science*, *7*(1), 1–16. https://doi.org/10.1186/s40645-020-00353-z

Try, S., Tanaka, S., Tanaka, K., Sayama, T., Oeurng, C., Uk, S., Takara, K., Hu, M., & Han, D. (2020c). Comparison of Gridded Precipitation Datasets for Rainfall-Runoff and Inundation Modeling in the Mekong River Basin. *PLoS ONE*, *15*(1), e0226814. https://doi.org/10.1371/journal.pone.0226814

Varis, O., Kummu, M., & Salmivaara, A. (2012). Ten Major Rivers in Monsoon Asia-Pacific: An Assessment of Vulnerability. *Applied Geography*, *32*(2), 441–454. https://doi.org/10.1016/J.APGEOG.2011.05.003

Yamamoto, K., Sayama, T., & Apip. (2021). Impact of Climate Change on Flood Inundation in a Tropical River Basin in Indonesia. *Progress in Earth and Planetary Science*, *8*(1), 1–15. https://doi.org/10.1186/S40645-020-00386-4/FIGURES/12

CHAPTER 3 Hydrological Changes in the Mekong River Basin under Future Hydropower Development and Reservoir Operations

3.1 Introduction

In the last decades, the Mekong River Basin (MRB) has experienced major economic growth including the construction of large water infrastructures such as hydropower dams and irrigation schemes. Hydropower development is an important movement toward renewable energy and low carbon emission for the Mekong region as set out in the Mekong River Commission (MRC)'s Strategic Plan and Basin Development Plan (MRC, 2019). Those developments would benefit the riparian countries in terms of oversea investment, energy supply, trade, and agricultural expansion (Räsänen et al., 2012). It also reduces flood exposure to the population in the region (Boulange et al., 2021). However, it is expected to impact the Mekong river's ecosystem, especially the flow regime, flood characteristics, fish biodiversity, and sediment transport (Lauri et al., 2012). The first hydropower, the Manwan dam, was constructed in the Upper Mekong Basin (UMB) in China in 1993. Since then, many hydropower dams have been built and planned in both mainstream and tributaries of the Mekong. Based on the MRC's hydropower database, there are 126 hydropower projects in total, including 11 mainstream dams in the Lower Mekong Basin (LMB). Most of the projects are still under construction or in the planning stage, but they will be completed in the near future (MRC, 2009).

The hydrological impact assessment of hydropower development in the MRB has been done by some researchers using different methods ranging from a simple statistical approach to a more complex modeling approach. Those studies conclude that hydropower developments have changed seasonal flow by decreasing the wet season flow and increasing the dry season flow. However, the degree of change varies between studies depending on the methods and assumptions (Hoang et al., 2019; Hoanh et al., 2010; Piman et al., 2013). The reservoir operation rule is one of the important components in assessing the impacts of hydropower. Nonetheless, such

information is normally unavailable. A good practice of reservoir operation should include an effective approach that can adapt for the future flow and optimize the use of river inflow for the capacity of the reservoir based on purposes such as ensuring a reliable water supply, maximizing the energy production, flood control, and so on. Such kind of effective approach can be achieved through reservoir optimization (Ginting et al., 2017; Padiyedath Gopalan et al., 2021). However, several assumptions and boundary conditions are required.

Hydrological modeling has been widely used in assessing changes in flow characteristics by many studies (Hoang et al., 2019; Hoanh et al., 2010; Lauri et al., 2012; Padiyedath Gopalan et al., 2021; Piman et al., 2013; Räsänen et al., 2012). Various models have been developed and applied in the MRB to understand the impact of hydropower development. They include the Soil and Water Assessment Tool (SWAT) model (Arnold et al., 1998), VMod model (Koponen et al., 2010), HEC-ResSim model (Klipsch & Hurst, 2007), and Rainfall-Runoff-Inundation (RRI) model (Sayama et al., 2012). Räsänen et al., (2012) used VMod for the hydrological simulation and CSUDP for the reservoir optimization to assess the downstream impacts due to hydropower development in the UMB. Lauri et al., (2012) used VMod and Linear programming optimization to study the impacts of climate change and reservoir operation on the hydrology of the MRB. (Piman et al., 2013) applied SWAT and HEC-ResSim to investigate the impact of hydro-power development and reservoir operation in the Sesan, Srepok, and Sekong Rivers on flow regimes. Previous studies mostly focused on the impact of hydropower in the UMB and main-stream hydropower in the LMB.

To further understand the hydrological impact of future hydropower development, especially those in the tributaries, this study aims to develop a simple storage model to define the reservoir operation and integrate it into a hydrologic model to analyze the changes in flow regimes in the MRB.

3.2 Methodology

3.2.1 Hydrologic Model Simulation

This study used the Rainfall-Runoff-Inundation (RRI) model to simulate the river discharge of the MRB. The model has been calibrated and validated by Try et al., (2020c) for the entire MRB using a global optimization algorithm developed by the University of Arizona, known as Shuffled Complex Evolution (SCE-UA). Thus, this study used the optimized parameters set to perform the simulation. For details on the model calibration and validation, refer to Try et al., (2020c). To

evaluate the model performance, we used two indicators: the Nash-Sutcliffe model Efficiency coefficient (NSE) and Root Mean Square Error ($RMSE$).

$$NSE = 1 - \frac{\sum(Q_{sim} - Q_{obs})^2}{\sum(Q_{obs} - \overline{Q_{obs}})^2} \tag{3.1}$$

$$RMSE = \sqrt{\frac{\sum(Q_{sim} - Q_{obs})^2}{n}} \tag{3.2}$$

where Q_{sim} and Q_{obs} are the simulated and observed discharge at time step *t*, $\overline{Q_{obs}}$ are the average observed discharge, and *n* is the number of data.

3.2.2 Reservoir Operation

Detailed information on hydropower dam operation rules in the Mekong River Basin is not available. However, we can assume that the dams are operated to maximize the hydropower generations. In fact, some previous studies (Hoang et al., 2019; Lauri et al., 2012; Räsänen et al., 2012) have conducted the optimization of the dam operations to estimate the outflow even for proposed dams. The optimization methods can be categorized into three types: linear programming, non-linear programming, and dynamic programming. Such programming can be used to estimate the outflow maximizing the hydropower given the storage volumes and turbine flow capacity by maintaining the continuity condition of water (Ginting et al., 2017).

In our study, we employed a non-linear programming coded by a MATLAB program (Deland, 2012) for estimating the optimized patterns of dam reservoir outflows for each dam in the basin. Here we optimized the dam reservoir operations for each dam with the objective function that maximizes the sum of the turbine flow with the simulated inflow. To perform the optimization of a series of reservoirs in the entire MRB is obviously time-consuming and technically challenging. Therefore, we proposed a simple storage model representing the general patterns of the optimized outflow. The incorporation of our proposed model into the RRI model allowed the program to perform the hydrological simulation with all the dam reservoirs, whose operation rules follow the general pattern. Then, we can assess the cumulative impact of cascade hydropower dams (i.e., a series of hydropower dams) in the MRB. The reservoir storage was calculated by the following equation at a monthly time-step:

$$S_t = S_{t-1} + Q_{in_{t-1}} - Q_{turb_{t-1}} - Q_{spill_{t-1}} \quad (3.3)$$

The boundary conditions adopted in the system are:

$$\Delta S = S_0 + Q_{in} - Q_{max} \quad (3.4)$$

If $Q_{in} < Q_{max}$:

- $\Delta S \geq S_{min} \Rightarrow \begin{cases} Q_{turb} = Q_{max} \\ Q_{spill} = 0 \end{cases}$
- $\Delta S < S_{min} \Rightarrow \begin{cases} Q_{turb} = Q_{in} + S_0 - S_{min} \\ Q_{spill} = 0 \end{cases}$

If $Q_{in} \geq Q_{max}$:

- $\Delta S \leq S_{max} \Rightarrow \begin{cases} Q_{turb} = Q_{max} \\ Q_{spill} = 0 \end{cases}$
- $\Delta S > S_{max} \Rightarrow \begin{cases} Q_{turb} = Q_{max} \\ Q_{spill} = S_0 + Q_{in} - Q_{max} - S_{max} \end{cases}$

where S_0 is the initial storage, S_{min} is the minimum storage, S_{max} is the maximum storage, ΔS is the storage change, Q_{in} is the river inflow, Q_{turb} is the flow released from the turbine, Q_{spill} is the water overflow through the spillway, Q_{max} is the turbine's maximum flow capacity.

3.2.3 Data Collection

For the hydrological modeling, this study used the Global Precipitation Climatology Centre (GPCC) rainfall product as suggested by Try et al., (2020c). Their study evaluated the performance of various gridded precipitation datasets for rain-fall-runoff and inundation modeling over the MRB and found that GPCC outperformed other datasets for long-term simulation. The topographic data was obtained from the Multi-Error-Removed-Improved-Terrain (MERIT DEM) (Yamazaki et al., 2017). The land use was extracted from the MODIS dataset (Friedl et al., 2010). The evapotranspiration data was taken from the Japanese 55-year Reanalysis dataset (JRA-55) (Kobayashi et al., 2015). The river cross-sections, river width (W) and depth

(D), were approximately estimated from equations (3.5) and (3.6) as a function of upstream area (A).

$$D = 0.0015 \times A^{0.7491} \quad (3.5)$$

$$W = 0.0520 \times A^{0.7596} \quad (3.6)$$

The hydropower information was given by the MRC and the ADB (ADB, 2004; MRC, 2009). It contained existing and proposed/planned hydropower projects in the LMB and mainstream dams in the UMB **(Figure 3.1)**. Two hydropower development scenarios were prepared for the hydrological analysis in this study. The present hydropower development scenario included all existing hydropower projects (98) in the MRB. The future hydropower development scenario consists of 126 hydropower projects in total. It included all existing and proposed/planned hydropower projects as well as Chinese dams in the UMB. The model simulation adopted the present hydropower development scenario to validate our simple storage model.

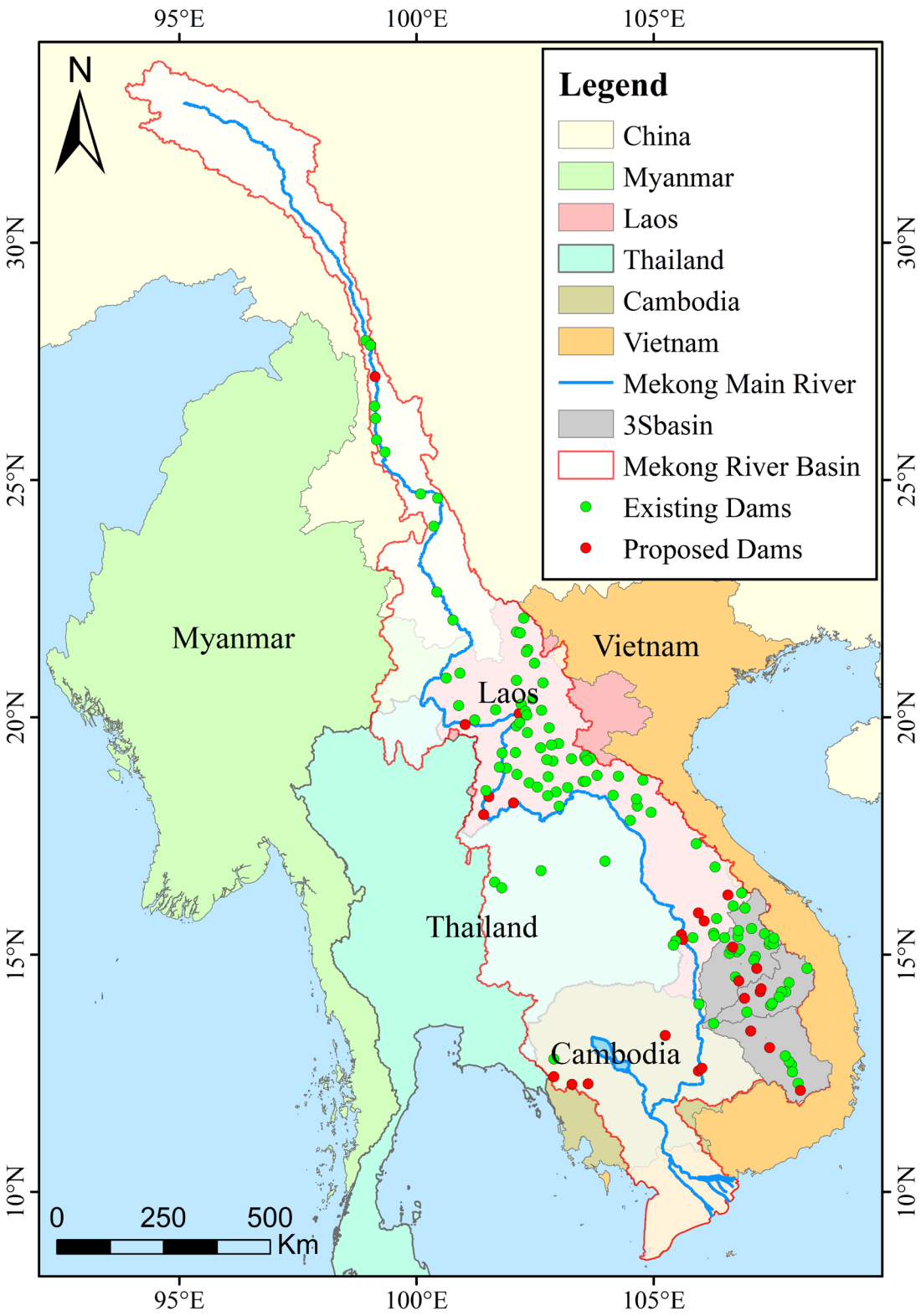

Figure 3.1 Location of the hydropower projects in the Mekong River Basin

3.3 Results and Discussion

3.3.1 Results of Reservoir Operation

In this study, we introduced a simple storage model to represent the optimized hydropower reservoir operations in the MRB. We compared our model with the non-linear programming method in estimating the monthly outflow from the reservoir. Two hydropower dams were selected for the evaluation period of 2010–2016: the Nam Tha-1 hydropower dam in the tributary of the LMB in Laos, and the Stung Treng hydropower dam in the mainstream of LMB in Cambodia. **Figure 3.2** and **Figure 3.3** show the average estimated monthly outflow from the two hydropower. The September outflow of the two reservoirs from our model was 290m^3/s and 36,695m^3/s. While the result from the optimization programming was 283m^3/s and 36,694m^3/s, respectively. The results suggested that the performance of our simple storage model was comparable with a more complicated optimization programming in estimating the monthly outflow of a reservoir. For the case of the Nam Tha-1 hydropower dam in **Figure 3.2**, the simple storage model released more water than the optimization in November and December. This pattern was observed for other dams also with comparatively high turbine flow capacity (290m^3/s for this case). While the optimization tended to keep the water for future use, the simple storage model just released all the water if the release was below the turbine flow. This indicated that an additional objective function may be effective for further stabilizing the outflow within the simple storage model.

3.3.2 Assessment of Hydropower Development Impact

The number of hydropower projects has significantly increased in the last decade. Many of them have started their operation since 2010. While other projects were expected to finish and fully operated by 2060 (MRC, 2009). We performed the simulation from 2010 to 2016 using the RRI model. The model performance was evaluated by the NSE and RMSE at Kratie, a station in the lower part of MRB. This station was selected based on its location and the availability of observed data. **Figure 3.4** shows the daily simulated and observed discharge at Kratie from 2010 to 2016. Without the hydropower development, the simulated discharge was slightly overestimated during the high flow season, especially the peak discharge, with NSE = 0.895 and RMSE = 3,728m^3/s. However, the reservoir operation overall reduced the peak flow and improved the simulated result with NSE = 0.908 and RMSE = 3,499m^3/s. This suggests that the incorporation of reservoir operation into the RRI model enhanced the model performance in reproducing the discharge and detecting the peak flow in the MRB.

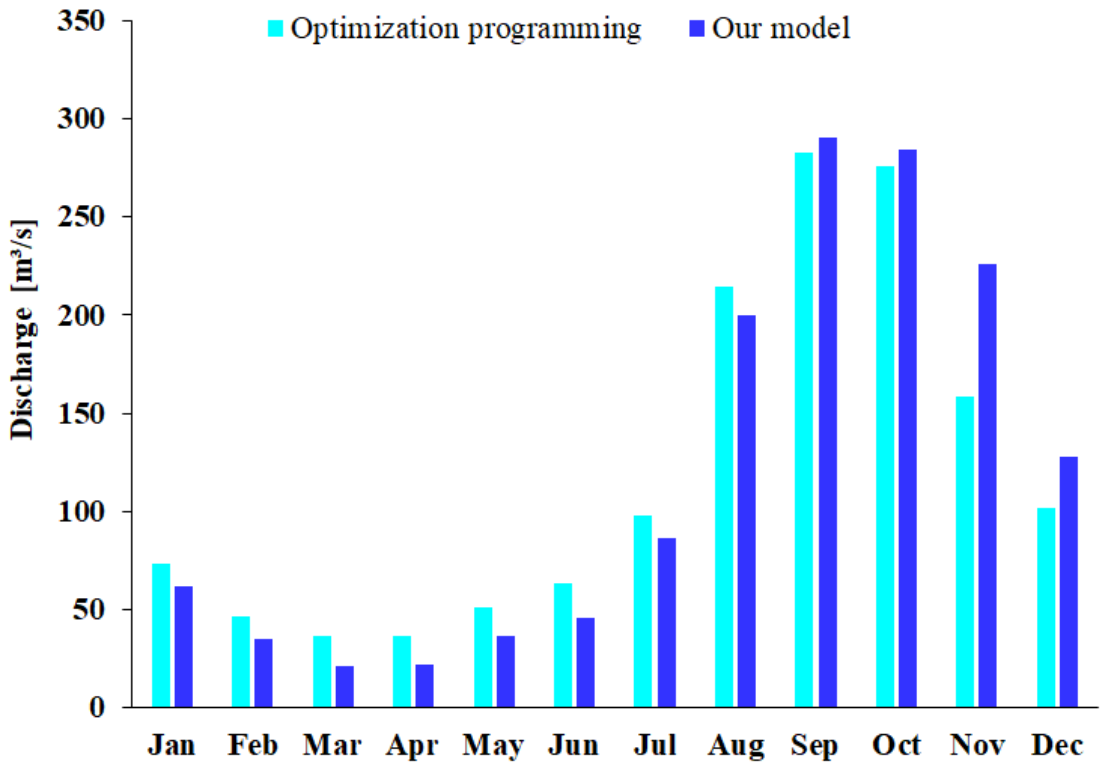

Figure 3.2 Estimated monthly outflow of the Nam Tha-1 hydropower dam

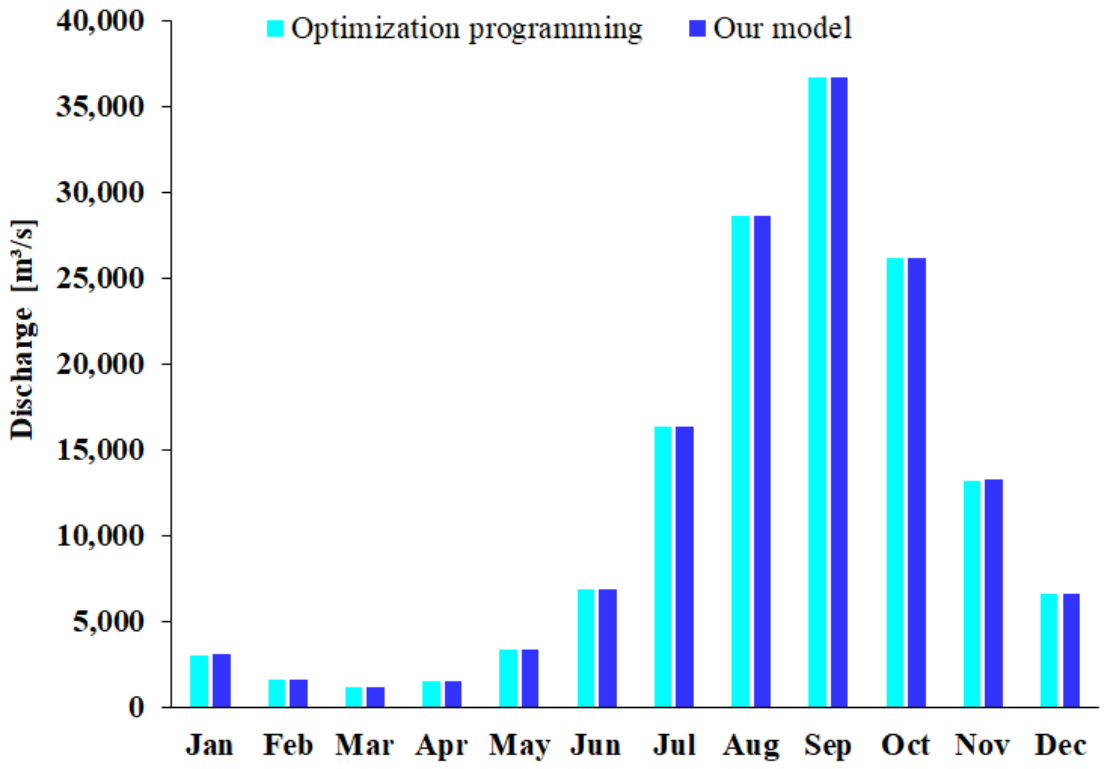

Figure 3.3 Estimated monthly outflow of the Stung Treng hydropower dam

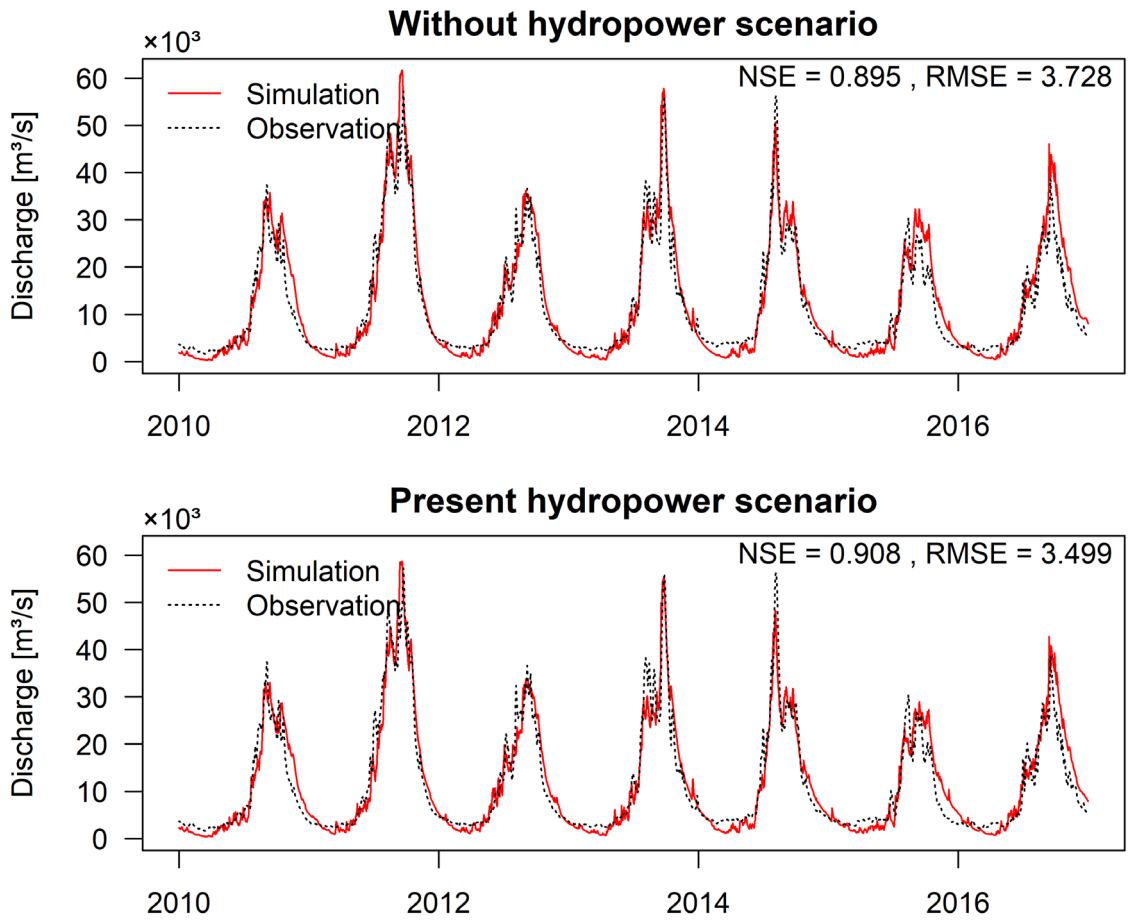

Figure 3.4 Simulated and observed daily discharge at Kratie from 2010 to 2016 without hydropower scenario and with present hydropower scenario

To further understand the hydrological changes due to hydropower development, we analyzed the seasonal and annual peak discharge under the present and future hydropower development scenario. Two stations along the mainstream of MRB were selected: Chiang Saen (the most upstream of LMB) and Kratie (the downstream of LMB). Under the future hydropower development scenario, the relative changes in monthly discharge ranged from -17% to +40% at Chiang Saen, and -16% to +100% at Kratie **(Figure 3.5)**. **Figure 3.6** presents the relative changes in discharge in the dry season (December–February), the wet season (July–September), and the annual peak discharge. With the future hydropower development, the dry seasonal flow was increased by 35% and 41% while the wet seasonal flow was decreased by 16% and 14% at Chiang Saen and Kratie, respectively. On the other hand, the annual peak discharge was also reduced at both stations **(Figure 3.7)**. The impacts of hydropower development can be seen as far as Kratie. However, the degree of change varied depending on the location. Due to the reservoir operation, the largest relative flow increases appeared in the early dry season when the reservoir started to

release the stored water. The increased flow during the dry season could mitigate the potential effects of droughts and expand agricultural activities. Our findings were comparable to other studies with a fairly similar monthly pattern of changes. Hoanh et al., (2010) and Räsänen et al., (2012) reported that June–November discharge at Chiang Saen would reduce by 17% and 22%, while our study suggested a 16% decrease. The direction of flow changes in this study also agreed with others on the seasonal scale as the high flow was decreased and the low flow was increased. However, the magnitude of alterations was slightly different among studies due to several factors such as study period, hydrologic model, assumption of boundary conditions, and reservoir operations rule. Lauri et al., (2012) and Hoang et al., (2019) found that dry seasonal flow at Kratie would increase by 90% and 63%, but our study estimated a 41% increase. Thus, the study of Lauri et al., (2012) estimated the largest flow changes while our study suggested a smaller change. The reduction of annual peak flow was due to the attenuation of water stored in the reservoir as it stored more water in the wet season and released water back in the dry season. Under the future hydropower development scenario, the flow at Kratie was significantly changed from the present hydropower development scenario while the flow at Chiang Saen was slightly changed. This can be explained through the number of proposed dams in the lower part of LMB. Since Chiang Saen is located in the most upstream of LMB, it received less impact from the future hydropower development compared to Kratie.

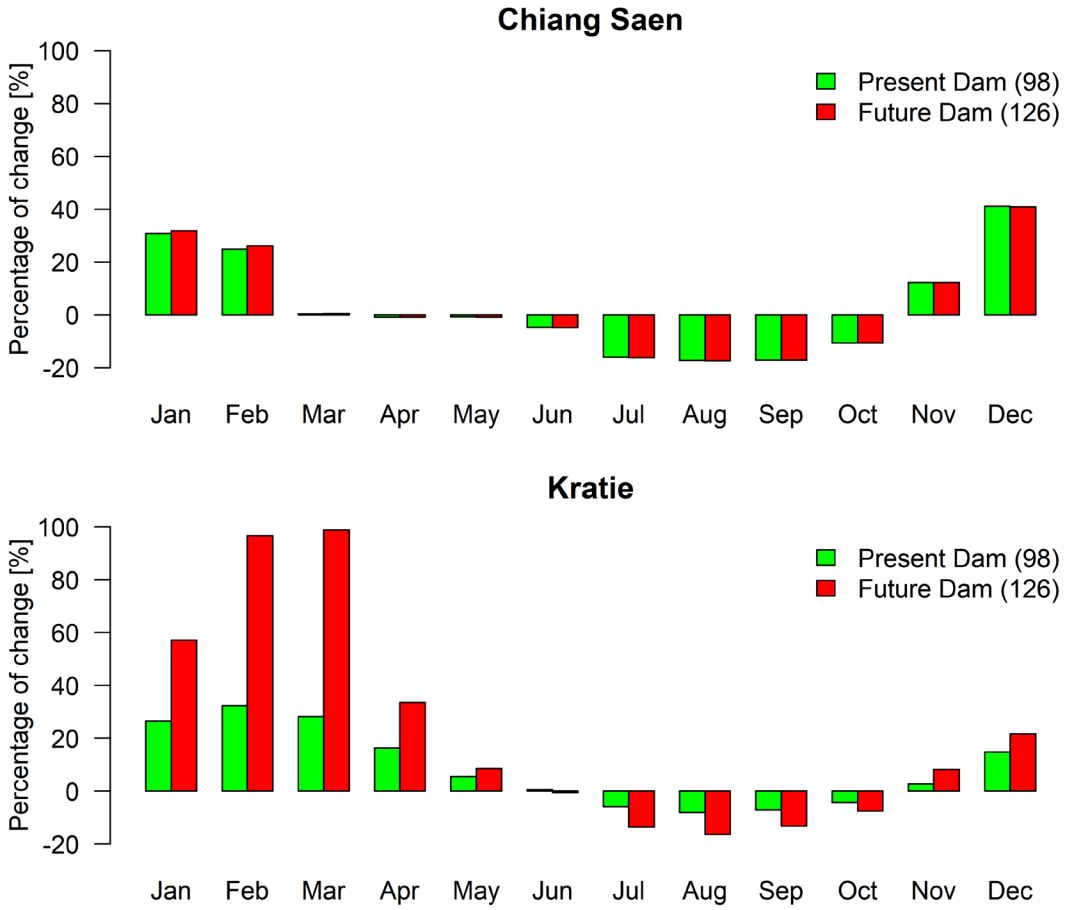

Figure 3.5 Relative changes of monthly discharge under present (98 dams) and future hydropower scenario (126 dams)

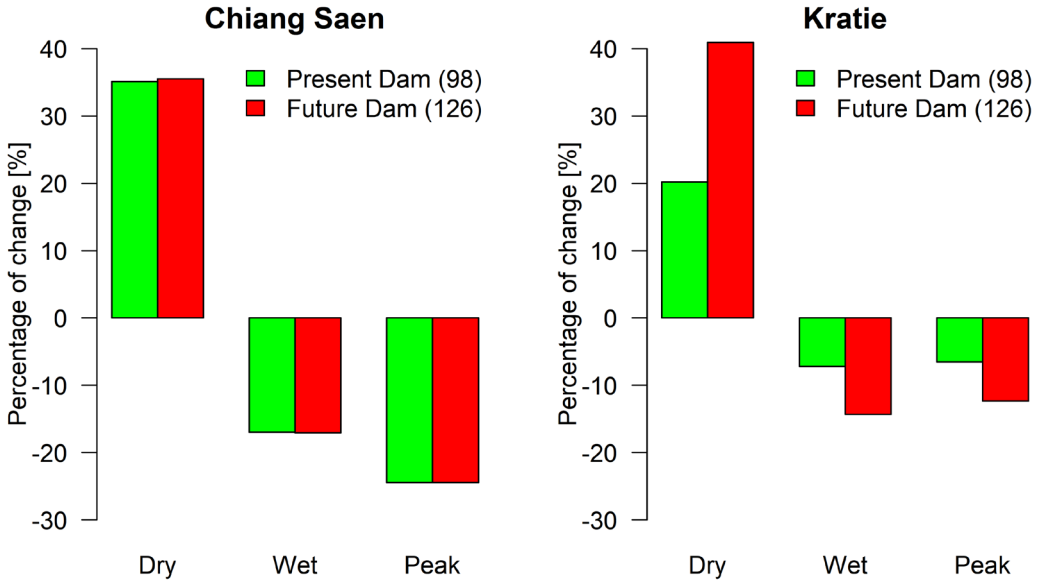

Figure 3.6 Relative changes of flow characteristics under present (98 dams) and future hydropower scenario (126 dams)

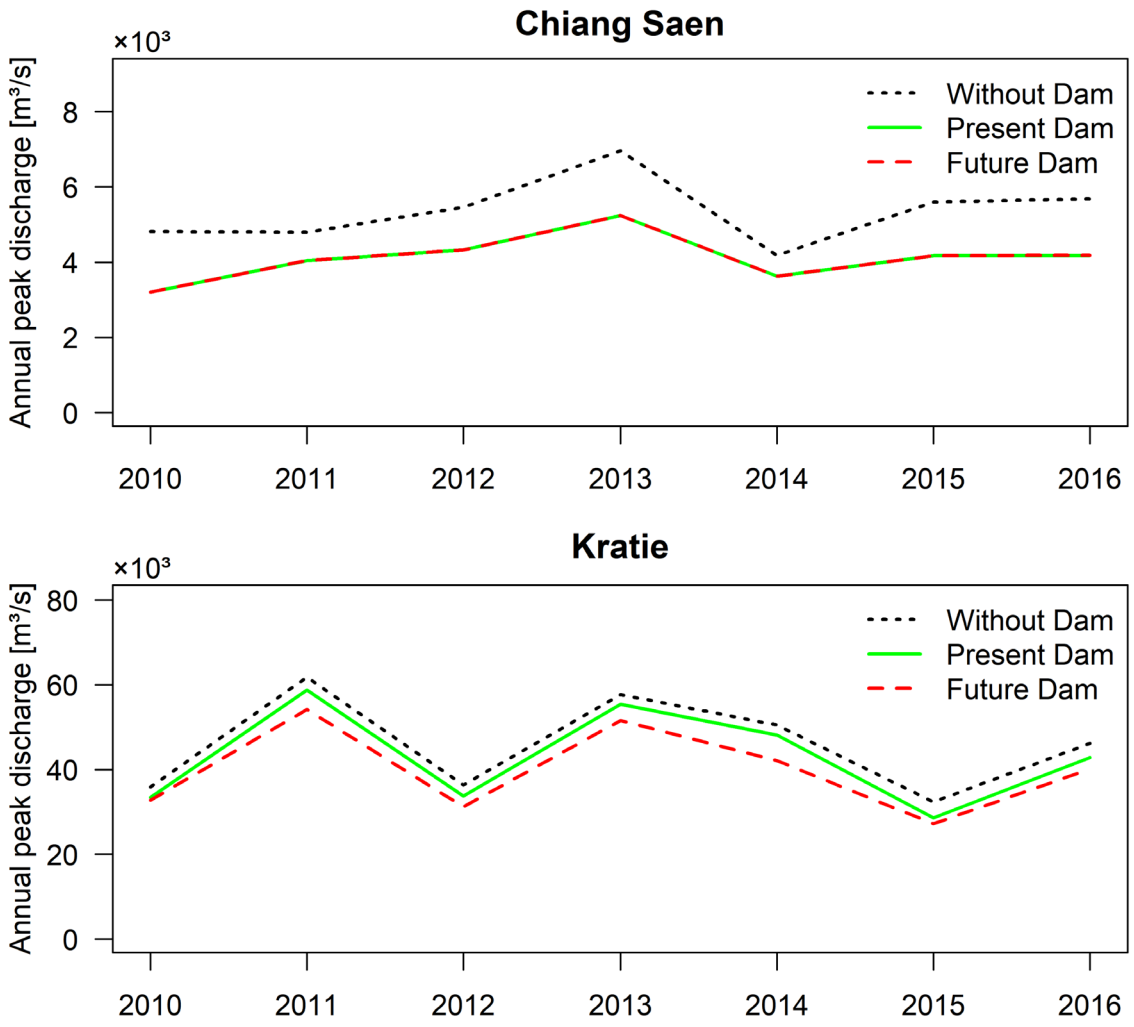

Figure 3.7 Simulated annual peak discharge at Chiang Saen and Kratie under different hydropower scenarios

3.4 Summary and Conclusion

In this chapter, we developed a simple storage model to define a reservoir operation, then incorporated it into the RRI model. We also assessed the hydrological impact of present and future hydropower development. The simulation was conducted from 2010 to 2016. The result showed that our model was capable of reproducing the discharge hydrograph in the MRB. We found that the hydropower development could impact the flow regime as far as Kratie. However, the degree of alteration would depend on the location. Relative changes in monthly discharge ranged from -17% to 40% and -16% to +100% at Chiang Saen and Kratie, respectively. Noticeably, the discharge at Kratie was significantly increased by over 40% in the dry season while decreased by about 15% in the wet season under the future hydropower development scenario. Nonetheless,

Kratie received larger impacts from the newly proposed dams compared to Chiang Saen due to its location. Further study is needed to consider both climate change and reservoir operations in order to understand broader environmental and social impacts in the MRB. This study is useful for the hydropower dam operation as well as policymakers for the sustainable development of the basin.

References

ADB. (2004). *Cumulative Impact Analysis and Nam Theun 2 Contributions - Final Report*. Asian Development Bank.

Arnold, J. G., Srinivasan, R., Muttiah, R. S., & Williams, J. R. (1998). Large Area Hydrologic Modeling and Assessment Part I: Model Development. *Journal of the American Water Resources Association*, *34*(1), 73–89. https://doi.org/10.1111/J.1752-1688.1998.TB05961.X

Boulange, J., Hanasaki, N., Yamazaki, D., & Pokhrel, Y. (2021). Role of Dams in Reducing Global Flood Exposure under Climate Change. *Nature Communications*, *12*(1), 1–7. https://doi.org/10.1038/s41467-020-20704-0

Deland, S. (2012). *Optimization in MATLAB: An Introduction to Quadtratic Program*. MATLAB Central File Exchange.

Friedl, M. A., Sulla-Menashe, D., Tan, B., Schneider, A., Ramankutty, N., Sibley, A., & Huang, X. (2010). MODIS Collection 5 Global Land Cover: Algorithm Refinements and Characterization of New Datasets. *Remote Sensing of Environment*, *114*(1), 168–182. https://doi.org/10.1016/J.RSE.2009.08.016

Ginting, B. M., Harlan, D., Taufik, A., & Ginting, H. (2017). Optimization of Reservoir Operation using Linear Program, Case Study of Riam Jerawi Reservoir, Indonesia. *International Journal of River Basin Management*, *15*(2), 187–198. https://doi.org/10.1080/15715124.2017.1298604

Hoang, L. P., van Vliet, M. T. H., Kummu, M., Lauri, H., Koponen, J., Supit, I., Leemans, R., Kabat, P., & Ludwig, F. (2019). The Mekong's Future Flows under Multiple Drivers: How Climate Change, Hydropower Developments and Irrigation Expansions Drive Hydrological Changes. *Science of the Total Environment*, *649*, 601–609. https://doi.org/10.1016/j.scitotenv.2018.08.160

Hoanh, C. T., Jirayoot, K., Lacombe, G., & Srinetr, V. (2010). *Impacts of Climate Change and Development on Mekong Flow Regimes First Assessment - 2009. MRC Technical Paper No. 29*. Mekong River Commission.

Klipsch, J. D., & Hurst, M. B. (2007). *HEC-ResSim Reservoir System Simulation User's Manual Version 3.0* (Vol. 512). US Army Corps of Engineers.

Kobayashi, S., Ota, Y., Harada, Y., Ebita, A., Moriya, M., Onoda, H., Onogi, K., Kamahori, H., Kobayashi, C., Endo, H., Miyaoka, K., & Takahashi, K. (2015). The JRA-55 reanalysis: General Specifications and Basic Characteristics. *Journal of the Meteorological Society of Japan. Ser. II*, *93*(1), 5–48. https://doi.org/10.2151/JMSJ.2015-001

Koponen, J., Lauri, H., Veijalainen, N., & Sarkkula, J. (2010). *HBV and IWRM Watershed Modelling User Guide*. Mekong River Commission.

Lauri, H., de Moel, H., Ward, P. J., Räsänen, T. A., Keskinen, M., & Kummu, M. (2012). Future Changes in Mekong River Hydrology: Impact of Climate Change and Reservoir Operation on Discharge. *Hydrology and Earth System Sciences*, *16*(12), 4603–4619. https://doi.org/10.5194/hess-16-4603-2012

MRC. (2009). *Database of the Existing, Under Construction and Planning/Proposed Hydropower Projects in the Lower Mekong Basin*. Mekong River Commission.

MRC. (2019). *The MRC Hydropower Mitigation Guidelines Vol. 1*. The Mekong River Commission.

Padiyedath Gopalan, S., Hanasaki, N., Champathong, A., & Tebakari, T. (2021). Impact Assessment of Reservoir Operation in the Context of Climate Change Adaptation in the Chao Phraya River basin. *Hydrological Processes*, *35*(1), e14005. https://doi.org/10.1002/HYP.14005

Piman, T., Lennaerts, T., & Southalack, P. (2013). Assessment of Hydrological Changes in the Lower Mekong Basin from Basin-Wide Development Scenarios. *Hydrological Processes*, *27*(15), 2115–2125. https://doi.org/https://doi.org/10.1002/hyp.9764

Räsänen, T. A., Koponen, J., Lauri, H., & Kummu, M. (2012). Downstream Hydrological Impacts of Hydropower Development in the Upper Mekong Basin. *Water Resources Management*, *26*(12), 3495–3513. https://doi.org/10.1007/s11269-012-0087-0

Sayama, T., Ozawa, G., Kawakami, T., Nabesaka, S., & Fukami, K. (2012). Rainfall–Runoff–Inundation Analysis of the 2010 Pakistan Flood in the Kabul River Basin. *Hydrological Sciences Journal*, *57*(2), 298–312. https://doi.org/10.1080/02626667.2011.644245

Try, S., Tanaka, S., Tanaka, K., Sayama, T., Oeurng, C., Uk, S., Takara, K., Hu, M., & Han, D. (2020). Comparison of Gridded Precipitation Datasets for Rainfall-Runoff and Inundation Modeling in the Mekong River Basin. *PLoS ONE*, *15*(1), e0226814. https://doi.org/10.1371/journal.pone.0226814

Yamazaki, D., Ikeshima, D., Tawatari, R., Yamaguchi, T., O'Loughlin, F., Neal, J. C., Sampson, C. C., Kanae, S., & Bates, P. D. (2017). A High-Accuracy Map of Global Terrain Elevations. *Geophysical Research Letters*, *44*(11), 5844–5853. https://doi.org/10.1002/2017GL072874

CHAPTER 4 Integrated Impact Assessment of Climate Change and Dam Operation on Streamflow and Inundation in the Mekong River Basin

4.1 Introduction

The Mekong River Basin (MRB), which originates from the Tibetan Plateau, is the largest transboundary river in Southeast Asia. With a length of approximately 4,800 km, the Mekong River travels from its source to the South China Sea, passing through six countries (upstream to downstream): China, Myanmar, Laos, Thailand, Cambodia, and Vietnam (MRC, 2005). A total catchment area of 795,000 km^2 and its river system is the livelihood of more than 70 million inhabitants, where fishery and agriculture are the main sources of income (Varis et al., 2012). The water resources of the MRB not only provide food and water to its dependents but also contribute significantly to the region's economic development. During the wet monsoon season, the unique flow reversal from the Mekong River to the Tonle Sap floodplain creates the most productive ecosystem, delivering fish and other biodiversity, sediments, and nutrients to Tonle Sap Lake (Arias et al., 2012). In addition, substantial economic development for member countries comes from hydropower development, as explained in the Strategic Plan and Basin Development of the Mekong River Commission (MRC) (MRC, 2019). The potential benefits generated from the hydropower sector alone are almost equivalent to the three major sectors of fisheries, agriculture, and navigation. In addition to electricity supply, hydropower developments could potentially expand agricultural activities during the dry season, function as flood protection during the high-flow season, and could also attract foreign investment and improve navigation systems (Intralawan et al., 2019).

Nonetheless, climate change, along with massive developments in hydropower at a rapid rate, has drastically changed the flow regime of the MRB. According to various studies, climate change is expected to alter temperature and rainfall patterns throughout the region, jeopardizing the hydrology of the basin. Using multiple general circulation models (GCM) from the Coupled

Model Intercomparison Project Phase 5 (CMIP5) climate projections, Hoang et al., (2016) analyzed the Mekong River flow under a changing climate. Seasonal and annual river discharges were found to increase (between +5% and +16%), but the degree of change depended on location. In addition, they suggested that the selection of GCM, as well as different versions of climate experiments, influenced the results of the flow changes. Try et al., (2020b) used high-resolution atmospheric general circulation model (AGCM) outputs to estimate the river flow alteration and hydrological extremes in the MRB due to changing climate. Their study estimated a 14% increase in annual precipitation and high flow (Q5) increased up to 30% at Kratie in downstream of the MRB under the high emission scenario of the representative concentration pathway (RCP8.5). Moreover, under the 4K increasing scenario from the database for Policy Decision-Making for Future Climate Change (d4PDF), Try et al., (2020a) found that increasing precipitation contributed to the severity of future extreme flood events, resulting in an increase in the flooding area and volume by nearly 40%. In addition to climate change, the MRB's water resources have been strained by the hydropower construction. Despite its benefits, such rapid developments are expected to impact water resource management and the seasonality of the flow regime. Many hydropower projects are being constructed and proposed throughout the basin, including 11 hydropower projects along the Lower Mekong Basin (LMB). Most will be completed in the next 10–20 years (Hecht et al., 2019). Several studies (Do et al., 2020; Li et al., 2017; Liu et al., 2016; Piman et al., 2013a; Räsänen et al., 2017) have studied the effects of hydropower construction on the MRB from various perspectives. The degree of impact differs from one study to another based on the study periods, dam scenarios, and reservoir operation rules. However, they share the same conclusion that reservoir operations alter river flow by increasing dry flow and decreasing wet flow. Moreover, hydropower can reduce peak flow and delay timing by up to one month (Pokhrel et al., 2018; Shin et al., 2020).

While many studies tend to focus on the individual impacts of either reservoir operations or climate change, the most important aspects of the cumulative impact of both drivers are often overlooked and not sufficiently studied, especially the impacts on flood inundation. Some studies prefer to focus on limited impacts of hydropower in only certain regions for case studies, such as the effects of hydropower construction in the Sesan, Sre Pok, and Sekong (3S) river basins (Arias et al., 2014; Piman et al., 2016; Wild & Loucks, 2014) and the effect of climate change and reservoir operation in the Upper Mekong Basin (UMB) (Han et al., 2019; Räsänen et al., 2017; Zhong et al., 2021). Motivated by this knowledge gap, the purpose of this study is to investigate the cumulative impact of climate change and hydropower operations (both existing and future hydropower projects) on flow alteration and flood inundation in the MRB using the latest Coupled

Model Intercomparison Project Phase 6 (CMIP6) climate projections. The study adopted a distributed rainfall-runoff-inundation (RRI) model coupled with a simple storage model (for reservoir operations) to simulate streamflow and inundation simultaneously for present and future climates.

4.2 Methodology

4.2.1 Rainfall-Runoff-Inundation Model Simulation

The study used the hydrologic RRI model to generate discharge and flood inundation. The two-dimensional distributed RRI model can simultaneously simulate runoff and inundation (Sayama et al., 2012). The RRI model was calibrated and validated from 2000 to 2007 at a daily time step for the MRB by Try et al. (2020c). The global optimization algorithm of the Shuffled Complex Evolution (SCE-UA) was used for the calibration process. The optimized parameter set was extracted and used in this study. For details on model calibration and validation, refer to Try et al. (2020c). The model performance was evaluated by two indicators, the Nash-Sutcliffe model Efficiency coefficient (NSE) and Coefficient of Determination (R^2):

$$NSE = 1 - \frac{\sum(Q_{sim} - Q_{obs})^2}{\sum(Q_{obs} - \overline{Q_{obs}})^2} \tag{4.1}$$

$$R^2 = \frac{\sum\left((Q_{sim} - \overline{Q_{sim}})(Q_{obs} - \overline{Q_{obs}})\right)^2}{\sum(Q_{sim} - \overline{Q_{sim}})^2 \sum(Q_{obs} - \overline{Q_{obs}})^2} \tag{4.2}$$

where Q_{obs} and Q_{sim} are the observed and simulated flow at time *t*, and $\overline{Q_{obs}}$ and $\overline{Q_{sim}}$ are the average observed and simulated flow, respectively.

The simulations were performed in two steps. First, the model was prepared for the entire MRB simulation to assess river discharge at a 2.5' resolution (≈ 5 km). Then, the finer-resolution model was set up with 1.5' (≈ 2.7 km) to simulate flood inundations in the LMB. The model input data included the precipitation, topography, land-use, evapotranspiration, and river geometry **(Table 4.1)**. Precipitation data from the Global Precipitation Climatology Centre was used for simulations (Ziese et al., 2018). Topographic data were received from the Multi-Error-Removed-Improved-Terrain digital elevation model (Yamazaki et al., 2017). Land-use data were derived from the Moderate Resolution Imaging Spectroradiometer dataset (Friedl et al., 2010). The

Table 4.1 Summary of data adopted in this study

Parameter	Resolution	Source
Precipitation	1º (≈ 120 km)	Ziese et al. (2018)
Topography	3 arc sec (≈ 90 m)	Yamazaki et al. (2017)
Land-use	500 m	Friedl et al. (2010)
Evapotranspiration	0.5625º (≈ 55 km)	Kobayashi et al. (2015)

evapotranspiration was taken from the Japanese 55-year Reanalysis database (Kobayashi et al., 2015). River geometry was estimated from the following equations:

$$D = C_D \times A^{S_D} \tag{4.3}$$

$$W = C_W \times A^{S_W} \tag{4.4}$$

where A is the upstream area [km^2], D is the river depth [m], W is the river width [m], and C_D, S_D, C_W, S_W are the river geometry parameters.

4.2.2 Hydropower Development Scenarios

The hydropower database, obtained from the MRC (MRC, 2009, 2019) and the Asian Development Bank (ADB, 2004), included existing/proposed hydropower in the LMB and Chinese dams in the UMB **(Figure 4.1)**. Two hydropower development scenarios were prepared for hydrological analysis in this study. The present development scenario consisted of 98 hydropower projects in the MRB. The future development scenario included 126 hydropower projects, including 23 mainstream dams. Because detailed operation rules are not available in the database, we estimated the general optimized patterns of the dam reservoir outflow for each dam. We used the basic information of each dam reservoir, including location, storage capacity, and turbine flow capacity, to develop the storage models, whose operation rules were estimated by optimizing their energy production considering the local flow regimes. Based on the optimized pattern, we obtained the general optimized patterns of the dam reservoir outflow. Reservoir models were then integrated into the RRI model to perform hydrological simulations. See Ly et al. (2021) for further details of the storage model incorporated in this study.

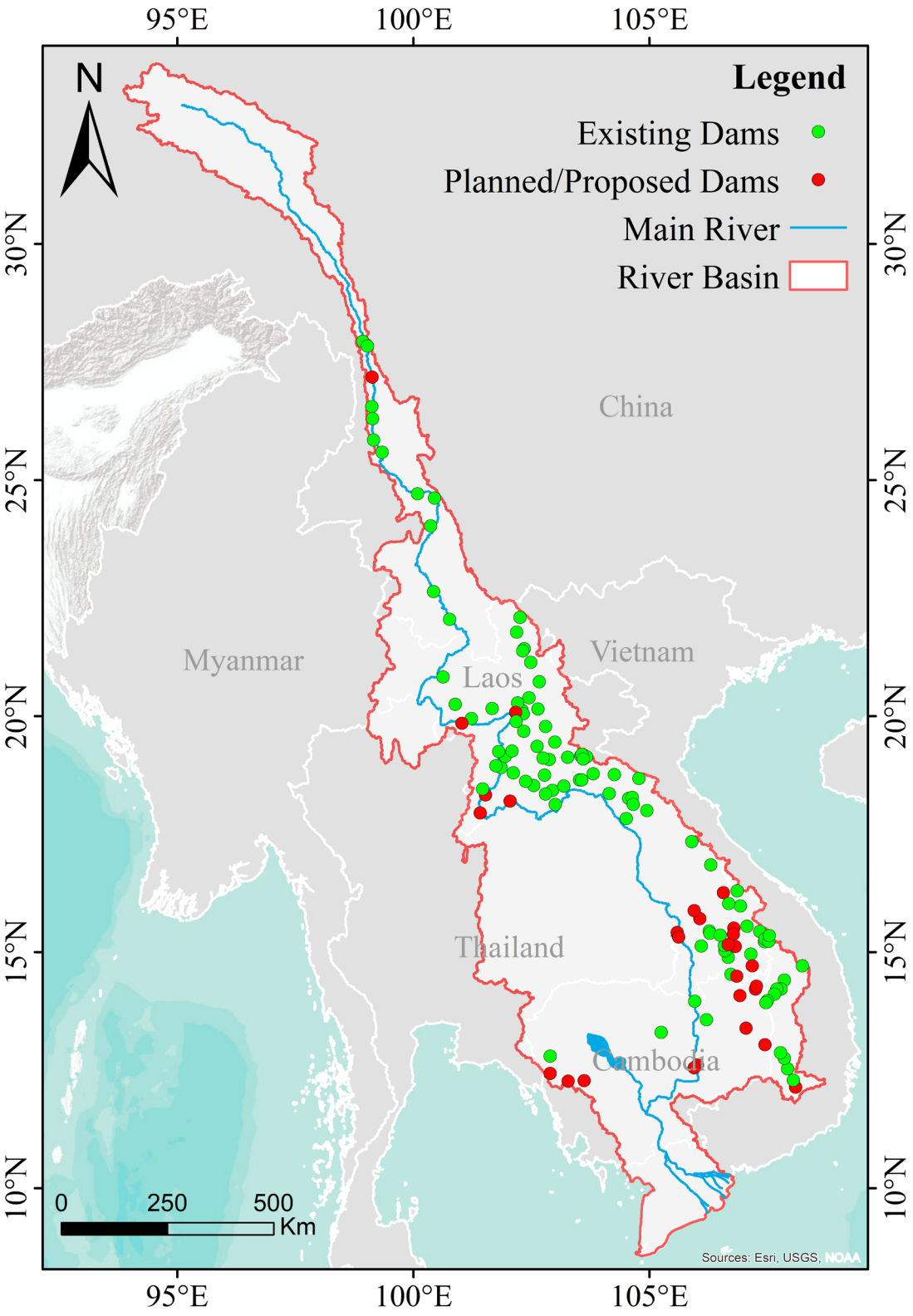

Figure 4.1 Existing and planned/proposed dams in the Mekong River basin

4.2.3 Climate Change Scenarios

General circulation models have been widely developed for climate change studies over time. The newly developed GCMs from CMIP6 promised some improvements and less bias than previous models from CMIP5 (Eyring et al., 2016; Try et al., 2022). The outputs of eight GCMs from CMIP6 were selected for this study **(Table 4.2)**. Two Share Socioeconomic Pathways (SSP) scenarios were adopted: SSP2-4.5 (middle of the road) and SSP5-8.5 (fossil-fueled development). The present period represented 1980–2014 and the future period was equally divided into three 25-year periods: near-future (2026–2050), mid-future (2051–2075), and far-future (2076–2100). Prior to further analysis, all eight GCMs were bias-corrected with GPCC precipitation using the linear scaling method:

$$P_{daily}^{BC} = P_{daily}^{gcm} \times \frac{P_{mon}^{obs}}{P_{mon}^{gcm}} \tag{4.5}$$

where P_{daily}^{BC} is the daily bias-corrected GCM precipitation, P_{daily}^{gcm} is the daily GCM precipitation, P_{mon}^{obs} is the average monthly GPCC precipitation, and P_{mon}^{gcm} is the average monthly GCM precipitation.

Table 4.2 List of the GCMs adopted in this study

Model Name	Country	Resolution (longitude × latitude in degrees)
ACCESS-CM2	Australia	1.9º × 1.3º
CNRM-CM6-1	France	1.4º × 1.4º
GFDL-CM4	United States	1.3º × 1.0º
IPSL-CM6A-LR	France	2.5º × 1.3º
MIROC6	Japan	1.4º × 1.4º
MPI-ESM1-2-LR	Germany	1.9º × 1.9º
MRI-ESM2-0	Japan	1.1º × 1.1º
NorESM2-MM	Norway	1.3º × 0.9º

4.2.4 Non-Parametric Kolmogorov-Smirnov Test

For better representations of the variation in flood extent during the study periods, a non-parametric statistical test, Kolmogorov–Smirnov (K-S), was used. The null hypothesis H_0 states that there is no significant difference in the cumulative distribution function between the two samples. The K-S test is defined using the following equation:

$$D_{n,m} = \sup_x |F_n(x) - F_m(x)| \tag{4.6}$$

When the likelihood of the two sample's different distributions exceeds a significant threshold, the null hypothesis H_0 is rejected. The two sample's different distributions are as follows:

$$D_{n,m} > c(\alpha)\sqrt{\frac{n+m}{nm}} \tag{4.7}$$

where, in Eq. (6), empirical distribution functions are denoted by $F_n(x)$ and $F_m(x)$ and supremum function is denoted by **sup**, and in both Eqs. (6) and (7), sample sizes are denoted by *n* and *m*. The value of $c(\alpha)$ is 1.36 at the 5% significance level.

4.3 Results

4.3.1 Performance of Model Simulation

The RRI model was calibrated from 2000 to 2003 and validated for the MRB from 2004 to 2007 by Try et al. (2020c). This study used the optimized parameters from the previous study to validate the RRI model again from 1985 to 2007 to confirm the model's performance for long-term simulation. Two performance indices, NSE and R^2, were calculated at the two gauging stations along the main river during the validation period. Based on the location and observed data availability, Chiang Saen (upstream) and Kratie (downstream) gauging stations were selected. **Figure 4.2** shows the observation and simulation of daily discharges during the validation period at the selected gauging stations. The performance indices at Chiang Saen were NSE = 0.53 and R^2 = 0.71. At Kratie, the model performance was better, with NSE = 0.89 and R^2 = 0.89. On the other hand, the observed and simulated monthly discharge was also compared during the validation period since this study analyzed the flow alteration at monthly and seasonal scales **(Figure 4.3)**. The model performance for Chiang Saen was NSE = 0.61 and R^2 = 0.82, while the

model performance for the downstream station of Kratie was NSE = 0.94 and R^2 = 0.94. The results indicated good agreement between the observation and simulation, particularly in the downstream region of the LMB. Thus, the RRI model was applied for further flood simulations in the LMB under climate change and hydropower operation. For the upper Mekong area (Chiang Saen), we mostly looked at flow alteration at monthly and seasonal scales, as the model performance in simulating monthly discharge was better.

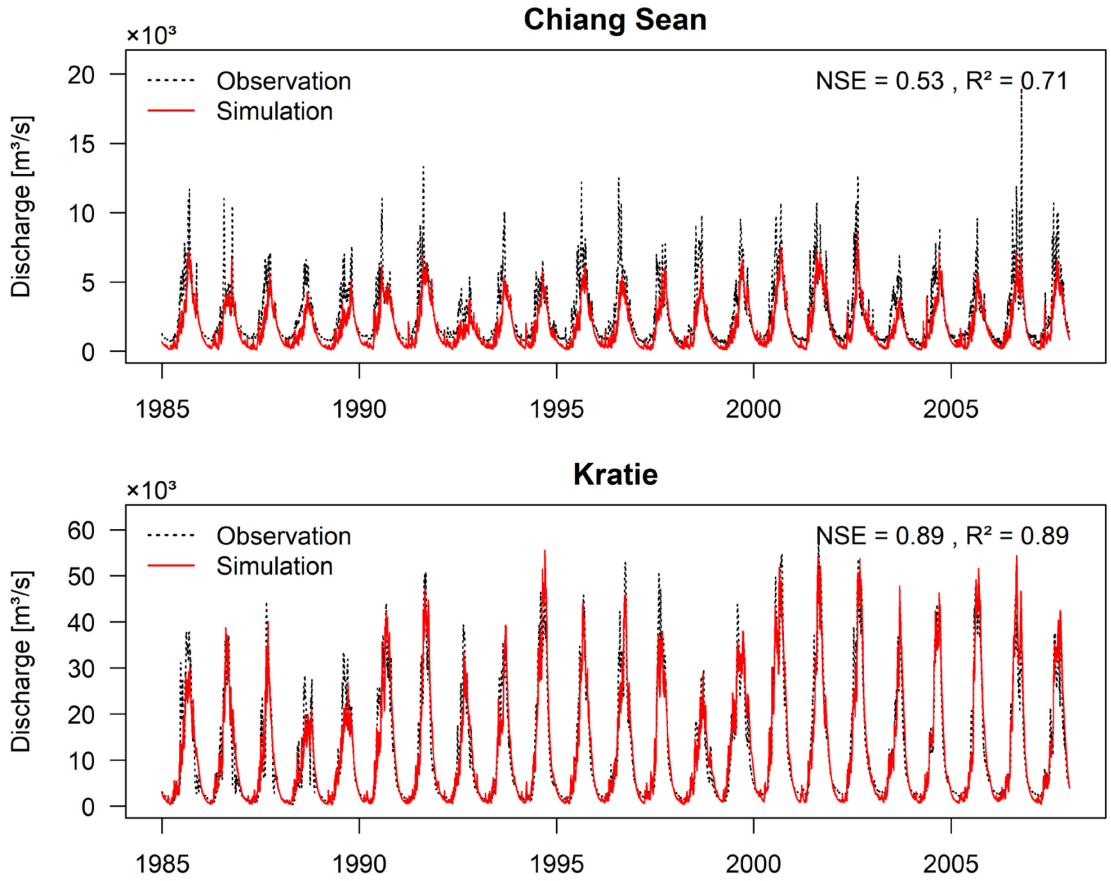

Figure 4.2 Observed and simulated daily discharges during the validation period (1985–2007) at Chiang Saen and Kratie

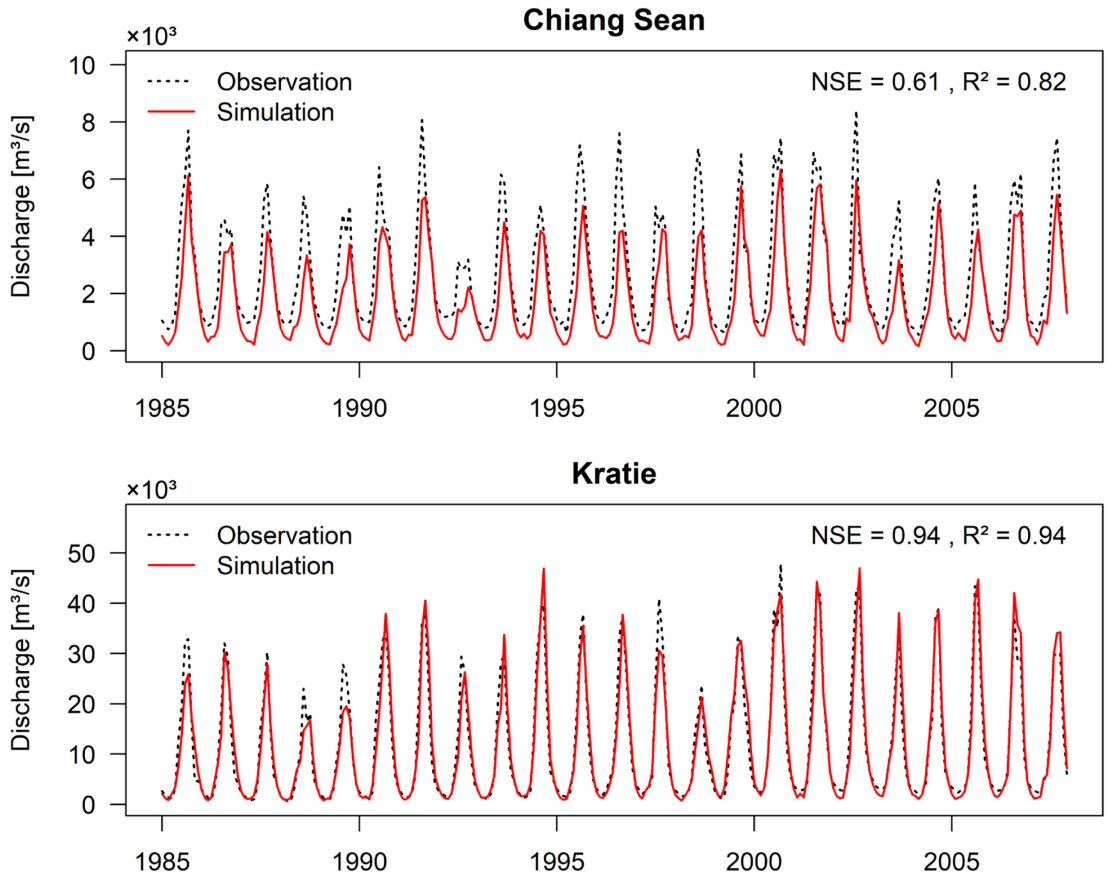

Figure 4.3 Observed and simulated monthly discharges during the validation period (1985–2007) at Chiang Saen and Kratie

4.3.2 Impacts of Hydropower on River Discharge

The impacts of hydropower were assessed by the RRI model using GPCC precipitation from 1982 to 2016 with two hydropower development scenarios. The same two hydrological stations along the MRB mainstream, Chiang Saen and Kratie, were selected to analyze the flow changes. **Figure 4.4** shows the relative changes in monthly average discharges at Chiang Saen and Kratie over the last three decades under present and future hydropower scenarios. Under the present hydropower scenarios (98 dams), the relative changes in monthly discharges at Chiang Saen and Kratie ranged from -22% to +102% and -7% to 55%, respectively. The newly proposed dams in the future hydropower scenario further altered the monthly average discharges at both stations. Under the future hydropower scenario, significant changes were observed at Kratie rather than at Chiang Saen; for instance, relative changes in February discharges doubled from the present scenario. A similar tendency was also observed in the wet months, including August and September. **Figure 4.5** presents the relative changes in the average discharges during the dry season (November–

April), wet season (May–October), and annual peak. At Kratie, dry flow increased by 14% while wet flow decreased by 5% under the present hydropower scenario, but it doubled to 28% and -10% in the future scenario, respectively. At Chiang Saen, dry flow increased by 36% and wet flow decreased by 17% under both hydropower scenarios (i.e., there was no significant difference in discharge changes between the hydropower scenarios at Chiang Saen). In addition, future hydropower reduced annual average peak discharges by 30% at Chiang Saen and 13% at Kratie.

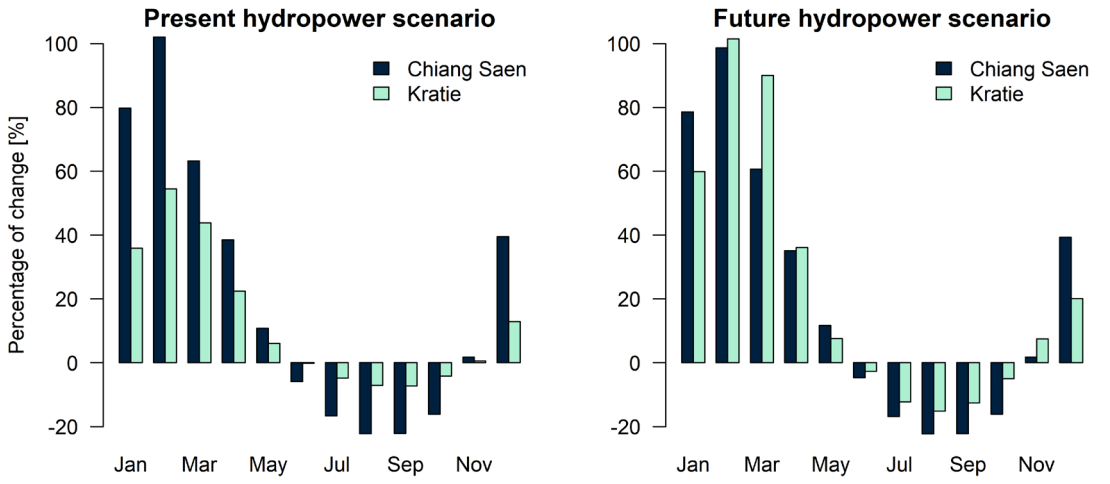

Figure 4.4 Relative changes in monthly discharges under hydropower scenarios

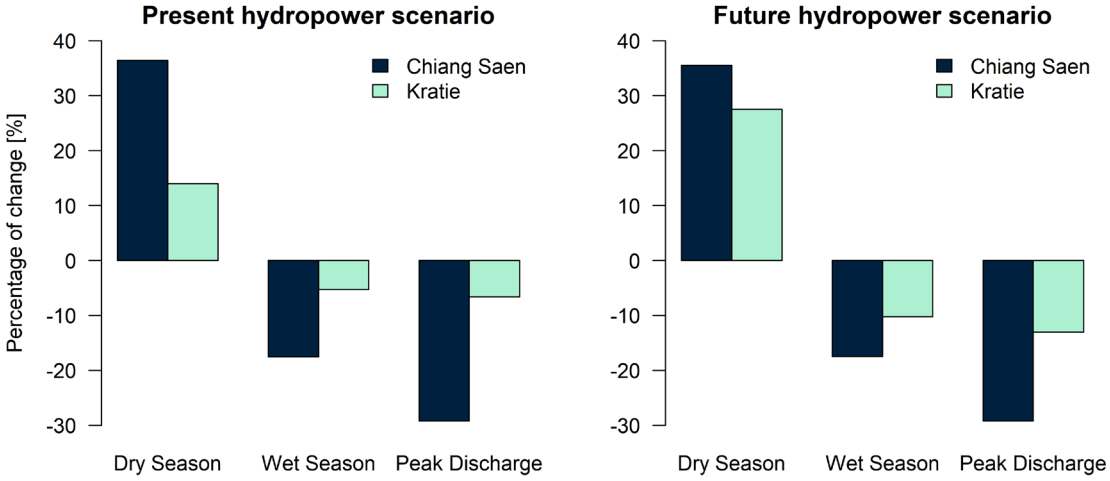

Figure 4.5 Relative changes in flow characteristics (seasonal flow and peak discharge) under different hydropower scenarios

4.3.3 Impacts of Climate Change on River Discharge

The eight GCMs from CMIP6 projections **(**recall **Table 4.2)** were used to analyze the impacts of climate change on river flow alteration. The model simulated river discharges for the present climate (1980–2014) and future climate (2026–2100) using two SSP scenarios (SSP2-4.5 and SSP5-8.5). **Figure 4.6** presents the simulated seasonal discharges under climate change scenarios at Chiang Saen and Kratie. For better representation of temporal changes in discharges, the future period was divided into three timeframes. The results showed a substantial increase both upstream (at Chiang Saen) and downstream (at Kratie). Despite the general increasing trend, the SSP5-8.5 scenario had more variation between GCMs, especially in the far-future (2076–2100), compared with the SSP2-4.5 scenario. The changes in seasonal discharges became more significant in the far-future at all stations during both the dry and wet seasons. Under the SSP5-8.5, the dry season discharges at Chiang Saen and Kratie increased from 4% and 10% in the near-future to 20% and 27% in the far-future, respectively. Discharge changes were slightly greater during the wet season

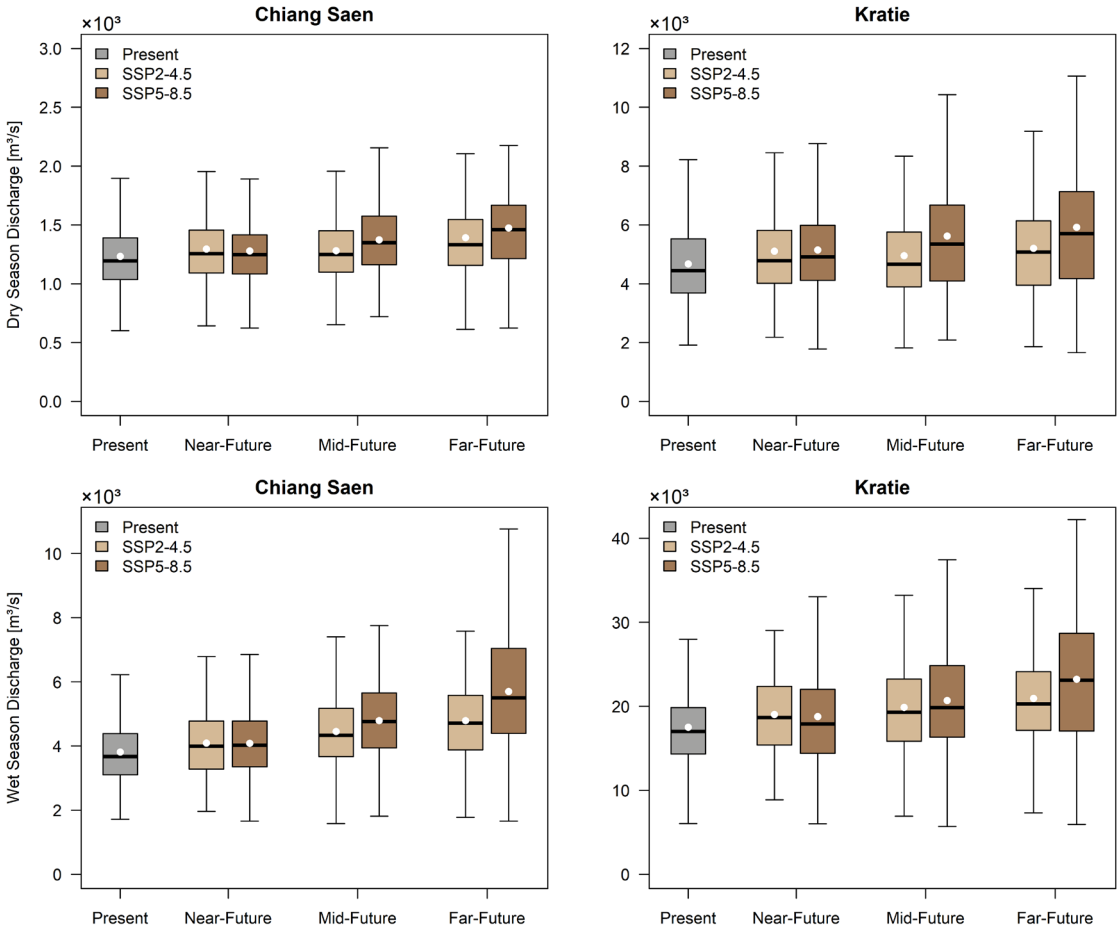

Figure 4.6 Simulated discharges in the dry season (top) and wet season (bottom) under present climate and projected future climate scenarios

than those in the dry season. It increased from 7% (7%) in the near-future to 49% (33%) in the far-future at Chiang Saen (Kratie). Overall, the degree of climate change impacts increased with the future timeframe (i.e., near-future < mid-future < far-future). On the other hand, peak discharges were computed and analyzed on the annual timescale for both present and future conditions. The time-series of the simulated annual peak discharges under climate change scenarios (SSP2-4.5 and SSP5-8.5) from 1980 to 2100 is presented in **Figure 4.7**. There was a noticeable increase in peak discharges in the far-future, especially under the SSP5-8.5 scenario. In comparison with the present condition, the peak discharges in the far-future at Chiang Saen and Kratie increased by an average of 50% and 43%, respectively. These increases in peak discharges would lead to a surge in flooded areas in the LMB.

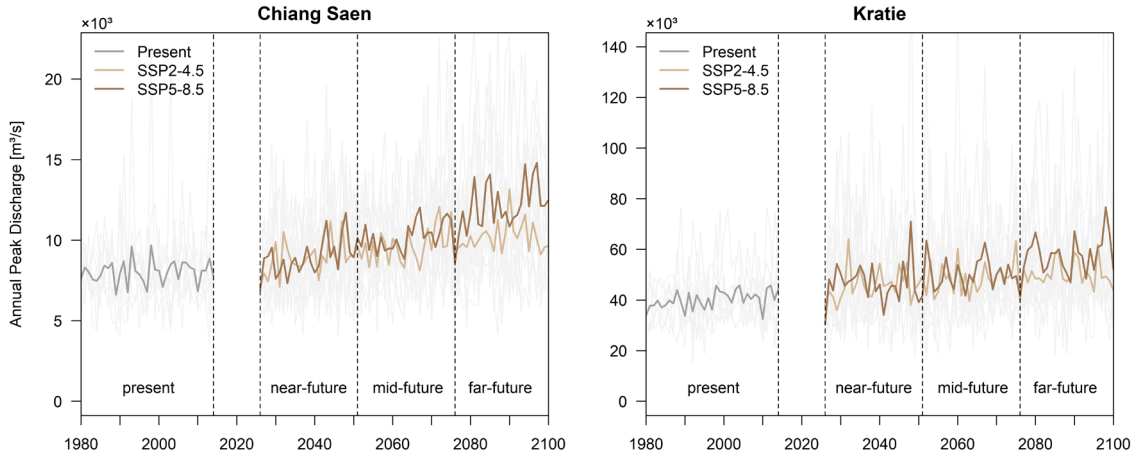

Figure 4.7 Time-series of simulated annual peak discharges from 1980 to 2100 under climate change

4.3.4 Cumulative Impacts of Hydropower and Climate Change on River Discharge

Using the RRI model, the cumulative impacts of hydropower and climate change on flow alteration were assessed on a seasonal timescale. Future changes were analyzed in three different timeframes: near-future, mid-future, and far-future. Overall, the seasonal discharges showed noticeable changes at all stations, but the direction and degree of changes differed between the seasons. At Chiang Saen, no significant changes in discharges were detected between the two hydropower development scenarios due to the fact that there is no newly proposed dam in the upper part of this station. **Figure 4.8** shows the simulated seasonal discharges under reservoir operations and climate change (SSP5-8.5) at Chiang Saen and Kratie. Discharges increased gradually from time to time during the dry season. The impacts can be seen clearly at both stations,

where reservoir operations (especially the future dam scenario) further increased the discharges in addition to climate change. Under future hydropower and climate change (SSP5-8.5 scenario), the relative changes in average dry flow at Chiang Saen and Kratie in the far-future increased by up to 60% and 61%, respectively. On the contrary, during the wet season, climate change substantially increased the discharge, while reservoir operations tended to reduce the effect of climate change by decreasing the discharge. Nevertheless, reservoir operations have not been able to fully diminish the effects of climate change. Consequently, it was still noticeable at both stations. Under climate change only (SSP5-8.5 scenario), the relative change in average wet flow at Chiang Saen and Kratie in the far-future increased by up to 49% and 33%, respectively. However, future hydropower will reduce the total changes to 32% and 19%, respectively. Although the effects of climate change dominated reservoir operations in most scenarios, there were exceptional cases in the near-future. Under climate change only (SSP5-8.5), the average wet flow at Chiang Saen and Kratie increased by up to 7% (both stations); nonetheless, it was reduced

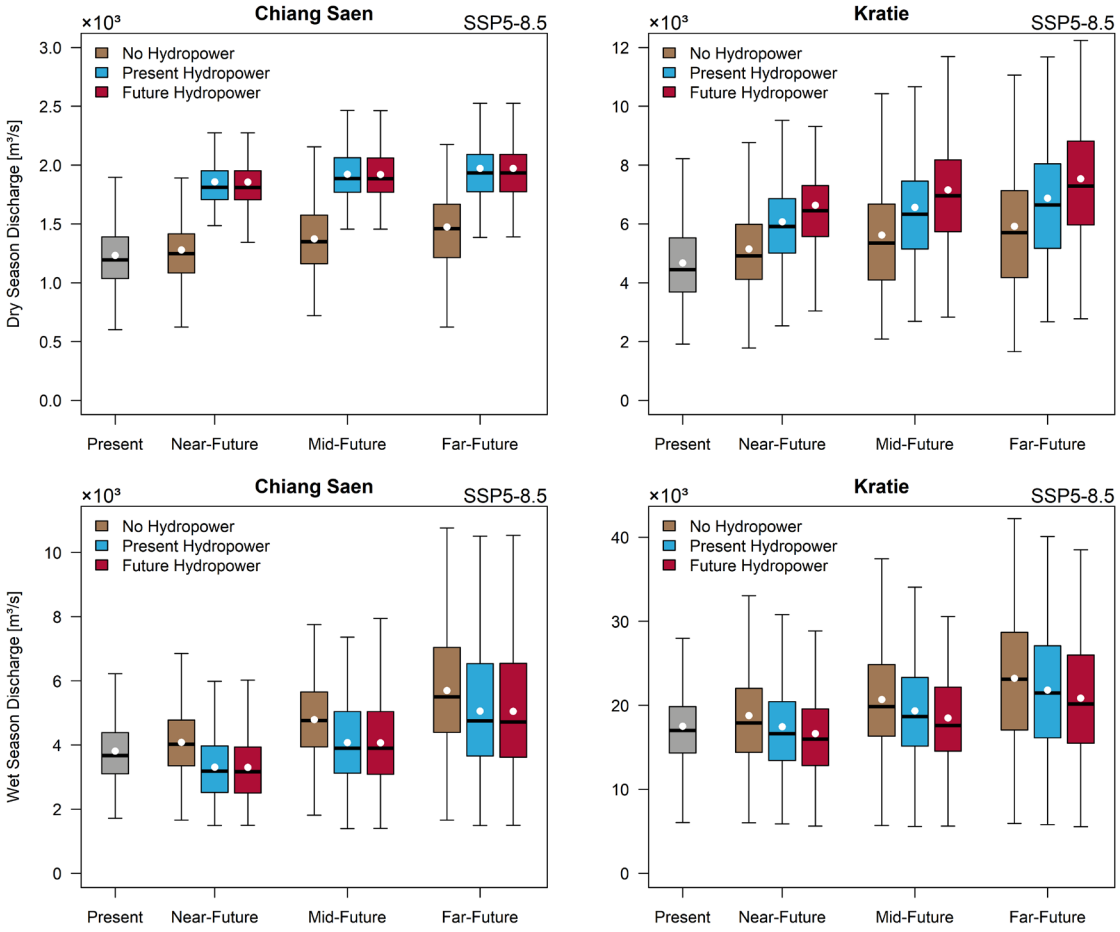

Figure 4.8 Simulated discharges in the dry season (top) and wet season (bottom) under reservoir operations and climate change (SSP5-8.5)

to -13% and -5%, respectively under combined impacts **(Table 4.3b)**. In the annual peak discharge, some compromise occurred between reservoir operations and climate change to some degree. A time-series of annual peak discharge at Chiang Saen and Kratie under combined impacts is presented in **Figure 4.9**. Depending on the scenarios, time frame, and location, the findings indicate that hydropower construction could mitigate climate change effects, as summarized in **Table 4.3a–Table 4.3c**.

Table 4.3a Summary of relative changes of dry season discharges under climate change and cumulative impacts

Dry season		Chiang Saen		Kratie	
		CC	Combined	CC	Combined
Near-future	SSP2-4.5	5%	52%	9%	41%
	SSP5-8.5	4%	51%	10%	42%
Mid-future	SSP2-4.5	4%	50%	6%	39%
	SSP5-8.5	11%	56%	20%	53%
Far-future	SSP2-4.5	13%	56%	11%	45%
	SSP5-8.5	20%	60%	27%	61%

Note: The combined impact was calculated with the future hydropower development scenario

Table 4.3b Summary of relative changes of wet season discharges under climate change and cumulative impacts

Wet season		Chiang Saen		Kratie	
		CC	Combined	CC	Combined
Near-future	SSP2-4.5	7%	-13%	9%	-4%
	SSP5-8.5	7%	-13%	7%	-5%
Mid-future	SSP2-4.5	17%	-3%	14%	1%
	SSP5-8.5	26%	7%	18%	6%
Far-future	SSP2-4.5	26%	6%	20%	6%
	SSP5-8.5	49%	32%	33%	19%

Note: The combined impact was calculated with the future hydropower development scenario

Table 4.3c Summary of relative changes of annual peak discharges under climate change and cumulative impacts

Peak discharge		Chiang Saen		Kratie	
		CC	Combined	CC	Combined
Near-future	SSP2-4.5	10%	-2%	14%	1%
	SSP5-8.5	11%	-2%	16%	3%
Mid-future	SSP2-4.5	20%	10%	21%	8%
	SSP5-8.5	28%	18%	23%	12%
Far-future	SSP2-4.5	27%	19%	25%	11%
	SSP5-8.5	50%	44%	43%	29%

Note: The combined impact was calculated with the future hydropower development scenario

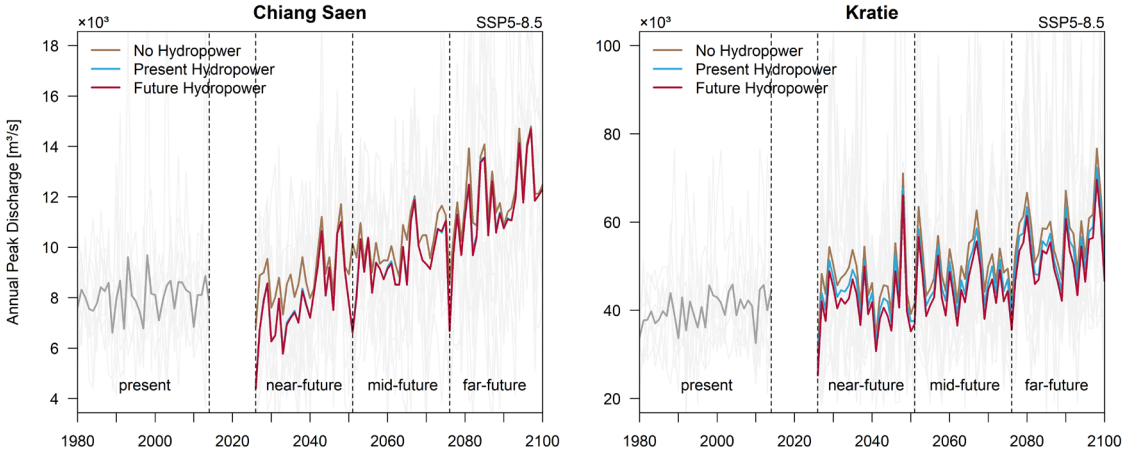

Figure 4.9 Time-series of simulated annual peak discharges from 1980 to 2100 under reservoir operations and climate change (SSP5-8.5)

4.3.5 Cumulative Impacts of Hydropower and Climate Change on Flood Extent

Flooding is one of the most important characteristics of the MRB because its floodplain creates remarkable biodiversity in the LMB. To further understand the effects of reservoir operations and climate change projections on the flood extent in the LMB, simulations were performed at a finer resolution of 1.5' (≈ 2.7 km). A water depth threshold of 0.5 m was chosen to distinguish between inundated and non-inundated areas. Moreover, the K-S test was conducted to determine the significant difference in flood variation during the study periods. The results showed an increase

in flood extent for all scenarios, ranging from +2% to +37%, compared to the present condition **(Table 4.4)**. **Figure 4.10** shows the changes in flood extent in the present and future conditions under hydropower development scenarios and climate change projections (SSP5-8.5). The largest relative changes occurred under the climate change only scenario in the far-future, up to +37%. The smallest relative changes were observed under the combined impacts in the near-future, at +2%. Hydropower plays a significant role in reducing the flood inundation in the LMB, although the climate change effects remain to some degree.

The results of the K-S test are shown in **Table 4.4**. The test showed significant differences for most scenarios at a significance level of 5% ($p < 0.05$), except for scenarios in the near-future, showing no significant difference ($p > 0.05$) between present and future conditions.

Table 4.4 Changes in flood inundation area and the K-S test results under climate change and cumulative impacts

Scenarios	Present	Near-future	Mid-future	Far-future
Climate Change	23,299 km^2	26,341 km^2 (+13%)*	28,291 km^2 (+21%)*	31,853 km^2 (+37%)*
Climate Change + Existing Dam		24,720 km^2 (+6%)	26,813 km^2 (+15%)*	30,568 km^2 (+31%)*
Climate Change + Future Dam		23,762 km^2 (+2%)	25,887 km^2 (+11%)*	29,649 km^2 (+27%)*

* Significant at the 95% confidence interval

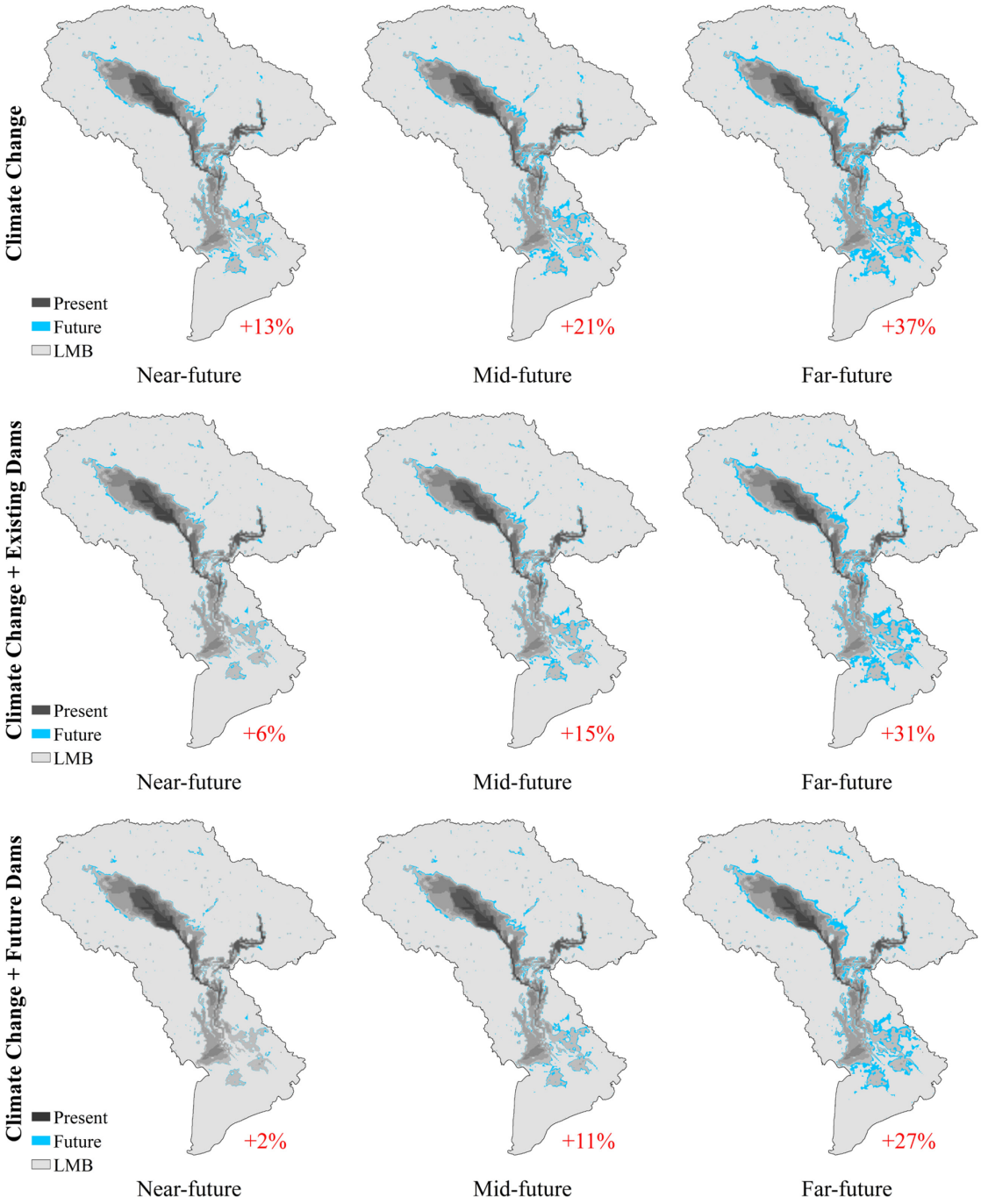

Figure 4.10 Comparison of inundated areas under different hydropower development and climate change scenarios (SSP5-8.5)

4.4 Discussion

This study investigated the seasonal flow and flood extents caused by the impacts of future climate change and reservoir operations in the MRB using the RRI model with CMIP6 GCMs. Various bias-corrected GCMs with different emission scenarios were considered to provide more robust and less uncertain results.

4.4.1 Main Findings

Our results suggested that reservoir operations substantially change the seasonal flow in the MRB, particularly under future hydropower development scenarios. The simulation results of the reservoir operations indicated an increase in dry seasonal flow and a decrease in wet seasonal flow at the two investigated stations. Flow alteration was detected from the upstream (Chiang Saen) to the downstream (Kratie). Under reservoir operations, the dry flow alteration started as early as December (early dry season), while the largest relative changes occurred in February. These changes could reduce water shortage issues and potentially increase agricultural activities for local residents. Our findings are in agreement with those of other studies (Hoang et al., 2019; Hoanh et al., 2010; Piman et al., 2013b), although the degree of change is slightly different between studies owing to boundary conditions, the choice of hydrologic model, operation conditions, and the study period. Under the future hydropower development scenario, our study projected a 28% increase in dry flow and a 10% decrease in wet flow at Kratie. Piman et al. (2013b) estimated increases of 29% and decreases of 13%, respectively.

Flow regimes are expected to change as a result of climate change, as reported in our study and many others (Han et al., 2019; Hoang et al., 2019; Ngo et al., 2018; Try et al., 2020a, 2020b). In addition, water resources are changing on a global scale, including the MRB. It is projected to alter the intensity and pattern of precipitation and evaporation, thus affecting runoff at the local scale (IPCC, 2007). Our findings from the eight CMIP6 GCMs suggested that climate change increased seasonal discharge and annual peak in all scenarios (SSP2-4.5 and SSP5-8.5) until the end of the century. On the other hand, reservoir operation reduced the effect of climate change by decreasing wet seasonal discharge and annual peak discharge across all scenarios and timeframes. In terms of the direction of the flow alterations, our results are in line with those of Lauri et al. (2012), Hoang et al. (2019), and Yun et al. (2020). Under combined drivers, dry, wet, and peak flows under SSP5-8.5, in the far-future at Kratie, increased up to 61%, 19%, and 29%,

respectively. Although there were some compromises between the two main drivers, climate change remained the dominant factor for flow alteration in the MRB.

In addition, our findings showed that climate change would trigger flood risk in the LMB under all scenarios by increasing the inundated area by up to 37% at the end of the century. Using AGCM outputs, Try et al. (2020b) found that climate change increased the inundated area in the LMB from 19% to 43%. Wang et al. (2017) highlighted significant increases in the mean annual maximum flood and flood frequency over the Mekong region, particularly in the lower basin. Perera et al. (2017) applied different projections of RCP8.5, with four SST boundary conditions to emphasize the severity of flooding and agricultural damage in the LMB. These studies agree with our findings regarding the direction and magnitude of these changes. Apart from climate change, reservoir operation is another aspect to consider when analyzing flood extent in the MRB. Yun et al. (2020) analyzed the changes in flood magnitude and frequency under changing climate and hydropower construction. Their study suggested some benefits of hydropower in eliminating flood risk, but their study period for climate change was between 2008 and 2016. In addition to existing studies, our study analyzed the cumulative impact of reservoir operations and climate change to the end of the century and highlighted the important role of hydropower in reducing the effect of climate change over the Mekong region. Moreover, this study adopted the latest climate projection dataset from CMIP6, with different SSP scenarios. Our findings indicated that hydropower development, especially future hydropower dams, could effectively reduce the flood magnitude in the flood prone areas of the LMB. The study further evaluated the significance of flood risk using statistical analysis. As a result, the changes in the inundated area were shown to be significant in most scenarios, except in the near-future timeframe.

4.4.2 Limitations

This study assessed the impacts of climate change and reservoir operations using a hydrologic model. However, several aspects, including irrigation water withdrawal and land-use change, were not considered. Future studies should include these drivers to provide a broader perspective on the changes in the hydrology of the MRB. However, owing to the limited information on reservoir operation rules, our study assumed that all hydropower is operated to maximize energy production. In actual operation, hydropower may have multiple functions, including drought relief, ecological sustainability, flood control, sediment control, and water supply. Therefore, different reservoir operation scenarios should be considered in future studies. The simulations of flood inundation were carried out at a spatial resolution of 2.7 km owing to the computational capacity. A finer resolution would provide more accurate predictions. Finally, this study adopted bias-

corrected global GCMs from the CMIP6 projections. Regional climate models or downscaled GCMs may provide better predictions of rainfall patterns.

4.5 Summary and Conclusion

This chapter assessed changes in river discharge and flood inundation induced by hydropower construction and climate change in the MRB using a hydrologic RRI model coupled with a reservoir operation model. This study adopted bias-corrected CMIP6 GCMs to analyze the changes in dry seasonal flow, wet seasonal flow, annual peak discharges, and flood extent for the present period (1980–2014) and future period (2026–2100). Our results indicated noticeable changes in seasonal flow and highlighted the important role of hydropower in reducing annual peak discharges, thus mitigating the flood risk in the LMB. Climate change has forcefully modified the flow regime from a monthly to an annual scale. The seasonal discharge and annual peak discharge increased considerably in all climate change scenarios. The largest changes were observed in the far-future under the high-emission scenario (SSP5-8.5). During the wet season, discharge at Kratie increased by 7% in the near-future and by 33% in the far-future; nonetheless, the flow changes under cumulative impacts decreased to -5% and 19%, respectively. Despite the effect of reservoir operations, climate change remained the dominant contributor to hydrological changes in the MRB. However, the magnitude of the impact varied between timeframes (i.e., near-, mid-, and far-future) and hydropower operations. This study provides concrete insights and broader perspectives for understanding the future hydrological alterations in the Mekong region.

References

ADB. (2004). *Cumulative Impact Analysis and Nam Theun 2 Contributions - Final Report*. Asian Development Bank.

Arias, M. E., Cochrane, T. A., Piman, T., Kummu, M., Caruso, B. S., & Killeen, T. J. (2012). Quantifying Changes in Flooding and Habitats in the Tonle Sap Lake (Cambodia) Caused by Water Infrastructure Development and Climate Change in the Mekong Basin. *Journal of Environmental Management*, *112*, 53–66. https://doi.org/10.1016/j.jenvman.2012.07.003

Arias, M. E., Piman, T., Lauri, H., Cochrane, T. A., & Kummu, M. (2014). Dams on Mekong Tributaries as Significant Contributors of Hydrological Alterations to the Tonle Sap Floodplain in Cambodia. *Hydrology and Earth System Sciences*, *18*(12), 5303–5315. https://doi.org/10.5194/hess-18-5303-2014

Do, P., Tian, F., Zhu, T., Zohidov, B., Ni, G., Lu, H., & Liu, H. (2020). Exploring Synergies in the Water-Food-Energy Nexus by using an Integrated Hydro-Economic Optimization Model for the Lancang-Mekong River Basin. *Science of The Total Environment*, *728*, 137996. https://doi.org/10.1016/j.scitotenv.2020.137996

Eyring, V., Bony, S., Meehl, G. A., Senior, C. A., Stevens, B., Stouffer, R. J., & Taylor, K. E. (2016). Overview of the Coupled Model Intercomparison Project Phase 6 (CMIP6) Experimental Design and Organization. *Geoscientific Model Development*, *9*(5), 1937–1958. https://doi.org/10.5194/GMD-9-1937-2016

Friedl, M. A., Sulla-Menashe, D., Tan, B., Schneider, A., Ramankutty, N., Sibley, A., & Huang, X. (2010). MODIS Collection 5 Global Land Cover: Algorithm Refinements and Characterization of New Datasets. *Remote Sensing of Environment*, *114*(1), 168–182. https://doi.org/10.1016/J.RSE.2009.08.016

Han, Z., Long, D., Fang, Y., Hou, A., & Hong, Y. (2019). Impacts of Climate Change and Human Activities on the Flow Regime of the Dammed Lancang River in Southwest China. *Journal of Hydrology*, *570*, 96–105. https://doi.org/10.1016/J.JHYDROL.2018.12.048

Hecht, J. S., Lacombe, G., Arias, M. E., Dang, T. D., & Piman, T. (2019). Hydropower Dams of the Mekong River Basin: A Review of Their Hydrological Impacts. *Journal of Hydrology*, *568*, 285–300. https://doi.org/10.1016/j.jhydrol.2018.10.045

Hoang, L. P., Lauri, H., Kummu, M., Koponen, J., van Vliet, M. T. H., Supit, I., Leemans, R., Kabat, P., & Ludwig, F. (2016). Mekong River Flow and Hydrological Extremes under Climate Change. *Hydrology and Earth System Sciences*, *20*(7), 3027–3041. https://doi.org/10.5194/hess-20-3027-2016

Hoang, L. P., van Vliet, M. T. H., Kummu, M., Lauri, H., Koponen, J., Supit, I., Leemans, R., Kabat, P., & Ludwig, F. (2019). The Mekong's Future Flows under Multiple Drivers: How Climate Change, Hydropower Developments and Irrigation Expansions Drive Hydrological Changes. *Science of the Total Environment*, *649*, 601–609. https://doi.org/10.1016/j.scitotenv.2018.08.160

Hoanh, C. T., Jirayoot, K., Lacombe, G., & Srinetr, V. (2010). *Impacts of Climate Change and Development on Mekong Flow Regimes First Assessment - 2009. MRC Technical Paper No. 29*. Mekong River Commission.

Intralawan, A., Smajgl, A., McConnell, W., Ahlquist, D. B., Ward, J., & Kramer, D. B. (2019). Reviewing Benefits and Costs of Hydropower Development Evidence From the Lower Mekong River Basin. *WIREs Water*, *6*(4), e1347. https://doi.org/10.1002/WAT2.1347

IPCC. (2007). *The Physical Science Basis: Working Group I Contribution to the Fourth Assessment Report of the Intergovernmental Panel on Climate Change* (Vol. 4). IPCC.

Kobayashi, S., Ota, Y., Harada, Y., Ebita, A., Moriya, M., Onoda, H., Onogi, K., Kamahori, H., Kobayashi, C., Endo, H., Miyaoka, K., & Takahashi, K. (2015). The JRA-55 reanalysis: General Specifications and Basic Characteristics. *Journal of the Meteorological Society of Japan. Ser. II*, *93*(1), 5–48. https://doi.org/10.2151/JMSJ.2015-001

Lauri, H., de Moel, H., Ward, P. J., Räsänen, T. A., Keskinen, M., & Kummu, M. (2012). Future Changes in Mekong River Hydrology: Impact of Climate Change and Reservoir Operation on Discharge. *Hydrology and Earth System Sciences*, *16*(12), 4603–4619. https://doi.org/10.5194/hess-16-4603-2012

Li, D., Long, D., Zhao, J., Lu, H., & Hong, Y. (2017). Observed Changes in Flow Regimes in the Mekong River Basin. *Journal of Hydrology*, *551*, 217–232. https://doi.org/10.1016/j.jhydrol.2017.05.061

Liu, K. T., Tseng, K. H., Shum, C. K., Liu, C. Y., Kuo, C. Y., Liu, G., Jia, Y., & Shang, K. (2016). Assessment of the Impact of Reservoirs in the Upper Mekong River using Satellite Radar

Altimetry and Remote Sensing Imageries. *Remote Sensing*, *8*(5), 367. https://doi.org/10.3390/RS8050367

Ly, S., Try, S., & Sayama, T. (2021). Hydrological Changes in the Mekong River Basin Under Future Hydropower Developments and Reservoir Operations. *Journal of Japan Society of Civil Engineers, Ser. B1 (Hydraulic Engineering)*, *77*(2), 259–264. https://doi.org/10.2208/jscejhe.77.2_I_259

MRC. (2005). *Overview of the Hydrology of the Mekong Basin*. The Mekong River Commission.

MRC. (2009). *Database of the Existing, Under Construction and Planning/Proposed Hydropower Projects in the Lower Mekong Basin*. Mekong River Commission.

MRC. (2019). *The MRC Hydropower Mitigation Guidelines Vol. 1*. The Mekong River Commission.

Ngo, L. A., Masih, I., Jiang, Y., & Douven, W. (2018). Impact of Reservoir Operation and Climate Change on the Hydrological Regime of the Sesan and Srepok Rivers in the Lower Mekong Basin. *Climatic Change*, *149*(1), 107–119. https://doi.org/10.1007/S10584-016-1875-Y

Perera, E. D. P., Sayama, T., Magome, J., Hasegawa, A., & Iwami, Y. (2017). RCP8.5-Based Future Flood Hazard Analysis for the Lower Mekong River Basin. *Hydrology*, *4*(4), 55. https://doi.org/10.3390/HYDROLOGY4040055

Piman, T., Cochrane, T. A., & Arias, M. E. (2016). Effect of Proposed Large Dams on Water Flows and Hydropower Production in the Sekong, Sesan and Srepok Rivers of the Mekong Basin. *River Research and Applications*, *32*(10), 2095–2108. https://doi.org/10.1002/rra.3045

Piman, T., Cochrane, T. A., Arias, M. E., Green, A., & Dat, D. N. (2013a). Assessment of Flow Changes from Hydropower Development and Operations in Sekong, Sesan, and Srepok Rivers of the Mekong Basin. *Journal of Water Resources Planning and Management*, *139*(6), 723–732. https://doi.org/10.1061/(ASCE)WR.1943-5452.0000286

Piman, T., Lennaerts, T., & Southalack, P. (2013b). Assessment of Hydrological Changes in the Lower Mekong Basin from Basin-Wide Development Scenarios. *Hydrological Processes*, *27*(15), 2115–2125. https://doi.org/https://doi.org/10.1002/hyp.9764

Pokhrel, Y., Shin, S., Lin, Z., Yamazaki, D., & Qi, J. (2018). Potential Disruption of Flood

Dynamics in the Lower Mekong River Basin due to Upstream Flow Regulation. *Scientific Reports*, *8*(1), 17767. https://doi.org/10.1038/s41598-018-35823-4

Räsänen, T. A., Someth, P., Lauri, H., Koponen, J., Sarkkula, J., & Kummu, M. (2017). Observed River Discharge Changes due to Hydropower Operations in the Upper Mekong Basin. *Journal of Hydrology*, *545*, 28–41. https://doi.org/10.1016/j.jhydrol.2016.12.023

Sayama, T., Ozawa, G., Kawakami, T., Nabesaka, S., & Fukami, K. (2012). Rainfall–Runoff–Inundation Analysis of the 2010 Pakistan Flood in the Kabul River Basin. *Hydrological Sciences Journal*, *57*(2), 298–312. https://doi.org/10.1080/02626667.2011.644245

Shin, S., Pokhrel, Y., Yamazaki, D., Huang, X., Torbick, N., Qi, J., Pattanakiat, S., Ngo-Duc, T., & Nguyen, T. D. (2020). High Resolution Modeling of River-Floodplain-Reservoir Inundation Dynamics in the Mekong River Basin. *Water Resources Research*, *56*(5), e2019WR026449. https://doi.org/10.1029/2019WR026449

Try, S., Tanaka, S., Tanaka, K., Sayama, T., Hu, M., Sok, T., & Oeurng, C. (2020a). Projection of Extreme Flood Inundation in the Mekong River Basin under 4K Increasing Scenario using Large Ensemble Climate Data. *Hydrological Processes*, *34*(22), 4350–4364. https://doi.org/10.1002/hyp.13859

Try, S., Tanaka, S., Tanaka, K., Sayama, T., Khujanazarov, T., & Oeurng, C. (2022). Comparison of CMIP5 and CMIP6 GCM Performance for Flood Projections in the Mekong River Basin. *Journal of Hydrology: Regional Studies*, *40*, 101035. https://doi.org/10.1016/J.EJRH.2022.101035

Try, S., Tanaka, S., Tanaka, K., Sayama, T., Lee, G., & Oeurng, C. (2020b). Assessing the Effects of Climate Change on Flood Inundation in the Lower Mekong Basin using High-Resolution AGCM Outputs. *Progress in Earth and Planetary Science*, *7*(1), 1–16. https://doi.org/10.1186/s40645-020-00353-z

Try, S., Tanaka, S., Tanaka, K., Sayama, T., Oeurng, C., Uk, S., Takara, K., Hu, M., & Han, D. (2020c). Comparison of Gridded Precipitation Datasets for Rainfall-Runoff and Inundation Modeling in the Mekong River Basin. *PLoS ONE*, *15*(1), e0226814. https://doi.org/10.1371/journal.pone.0226814

Varis, O., Kummu, M., & Salmivaara, A. (2012). Ten Major Rivers in Monsoon Asia-Pacific: An Assessment of Vulnerability. *Applied Geography*, *32*(2), 441–454.

https://doi.org/10.1016/J.APGEOG.2011.05.003

Wang, W., Lu, H., Ruby Leung, L., Li, H. Y., Zhao, J., Tian, F., Yang, K., & Sothea, K. (2017). Dam Construction in Lancang-Mekong River Basin Could Mitigate Future Flood Risk from Warming-Induced Intensified Rainfall. *Geophysical Research Letters*, *44*(20), 10,378-10,386. https://doi.org/10.1002/2017GL075037

Wild, T. B., & Loucks, D. P. (2014). Managing Flow, Sediment, and Hydropower Regimes in the Sre Pok, Se San, and Se Kong Rivers of the Mekong Basin. *Water Resources Research*, *50*(6), 5141–5157. https://doi.org/10.1002/2014WR015457

Yamazaki, D., Ikeshima, D., Tawatari, R., Yamaguchi, T., O'Loughlin, F., Neal, J. C., Sampson, C. C., Kanae, S., & Bates, P. D. (2017). A High-Accuracy Map of Global Terrain Elevations. *Geophysical Research Letters*, *44*(11), 5844–5853. https://doi.org/10.1002/2017GL072874

Yun, X., Tang, Q., Wang, J., Liu, X., Zhang, Y., Lu, H., Wang, Y., Zhang, L., & Chen, D. (2020). Impacts of Climate Change and Reservoir Operation on Streamflow and Flood Characteristics in the Lancang-Mekong River Basin. *Journal of Hydrology*, *590*, 125472. https://doi.org/10.1016/J.JHYDROL.2020.125472

Zhong, R., Zhao, T., & Chen, X. (2021). Evaluating the Tradeoff between Hydropower Benefit and Ecological Interest under Climate Change: How Will the Water-Energy-Ecosystem Nexus Evolve in the Upper Mekong Basin? *Energy*, *237*, 121518. https://doi.org/10.1016/J.ENERGY.2021.121518

Ziese, M., Rauthe-Schöch, A., Becker, A., Finger, P., Meyer-Christoffer, A., & Schneider, U. (2018). *GPCC Full Data Daily Version.2018 at 1.0°: Daily Land-Surface Precipitation from Rain-Gauges built on GTS-based and Historic Data*. Global Precipitation Climatology Centre. https://doi.org/10.5676/DWD_GPCC/FD_D_V2018_100

CHAPTER 5 Effect of Climate Change on Hydropower Generation in the Mekong River Basin

5.1 Introduction

Population growth, urbanization, and economic development in the Mekong River Basin (MRB) have led to an increase in energy consumption in all the member countries. In the last decades, electricity demand has grown faster by 10% per annum. The average electricity consumption for an individual was approximately 950 kilowatt-hours (kWh), with Thailand having the highest consumption of over 2,000 kWh and Cambodia has the lowest consumption of just 55 kWh (ADB, 2008). In order to maintain energy security while also reducing the carbon emissions in the atmosphere, interest in renewable energy sources such as hydroelectric dams has been increased significantly in the Mekong region. Hydropower could potentially reduce greenhouse gas (GHG) emissions by up to 13%, with significant reductions in Sulphur Dioxide (SO_2) (the primary cause of acid rain) and Nitrous Oxide (N_2O) from the atmosphere (Richard & Tran, 2014). The abundant water resources and location of the MRB could provide the greatest potential for hydropower development. The hydropower potential of the region is estimated to be 43,000 MW, with over a hundred operational reservoirs by 2021 (Peter et al., 2007; Yun et al., 2021). The operation of hydropower dams have been criticized for changing the flow region and natural ecosystem of the basin (Arias et al., 2014; Ly et al., 2021; Piman et al., 2016; Räsänen et al., 2017; Try et al., 2020a; Yun et al., 2020). However, hydropower could provide clean energy, additional water for irrigation during the dry season, and navigation, which could largely contribute to the national economic growth of the riparian countries (Hecht et al., 2019; Pokhrel et al., 2018). The future hydropower generation not only relies on the current river flow variation but also the future water availability induced by climate change.

Climate change has become one of the most pressing global concerns, posing a threat to the environment and natural resources. The hydrologic cycle has been significantly altered globally, including in the Mekong River Basin, as a result of air temperature increases and changes in precipitation patterns (Beyene et al., 2010; Wang et al., 2013; Wu et al., 2016). By the end of the 21st century, the global average temperature is expected to rise from 1.0°C in the lowest emission

scenario to 3.7°C in the highest emission scenario (IPCC, 2014). Like other river catchments in the world, the flow regime in the Mekong River Basin will be adversely impacted by climate change (Hoanh et al., 2010; Lauri et al., 2012). Using the high-resolution atmospheric general circulation model (AGCM), Try et al., (2020a) estimated the impact of future climate projections on the streamflow in the MRB. Their findings found that the annual precipitation will increase by 14% and river flow exceeded 5% of the time (Q_5) in the downstream of MRB will increase by 30% under the high emission scenario. On the other hand, Hoang et al., (2016) suggested that climate change is expected to alter the seasonal and annual river discharge of the MRB, but the magnitude of change may vary by location. Besides, the future hydrologic system of the MRB's sub-basin, such as the Tonle Sap Lake Basin and 3S (Sesan, Sre Pok, and Sekong) River Basin, will also be affected by climate change (Oeurng et al., 2019; Shrestha et al., 2016).

Several studies have analyzed the impact of climate change on hydropower generation on a global scale, national scale, and basin-scale; however, there is a limited study on the MRB (Fan et al., 2020; Mohor et al., 2015; Van Vliet et al., 2016). Motivated by these knowledge gaps, this study aims to assess the impact of climate change on hydropower production using the most recent climate projections from the Coupled Model Intercomparison Project Phase 6 (CMIP6). The following research questions are addressed in the study:

1. How does climate change alter the potential annual discharge in the future?
2. How does the actual hydropower generation differ from potential hydropower generation?
3. What types of hydropower characteristics should be prioritized in the MRB for future hydropower development?
4. Under the future climate projections, which regions can be expected to generate more energy?

5.2 Methodology

5.2.1 Hydrologic Model Simulation

This study used the two-dimensional distributed Rainfall-Runoff-Inundation (RRI) model coupled with a reservoir model to simulate the effect of climate change on hydropower generation (Ly et al., 2021; Sayama et al., 2012). The RRI model was previously calibrated using the global optimization algorithm of the Shuffled Complex Evolution (SCE-UA) for the entire MRB. Details of the calibration and validation process were described in Try et al., (2020). The river discharge was simulated at a spatial resolution of 2.5 arc-minute (approximate 5 km) for the whole MRB

(Figure 5.1). The topographic data obtained from the Multi-Error-Removed-Improved-Terrain (MERIT DEM) included the digital elevation model (DEM), flow direction (DIR), and flow accumulation (ACC) (Yamazaki et al., 2017). The topographic data was scaled up from the original resolution of 3 arc-second (approximate 90 m) to 2.5 arc-minute in order to reduce the simulation time of the RRI model. The land-use data was derived from the Land Cover Product of the Moderate Resolution Imaging Spectroradiometer (MCD12Q1) (Friedl et al., 2010). The land-use type was reclassified into three main categories (i.e., permanent water body, agriculture, and forest). Due to the insufficient observed evapotranspiration data, the Japanese 55-year Reanalysis dataset (JRA-55) with a 3-hour temporal resolution was used (Kobayashi et al., 2015). River cross-sections were assumed to be rectangles and were estimated by the following equation:

$$D = 0.0015 \times A^{0.7491} \tag{5.1}$$

$$W = 0.0520 \times A^{0.7596} \tag{5.2}$$

where A is the upstream area [km^2], D is the river depth [m], W is the river width [m]

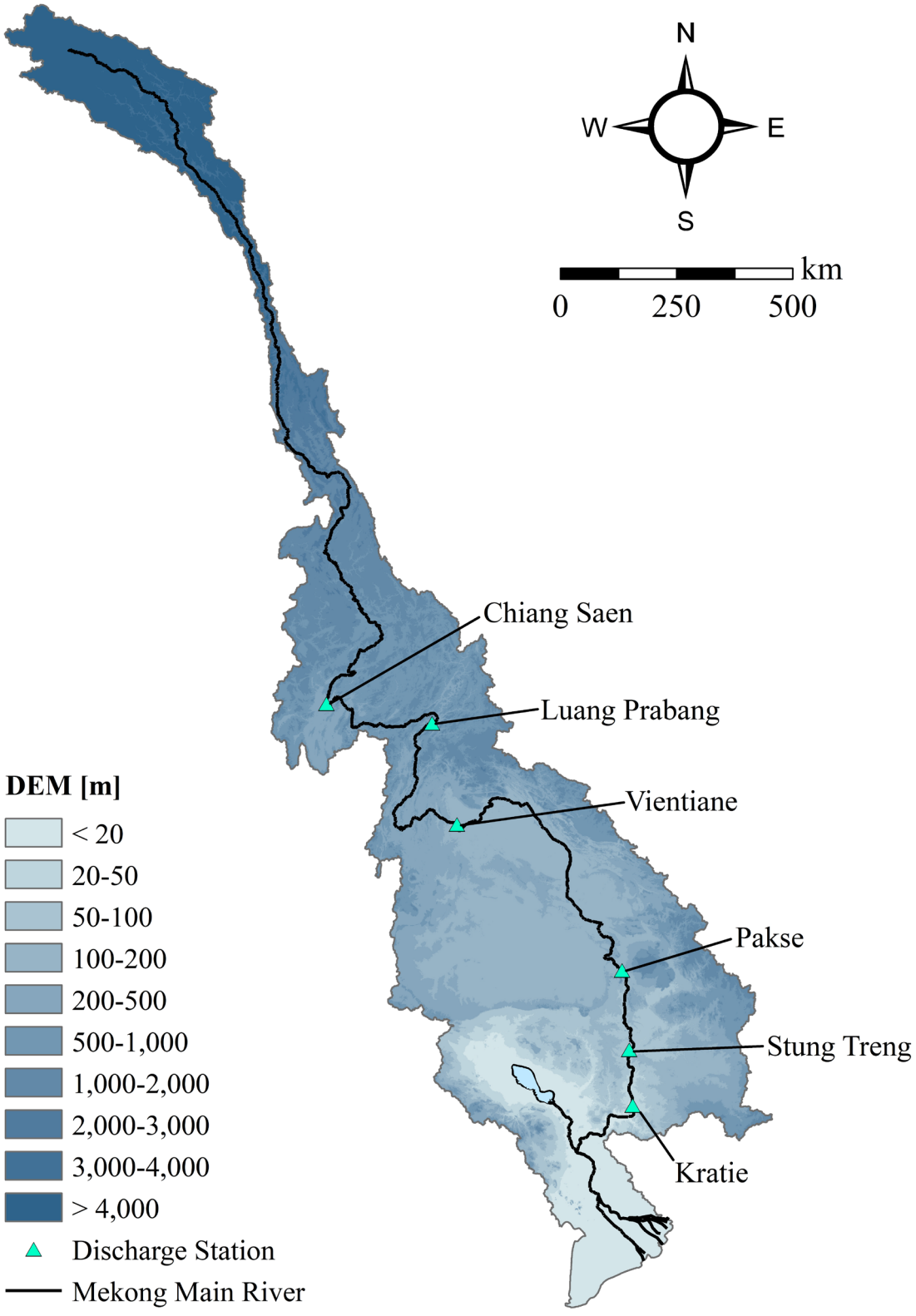

Figure 5.1 Digital elevation model of the Mekong River Basin

5.2.2 Climate Change Projection

To evaluate the effect of climate change on hydropower generation in the MRB, this study adopted eight General Circulation Models (GCM) from the CMIP6 projection. The dataset was obtained from the World Climate Research Program (WCRP) website, https://esgf-node.llnl.gov/search/cmip6/. Recently released by the Intergovernmental Panel on Climate Change (IPCC), the new CMIP6 climate change dataset included wider equilibrium climate sensitivity (ECS) with an increasing temperature ranging from 1.5°C to 4.5°C (IPCC, 2014). The CMIP6 provided a high-resolution GCM model (i.e., HighResMIP experiments) with uncertainty reduction over the previous CMIP5 and CMIP3 (Eyring et al., 2016; Try et al., 2022). The CMIP5 forecasted future climate conditions based on four different greenhouse gas emission scenarios of representative concentration pathways (RCPs), namely RCP2.6, RCP4.5, RCP6.0, and RCP8.5. In contrast, the new CMIP6 developed five scenarios known as shared socioeconomic pathways (SSPs), namely SSP1-2.6, SSP2-4.5, SSP4-6.0, and SSP5-8.5, which take socioeconomic factors like population growth, economic, urbanization, and other factors into account **(Figure 5.2)**. For this study, two SSP scenarios were considered: SSP2-4.5 (middle of the road) and SSP5-8.5 (fossil-fueled development). Prior to simulations, the GCMs were bias-corrected with GPCC precipitation using the linear scaling method in order to improve the model accuracy and fit with the ground precipitation. The eight GCMs from CMIP6 (**Table 5.1**) were used to access the impacts of climate change on river flow. The present climate corresponds to 1980–2014, while the future climate corresponds to 2026–2100.

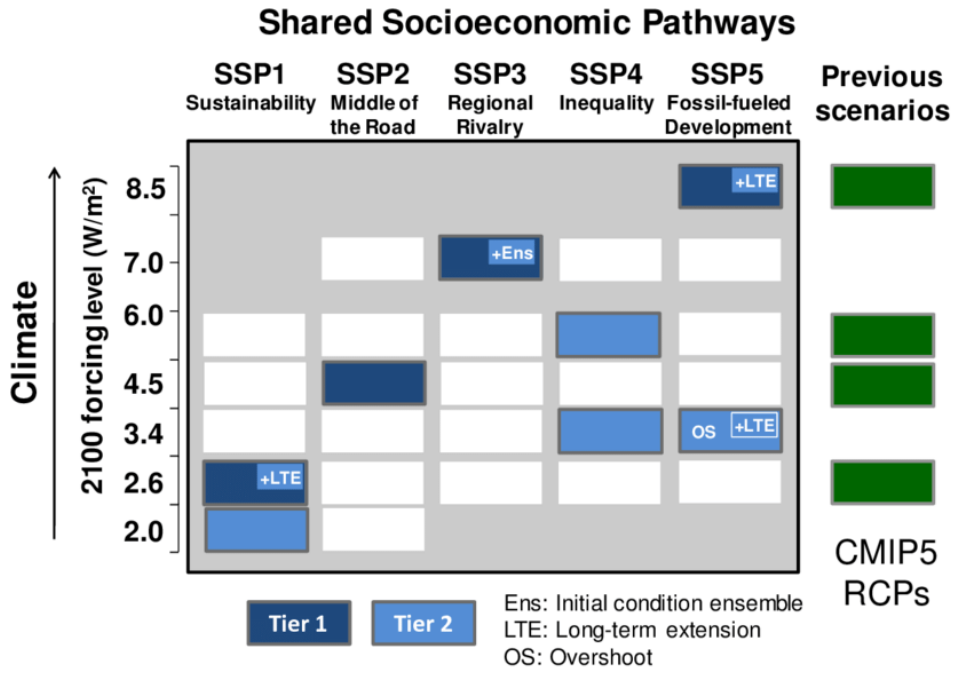

Figure 5.2 Comparison of SSP and RCP scenarios (O'Neill et al., 2016)

Table 5.1 Brief information on selected CMIP GCM models

N°	Model Name	Resolution	Developing Research Institute	References
		Lon. × Lat.		
1	CNRM-CM6-1	1.40625 × 1.40625	Centre National de Recherches Météorologiques (CNRM) and Cerfacs, France	Voldoire et al., (2019)
2	IPSL-CM6A-LR	2.5 × 1.25874	Institut Pierre-Simon Laplace, France	Boucher et al., (2020)
3	MIROC6	1. 40625 × 1.40625	Center for Climate System Research, University of Tokyo, Japan Agency for Marine-Earth Science and Technology, and National Institute for Environmental Studies, Japan	Tatebe et al., (2019)
4	MPI-ESM1-2-LR	1.875 × 1.875	Max Planck Institute for Meteorology, Germany	Mauritsen et al., (2019)
5	MRI-ESM2.0	1.125 × 1.125	Meteorological Research Institute, Japan	Yukimoto et al., (2019)
6	ACCESS-CM2	1.875 × 1.25	Commonwealth Scientific and Industrial Research Organization and Bureau of Meteorology, Australia	Bi et al., (2020)
7	GFDL-CM4	1.25 × 1.0	National Oceanic and Atmospheric Administration's Geophysical Fluid Dynamics Laboratory, USA	Held et al., (2019)
8	NorESM2	1.25 × 0.9375	Norwegian Climate Center, Norway	Seland et al., (2020)

5.2.3 Reservoir Operation Modeling

There was no comprehensive information on hydropower operation rules. Therefore, release flows were estimated for each time step using a simple storage model proposed by Ly et al., (2021). The model estimated the optimum reservoir outflow patterns for each dam. The main objective function of the model was to maximize production outflows (i.e., outflows through the turbines), thus maximizing hydropower production. The reservoir operation model required a set of parameters, including inflow, reservoir active storage, and turbine capacity. The reservoir operation model was integrated into the RRI model to simulate the discharge under hydropower development and climate change. The reservoir storage at each time step was calculated by the following equation:

$$S_t = S_{t-1} + Q_{in_{t-1}} - Q_{turb_{t-1}} - Q_{spill_{t-1}} \quad (5.3)$$

The released flows from the turbine are determined by the following rules:

$$\Delta S = S_0 + Q_{in} - Q_{max} \quad (5.4)$$

If $Q_{in} < Q_{max}$:

- $\Delta S \geq S_{min} \Rightarrow \begin{cases} Q_{turb} = Q_{max} \\ Q_{spill} = 0 \end{cases}$

- $\Delta S < S_{min} \Rightarrow \begin{cases} Q_{turb} = Q_{in} + S_0 - S_{min} \\ Q_{spill} = 0 \end{cases}$

If $Q_{in} \geq Q_{max}$:

- $\Delta S \leq S_{max} \Rightarrow \begin{cases} Q_{turb} = Q_{max} \\ Q_{spill} = 0 \end{cases}$

- $\Delta S > S_{max} \Rightarrow \begin{cases} Q_{turb} = Q_{max} \\ Q_{spill} = S_0 + Q_{in} - Q_{max} - S_{max} \end{cases}$

where S_0 is the initial storage, S_{min} is the minimum storage, S_{max} is the maximum storage, ΔS is the storage change, Q_{in} is the river inflow, Q_{turb} is the flow released from the turbine, Q_{spill} is the overflow through the spillway, Q_{max} is the turbine's maximum flow capacity.

Two hydropower scenarios were prepared for this study based on the database provided by the Mekong River Commission (MRC) (MRC, 2009, 2019c). The present hydropower scenario consisted of 98 projects, most of which are located in the tributaries of the LMB. The future hydropower scenarios included 126 projects on mainstreams (23 projects) and tributaries (103 projects) of the MRB, equivalent to total active storage of 108 km^3 **(Figure 5.3)**. The majority of these dams will be fully functional by 2040 (MRC, 2019a).

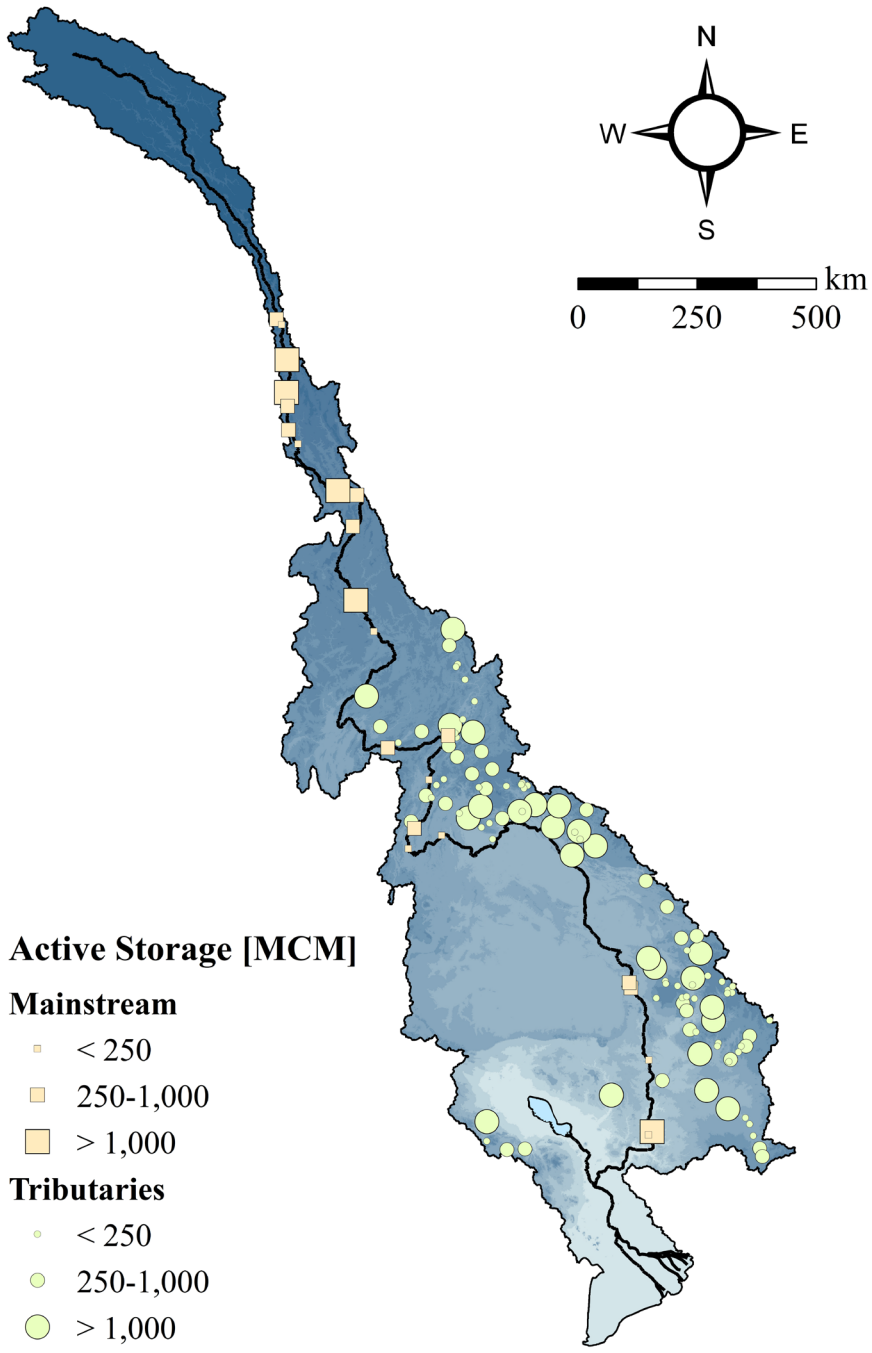

Figure 5.3 Active storage of the mainstream and tributaries dams

Given the inflow to the turbines, the hydropower generation can be expressed as follows:

$$E = \eta \times \rho \times g \times H \times Q_{turb} \quad (5.4)$$

where E is the energy generated through the turbines
η is the turbine efficiency
ρ is the water density
g is the gravitational acceleration
H is the hydraulic head

5.2.4 Data Analysis

Characteristics of the hydropower in the MRB were analyzed to determine their potential in generating energy under future climate projections. Several types of analysis were performed: the analysis of turbine flow capacity, the analysis of future flow increase based on flow duration curve, and the analysis of the location of hydropower for potential future energy generation.

Hydropower Classification Based on Turbine Flow Capacity

Hydropower projects in the MRB were classified into three types based on their turbine flow capacity. Type-A hydropower was characterized as having a turbine flow capacity larger than Q_{25} (discharge exceeded 25% of the time). Hydropower with turbine flow capacity between Q_{25} (discharge exceeded 25% of the time) and Q_{50} (discharge exceeded 50% of the time) was classified as Type-B, while the remainder was classified as Type-C.

Table 5.2 Classification of hydropower based on the turbine flow capacity

Type of Hydropower	Condition of Turbine Capacity
Type-A	turbine flow capacity $\geq Q_{25}$
Type-B	$Q_{25} >$ turbine flow capacity $\geq Q_{50}$
Type-C	turbine flow capacity $< Q_{50}$

Future Flow Increase Classification Based on Flow Duration Curve

Future flow increase was categorized into three groups based on the flow duration curve (FDC). First, the flow increase was divided into four zones: Zone A ($Q \geq Q_{25}$), Zone B ($Q_{25} > Q \geq Q_{50}$), Zone C ($Q_{50} > Q \geq Q_{75}$), and Zone D ($Q < Q_{75}$). **Figure 5.4** shows the graphical representation of the future flow increase zone. Then, the future flow increase was classified into three groups as shown in **Table 5.3**.

Table 5.3 Classification of future flow increase based on flow duration curve

Category of Future Flow Increase	Condition
High-flow increase	$\frac{Zone\ A}{\sum \Delta Q} \geq 50\%$
Uniform increase	$\frac{Zone\ A - Zone\ C}{\sum \Delta Q} = \pm 10\%$
Low-flow increase	$\frac{Zone\ C + Zone\ D}{\sum \Delta Q} > 50\%$

where $\sum \Delta Q$ is the total flow change between the present and future climate.

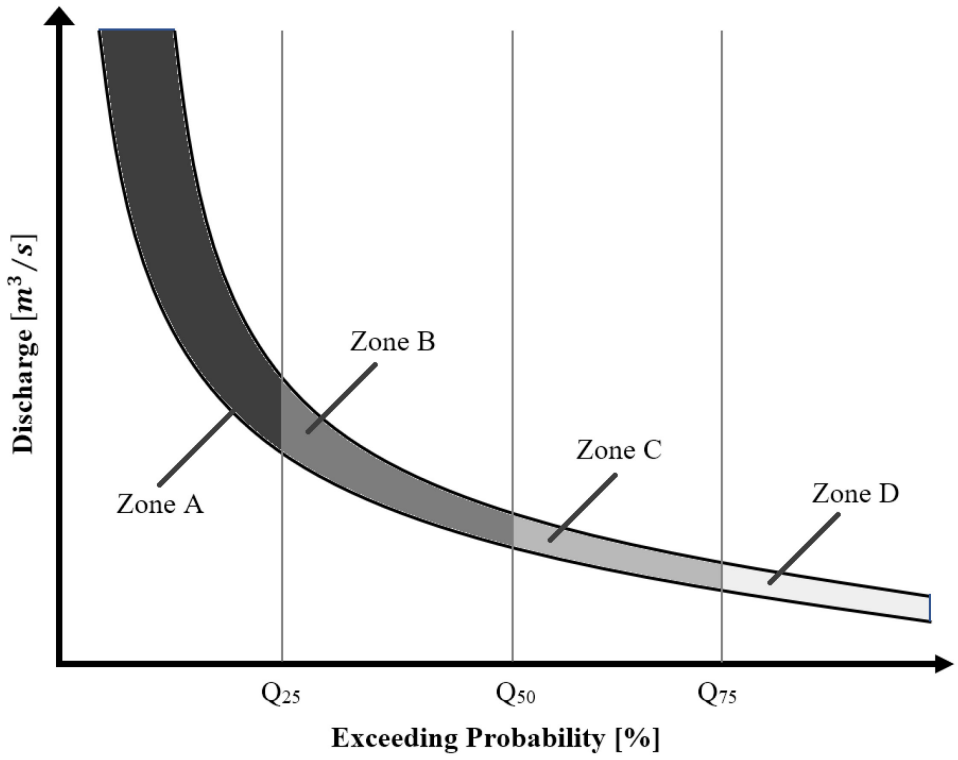

Figure 5.4 Graphical representation of future flow increase zone

Classification of Hydropower Location

To determine the potential location for future hydropower generation under climate change, the hydropower projects were divided into four main regions: mainstream of the UMB mainstream of the LMB, 3S (Sesan, Sre Pok, and Sekong) River system, and tributaries of the MRB.

Through these classifications and data analysis, types of hydropower and regions to be prioritized for further development can be defined.

5.3 Results

5.3.1 River Discharge under Future Climate Projections

Using the RRI model, the river discharge was simulated for the present period and the future period under different climate change scenarios. **Figure 5.5** shows the simulated annual discharge under different climate scenarios (SSP2-4.5 and SSP5-8.5) from 1980 to 2100. Two hydrological stations along the main river were selected to analyze the overall flow changes in the MRB: Chiang Saen (upstream) and Kratie (downstream). Compared to the present climate scenario, the relative changes in annual discharge at Chiang Saen range from -3.6% to +61.5% for the SSP2-4.5 scenario and from -2.7% to +86.9% for the SSP5-8.5 scenario depending on the GCMs, with an average change of +14.4% and +23.6%, respectively. The relative changes in annual discharge at Kratie range from -3.9% to +35.6% for the SSP2-4.5 scenario and from -16% to +66% for the SSP5-8.5 scenario, with an average change of +12.9% and +17.1%, respectively. The simulation results showed a large variation among GCMs, however; the future climate indicated an increasing trend in the annual river discharge in all scenarios with a noticeable change in the far-future period. The difference in magnitude of annual average discharge increased with the future timeframe (i.e., near-future < mid-future < far-future). These increases in annual discharge would be beneficial to hydropower generation, thus, contributing to the economic growth of the riparian countries in the MRB.

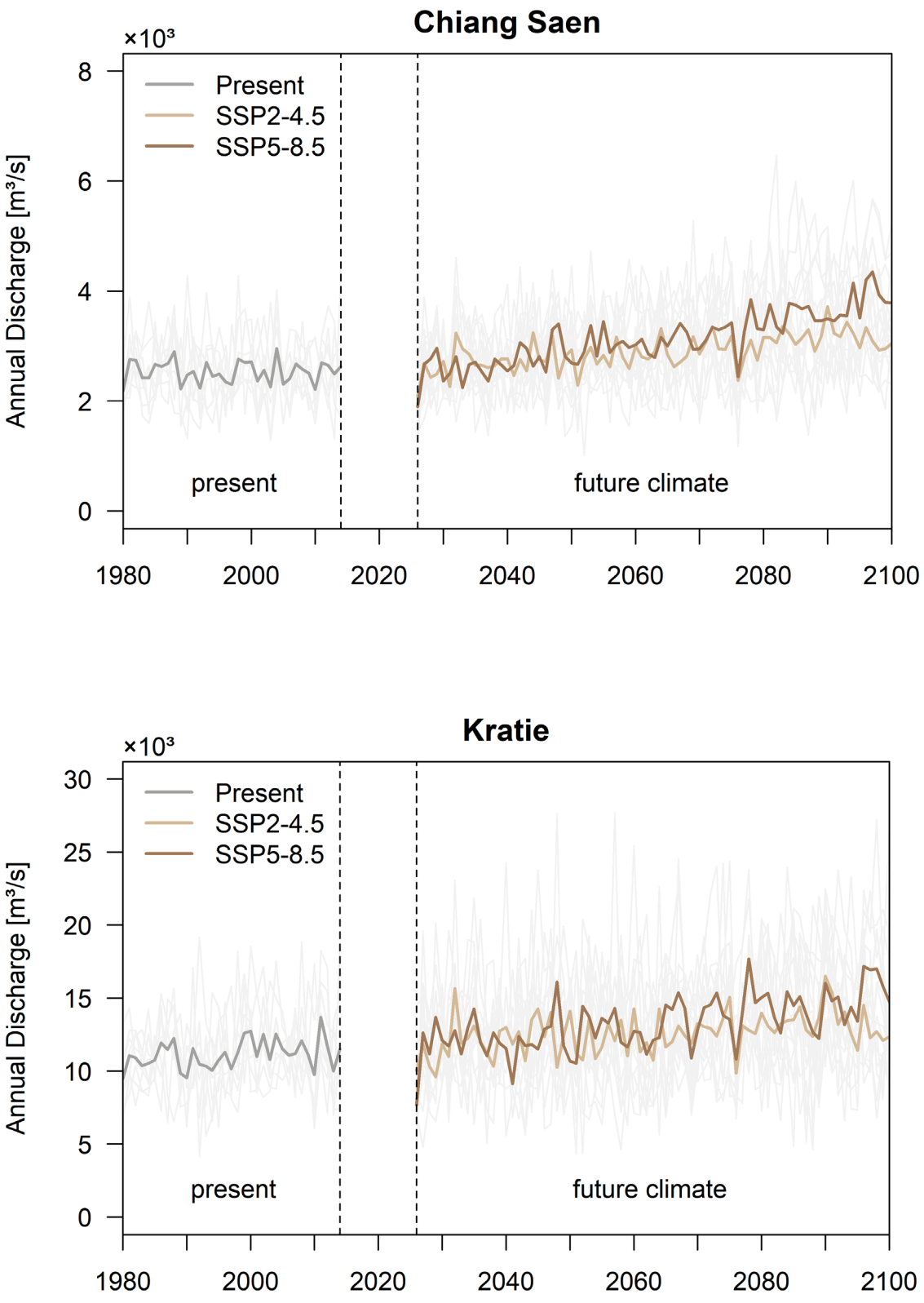

Figure 5.5 Simulated annual discharge from 1980 to 2100 under different climate scenarios

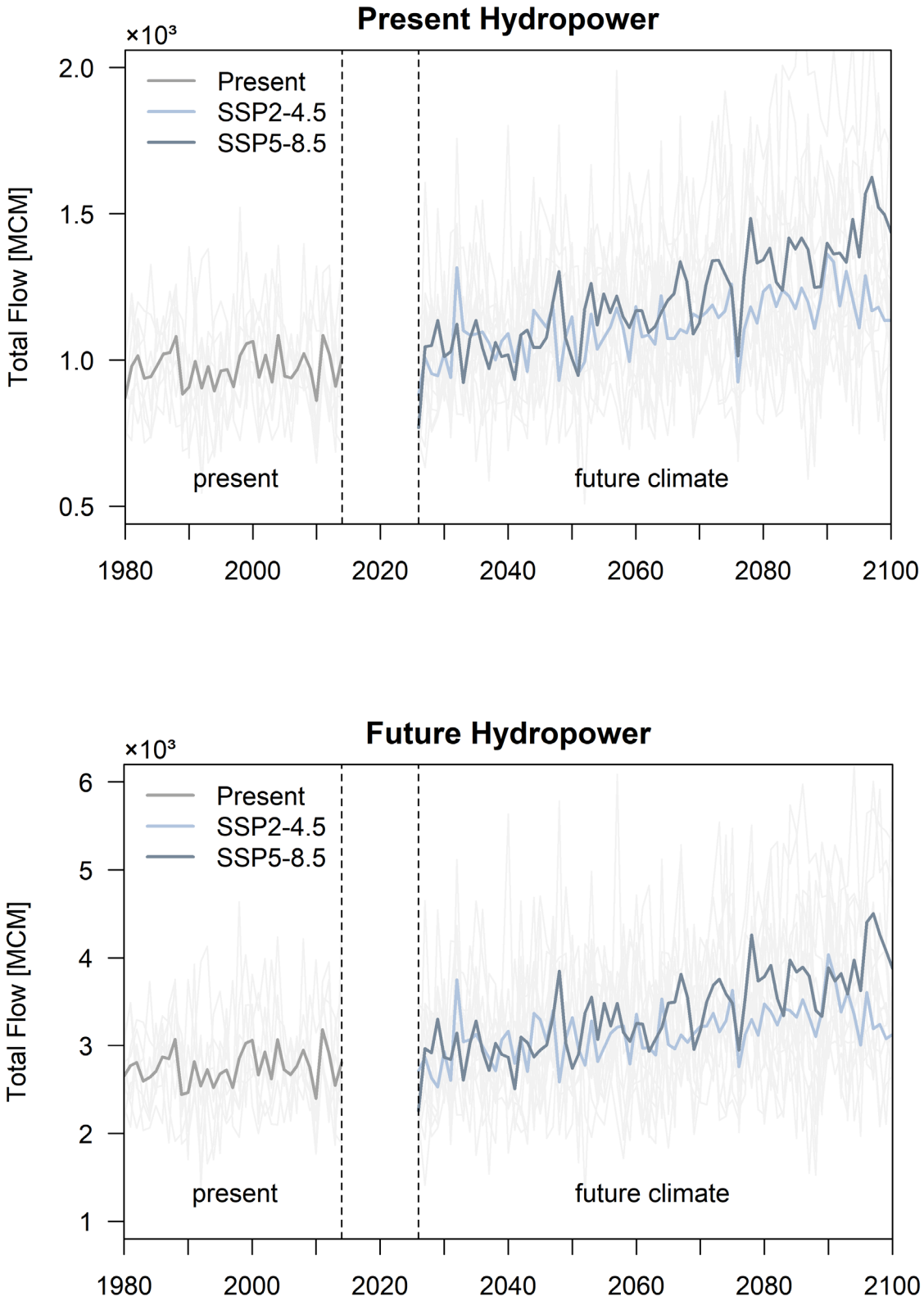

Figure 5.6 Changes in total inflow to the turbines of present and future hydropower under different climate scenarios

Furthermore, total inflow to the turbines of present hydropower and future hydropower were evaluated to better understand the potential flow changes in the MRB. **Figure 5.6** showed the total inflow to the turbines of present and future hydropower from 1980 to 2100 under different climate scenarios. Similar to the annual discharge at Chiang Saen and Kratie, the total inflow of both present and future hydropower was increasing under climate change. For the present hydropower scenario, the total inflow increased from 974 MCM (present climate) to 1,121 MCM for the SSP2-4.5 scenario, and to 1,206 MCM for the SSP5-8.5 scenario. For the future hydropower scenario, the total inflow increased from 2,753 MCM (present climate) to 3,147 MCM and 3,368 MCM for the SSP2-4.5 and SSP5-8.5 scenarios, respectively.

5.3.2 Climate Change Impacts on Energy Production

Climate change is expected to change total inflow through turbines, thus, affecting hydropower generation. Although the total inflow was estimated to increase in all climate scenarios, hydropower generation will decrease in some GCMs compared to the present climate. Under the present hydropower (98 dams), the total inflow will increase on average by 15% for the SSP2-4.5 scenario, and 24% for the SSP5-8.5 scenario **(Figure 5.7)**. On the other hand, the total inflow of the future hydropower (126 dams) will increase on average by 14% and 22% for SSP2-4.5 and SSP5-8.5 scenarios, respectively **(Figure 5.8)**. In contrast, the energy generation was expected to increase on average by only 2% (3%) under the SSP2-4.5 (SSP5-8.5) for the present hydropower, and only 3% (5%) under the SSP2-4.5 (SSP5-8.5) for the future hydropower **(Figure 5.9)**. The small increase rate in energy production compared to the increase rate in total inflow was due to the limited turbine flow capacity of the hydropower. In addition, if the increase of the total inflow is concentrated in the higher discharge than the turbine flow capacity, the increasing rate of the hydropower production will be limited compared to the increase in the total flow. Restricted by the turbine capacity, excessive inflow will be abandoned through the spillway without generating additional energy. Overall, the hydropower generation showed an increasing trend in the future climate projections; however, the degree of change varies between selected GCMs.

The relative changes in average annual energy production compared to the present climate of the present hydropower scenario (ED_PS) is presented in **Table 5.4**. Average annual energy production for the present hydropower scenario varied from -1.87% to +7.19% for the SSP2-4.5 scenario and from -1.07% to +6.92% for the SSP5-8.5 scenario. In comparison to the present climate, both SSP2-4.5 and SSP5-8.5 showed a small increase in annual energy production. However, the future hydropower scenario resulted in a significant increase in average annual energy production, exceeding 100% in some future climate projections, compared to ED_PS.

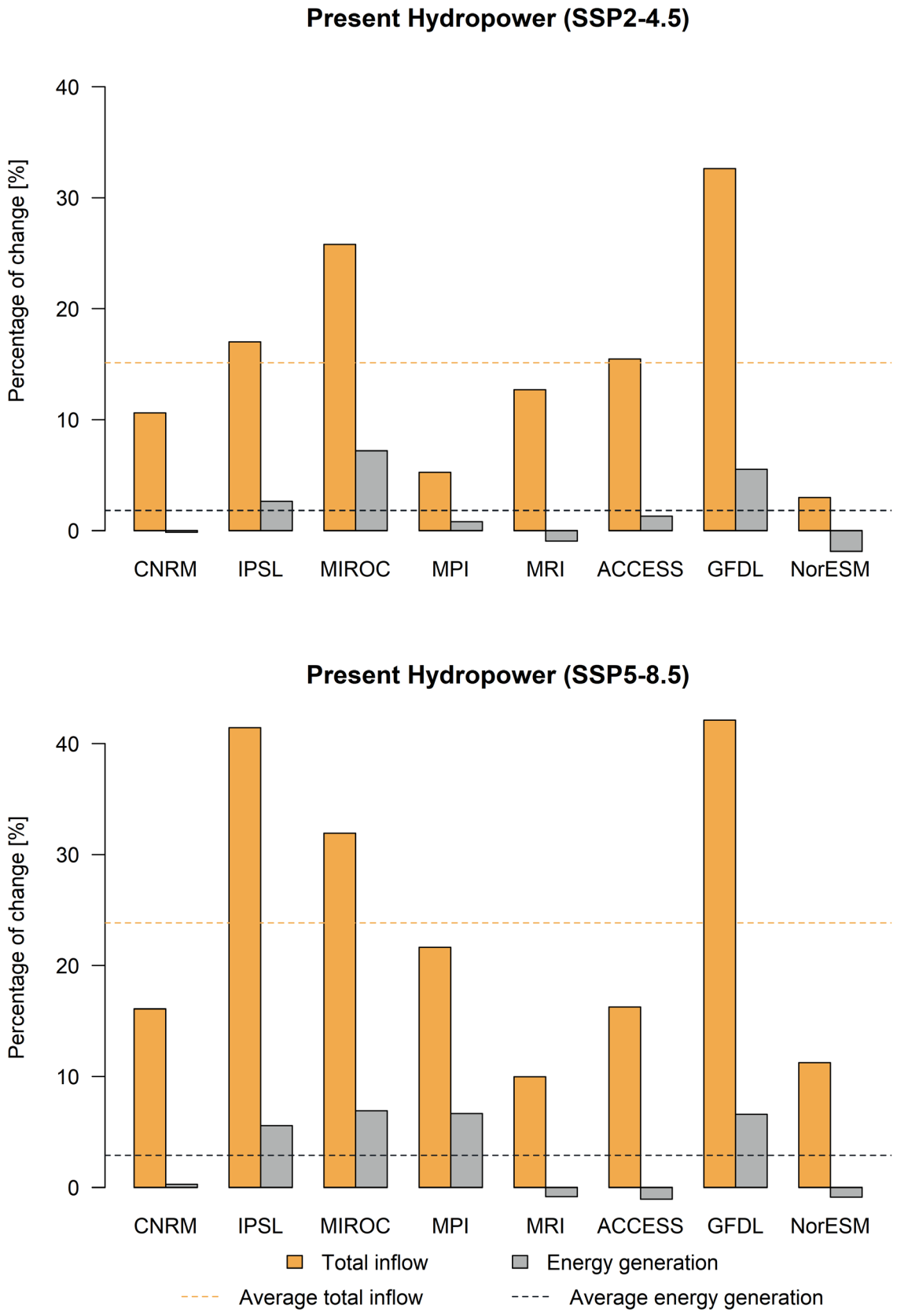

Figure 5.7 Relative changes in total inflow and energy generation of the present hydropower development scenario

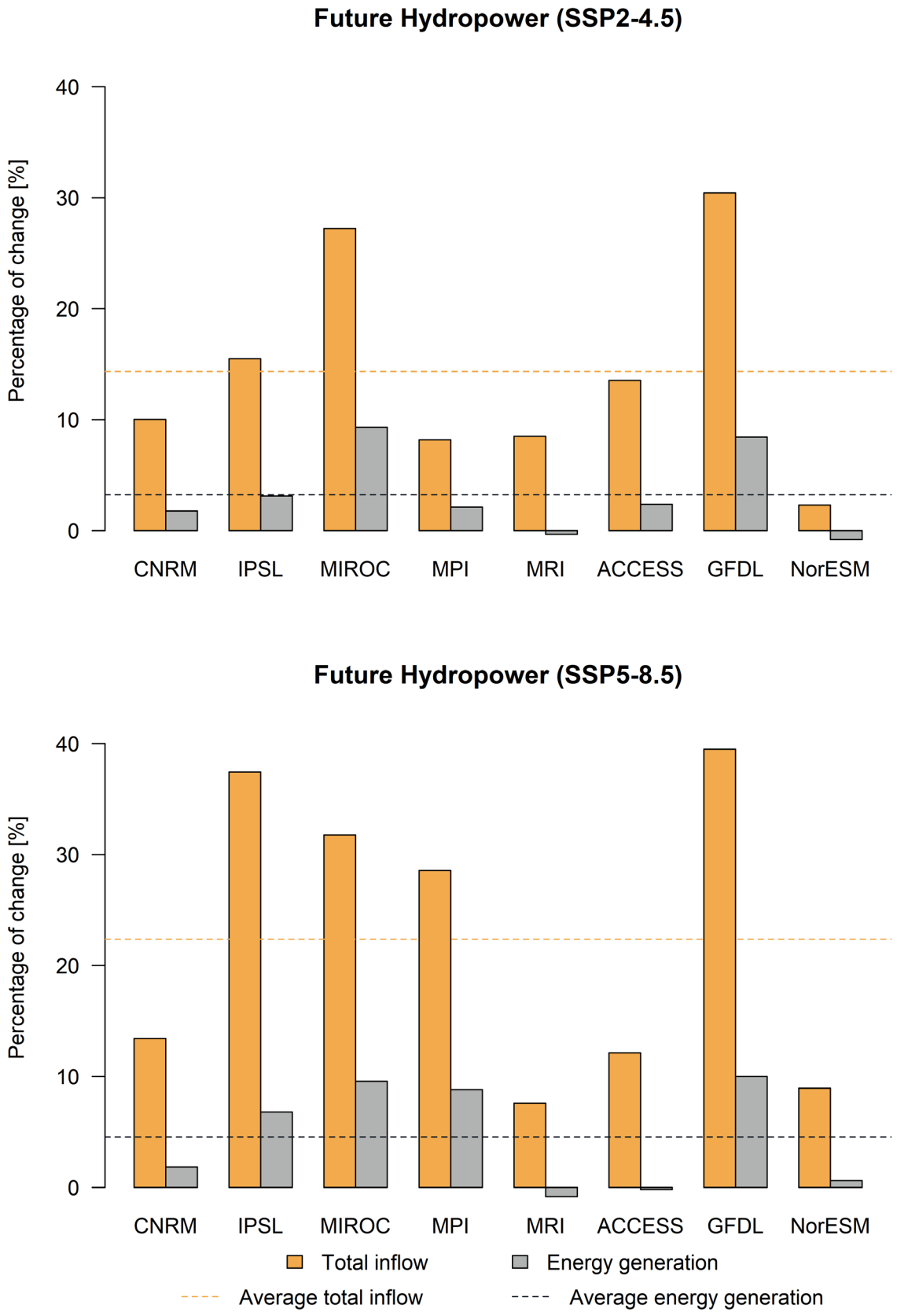

Figure 5.8 Relative changes in total inflow and energy generation of the future hydropower development scenario

Table 5.4 Relative changes in average annual energy production under climate change scenarios compared to ED_PS scenario

Scenario	Change (%)	Scenario	Change (%)
ED_PS	–	FD_PS	91.7
ED_SSP2-4.5_CNRM	-0.14	FD_SSP2-4.5_CNRM	93.5
ED_SSP2-4.5_IPSL	2.62	FD_SSP2-4.5_IPSL	97.0
ED_SSP2-4.5_MIROC	7.19	FD_SSP2-4.5_MIROC	110.6
ED_SSP2-4.5_MPI	0.79	FD_SSP2-4.5_MPI	96.5
ED_SSP2-4.5_MRI	-0.96	FD_SSP2-4.5_MRI	92.1
ED_SSP2-4.5_ACCESS	1.30	FD_SSP2-4.5_ACCESS	97.1
ED_SSP2-4.5_GFDL	5.51	FD_SSP2-4.5_GFDL	105.7
ED_SSP2-4.5_NorESM	-1.87	FD_SSP2-4.5_NorESM	90.5
ED_SSP5-8.5_CNRM	0.25	FD_SSP5-8.5_CNRM	93.6
ED_SSP5-8.5_IPSL	5.54	FD_SSP5-8.5_IPSL	104.0
ED_SSP5-8.5_MIROC	6.92	FD_SSP5-8.5_MIROC	111.0
ED_SSP5-8.5_MPI	6.65	FD_SSP5-8.5_MPI	109.4
ED_SSP5-8.5_MRI	-0.84	FD_SSP5-8.5_MRI	91.1
ED_SSP5-8.5_ACCESS	-1.07	FD_SSP5-8.5_ACCESS	92.2
ED_SSP5-8.5_GFDL	6.59	FD_SSP5-8.5_GFDL	108.7
ED_SSP5-8.5_NorESM	-0.88	FD_SSP5-8.5_NorESM	93.2

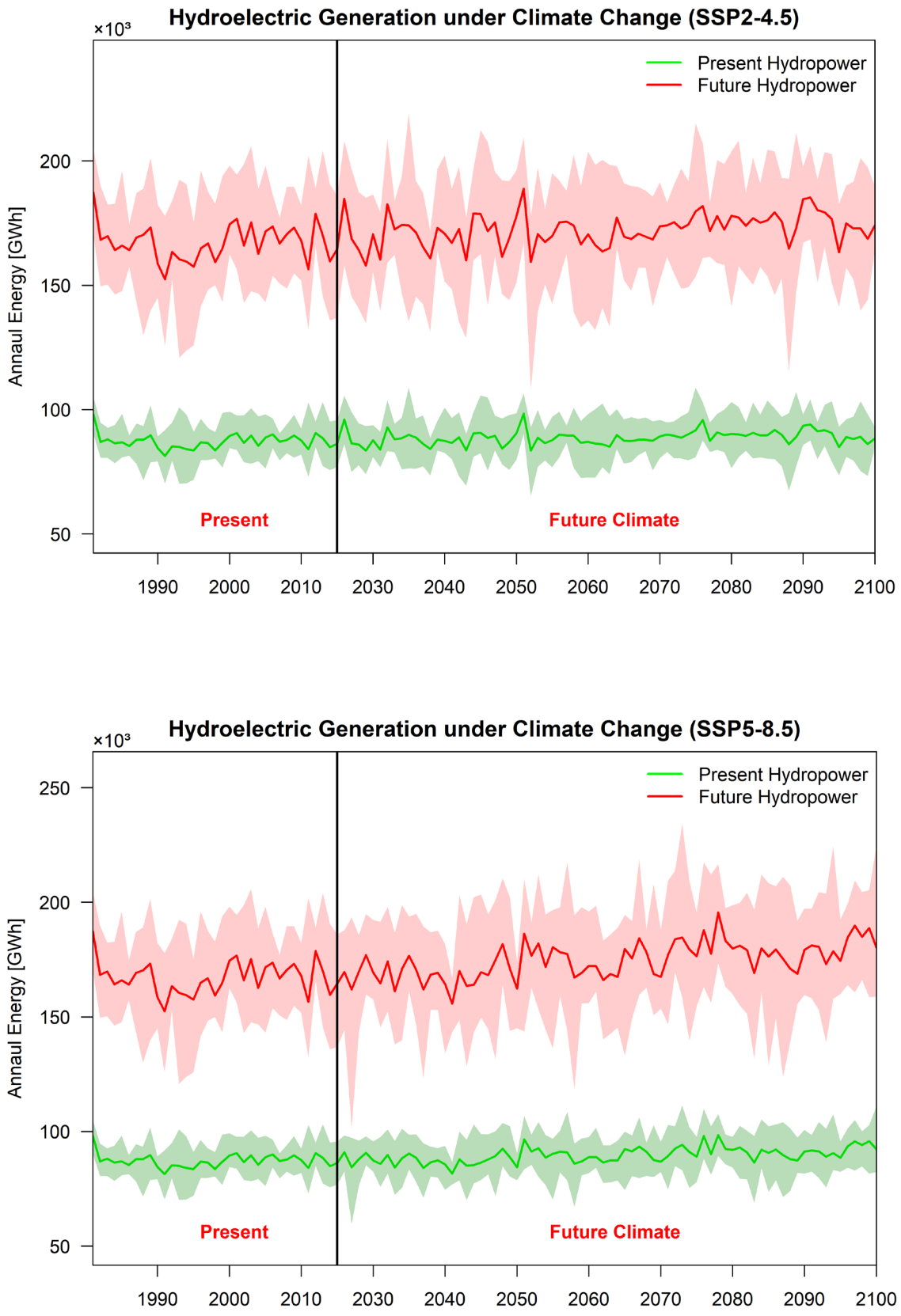

Figure 5.9 Annual energy production under different climate projections

5.3.3 Characterization of Hydropower in the Mekong River Basin

The future hydropower scenario in the MRB was classified based on the characteristics of turbine flow capacity and the flow duration curves to identify its future potential in energy generation. According to data analysis based on turbine flow capacity, Type-A hydropower accounted for 67% of all future hydropower adopted in this study, followed by Type-B (20%) and Type-C (13%). In addition, the majority of river discharge was increased in high flow in the future, based on the flow duration curve analysis. Results from data analysis indicated that most of the hydropower in the MRB was type-A with the future high-flow increase, accounting for more than half of the total hydropower **(Figure 5.10)**.

Dam type-A and type-B are primarily found in the LMB, particularly in the Mekong's tributaries and 3S river basin. On the other hand, dam type-C is mainly located in the UMB of China. Compared to the present climate, dam type-C in China had the potential to increase hydropower

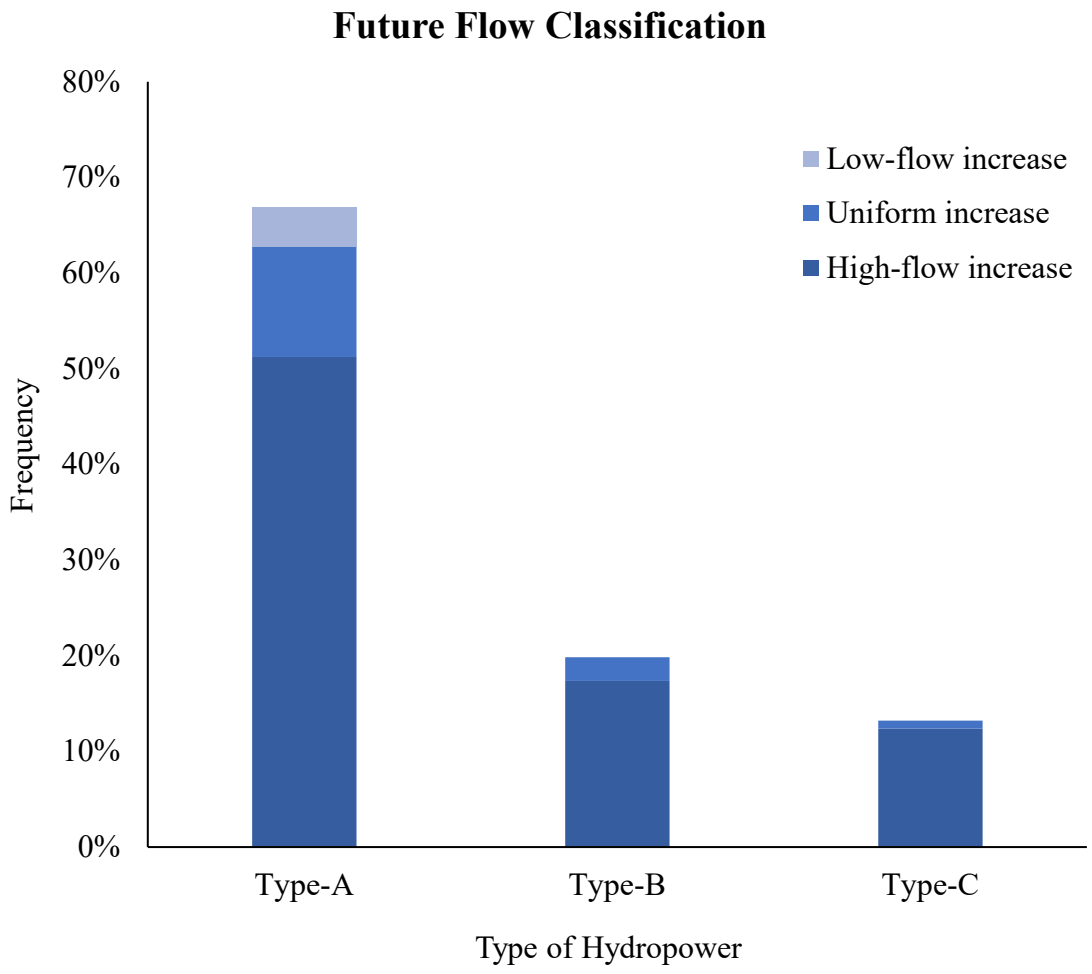

Figure 5.10 Characteristics of hydropower in the Mekong River Basin

production by over 50% under climate change (SSP5-8.5), while dam type-A and type-B could increase their energy generation by less than 50% **(Figure 5.11)**. However, the actual future increase of hydropower production of dam type-C was estimated to be less than 10% due to its characteristics (i.e., small turbine capacity and future high-flow increase) **(Figure 5.12)**. A similar tendency also occurred on dam type-A and type-B, particularly along the Mekong mainstream. Hydropower with future high-flow increase and large turbine flow capacity had greater hydropower potential since most of the inflow could go through the turbine for energy generation. Hydropower with a small turbine flow capacity, on the other hand, cannot benefit from increased inflows due to climate change because the excessive inflow will pass through the spillway instead of the turbines.

5.3.4 Direction of the Future Hydropower Development under Future Climate Projections

As hydropower production is highly dependent on inflow and turbine flow capacity, the energy generation may vary significantly owing to those factors. Although climate change increased annual total inflow, the limited turbine flow capacity prevented them from fully utilizing all inflow for energy production. To take the advantage of total inflow increase by climate change, strategies such as enlarging turbine flow capacity should be implemented. In addition, to identify the potential regions for future development, the hydropower plants in the MRB were divided into four main regions: the UMB mainstream, the LMB mainstream, the 3S region, and the Mekong tributaries. The turbine flow capacity was then increased by 10%, 30%, and 50%, respectively, to estimate the additional energy production for each region **(Figure 5.13**–**Figure 5.16).** Water loss through the spillway tended to decrease as turbine flow capacity was increased, while energy production tended to increase. The finding showed that hydropower in the UMB and LMB mainstream can generate more energy than those from the Mekong tributaries when the turbine capacity was increased. Mainstream hydropower can generate up to 10% more energy with a 50% increase in turbine capacity. The 3S region, on the other hand, can generate about 1.2% of additional energy, and the Mekong tributaries can generate about 2.6%.

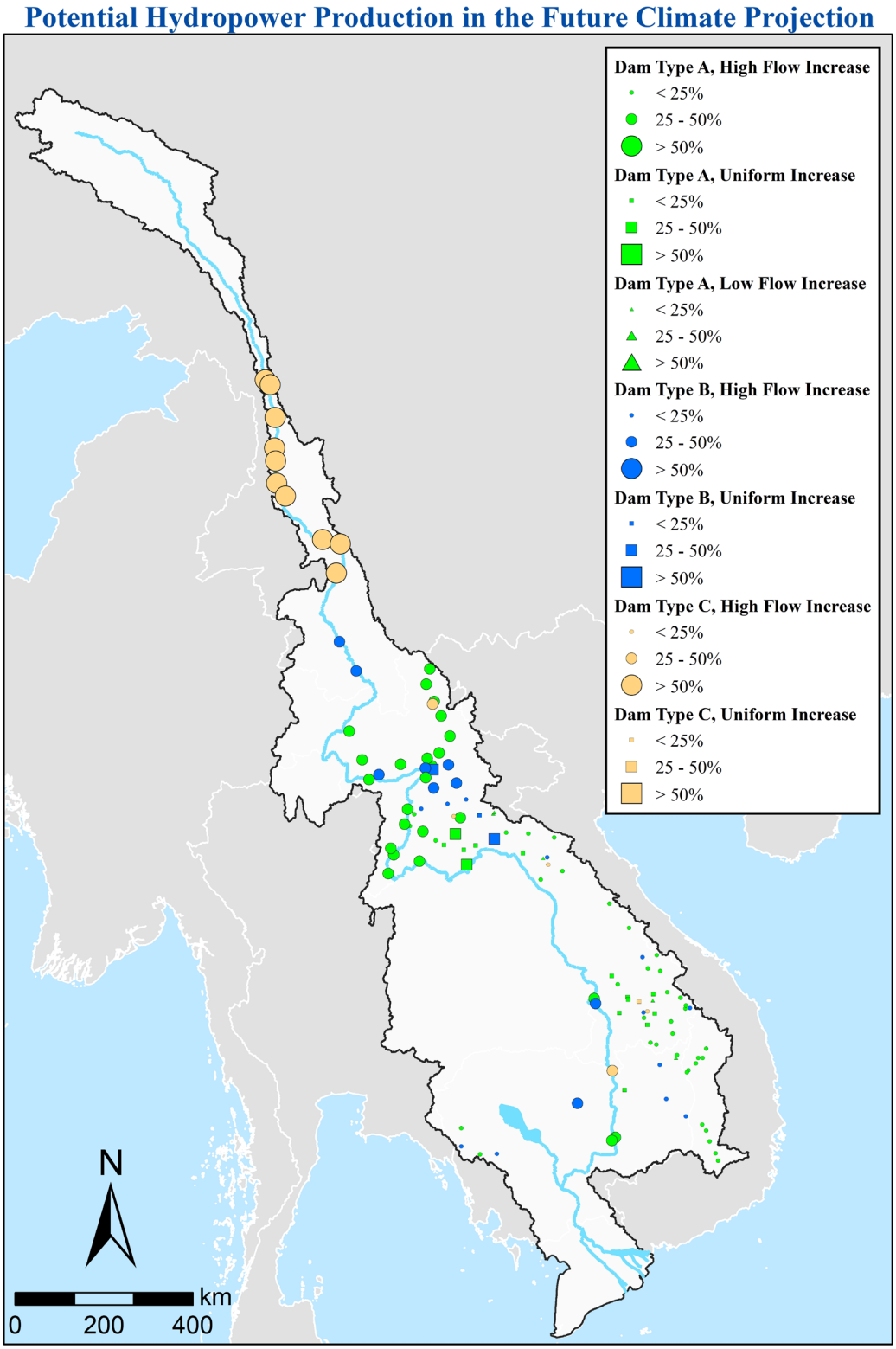

Figure 5.11 Potential increase of hydropower production in the MRB under future climate projection (SSP5-8.5)

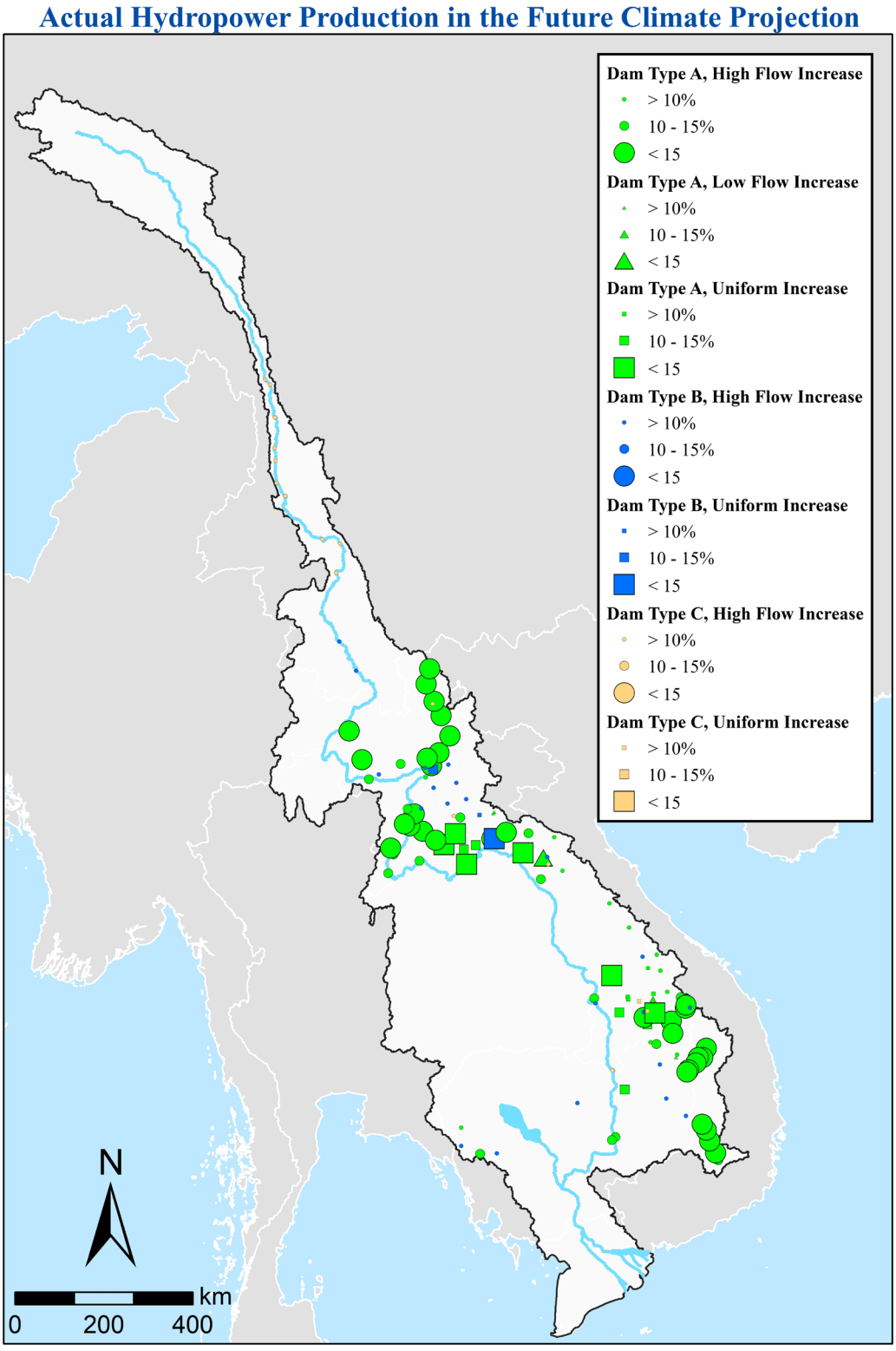

Figure 5.12 Actual Increase of hydropower production in the MRB under future climate projection (SSP5-8.5)

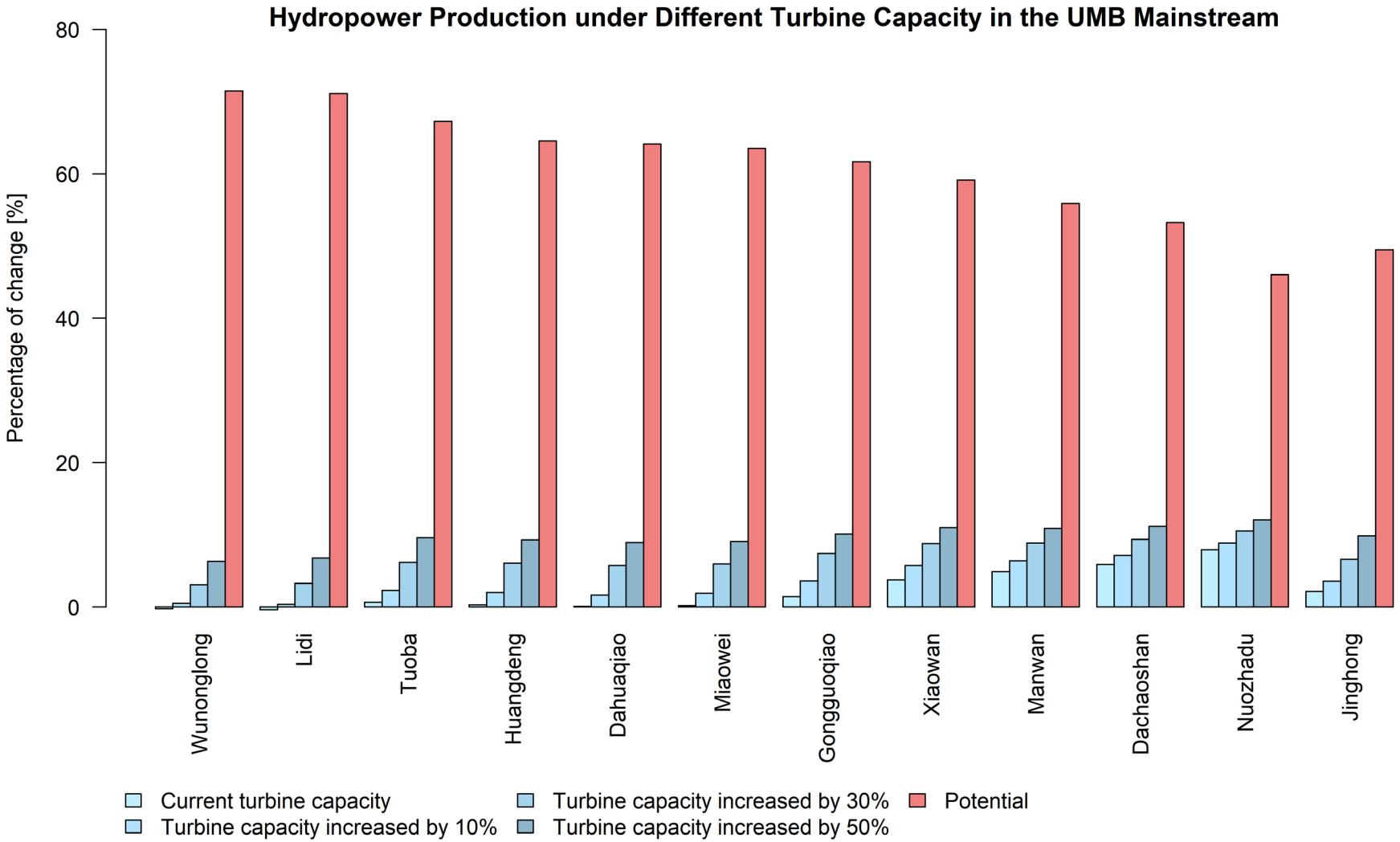

Figure 5.13 Projected hydropower production under different turbine flow capacity of the dams in the UMB mainstream

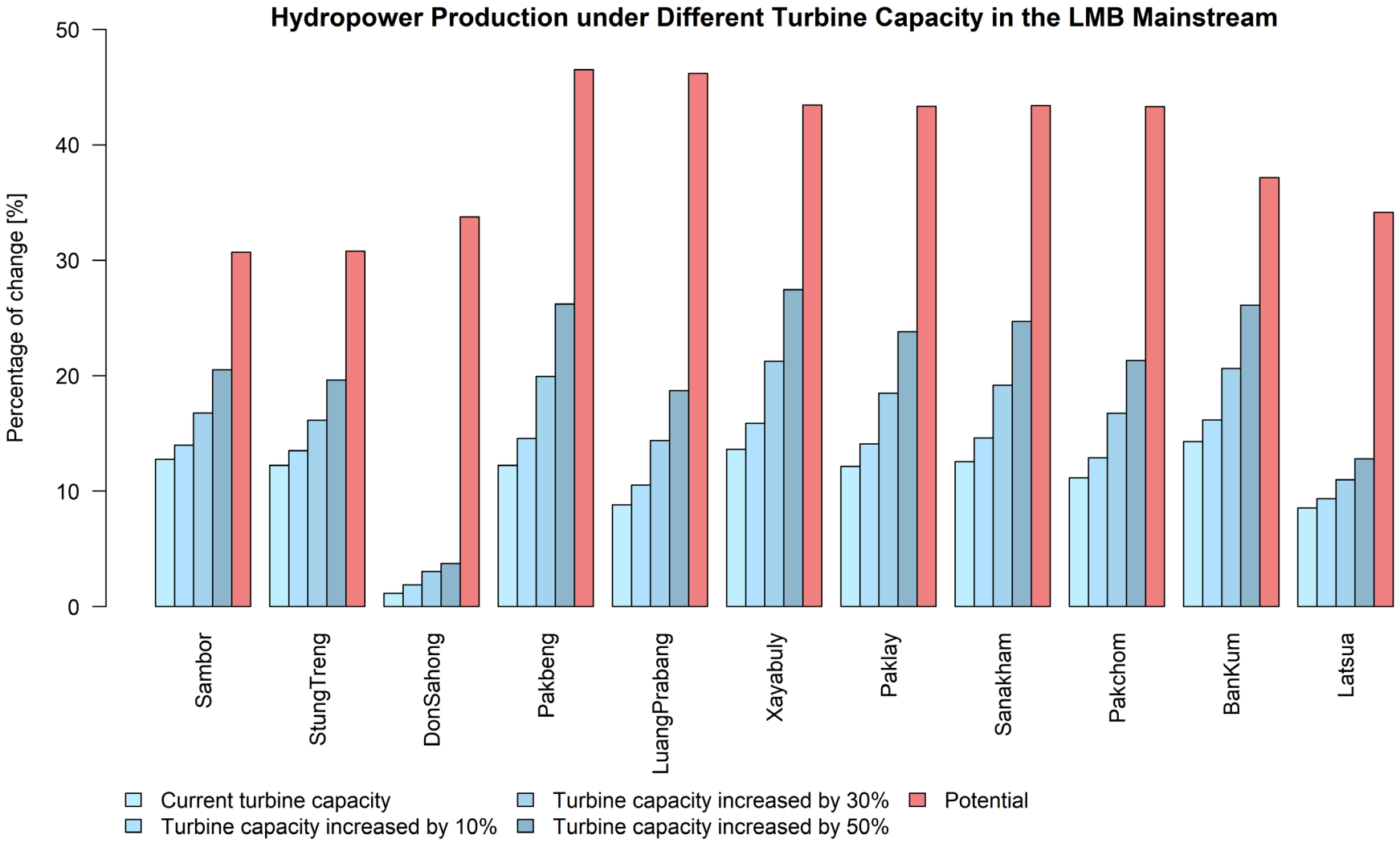

Figure 5.14 Projected hydropower production under different turbine flow capacity of the dams in the LMB mainstream

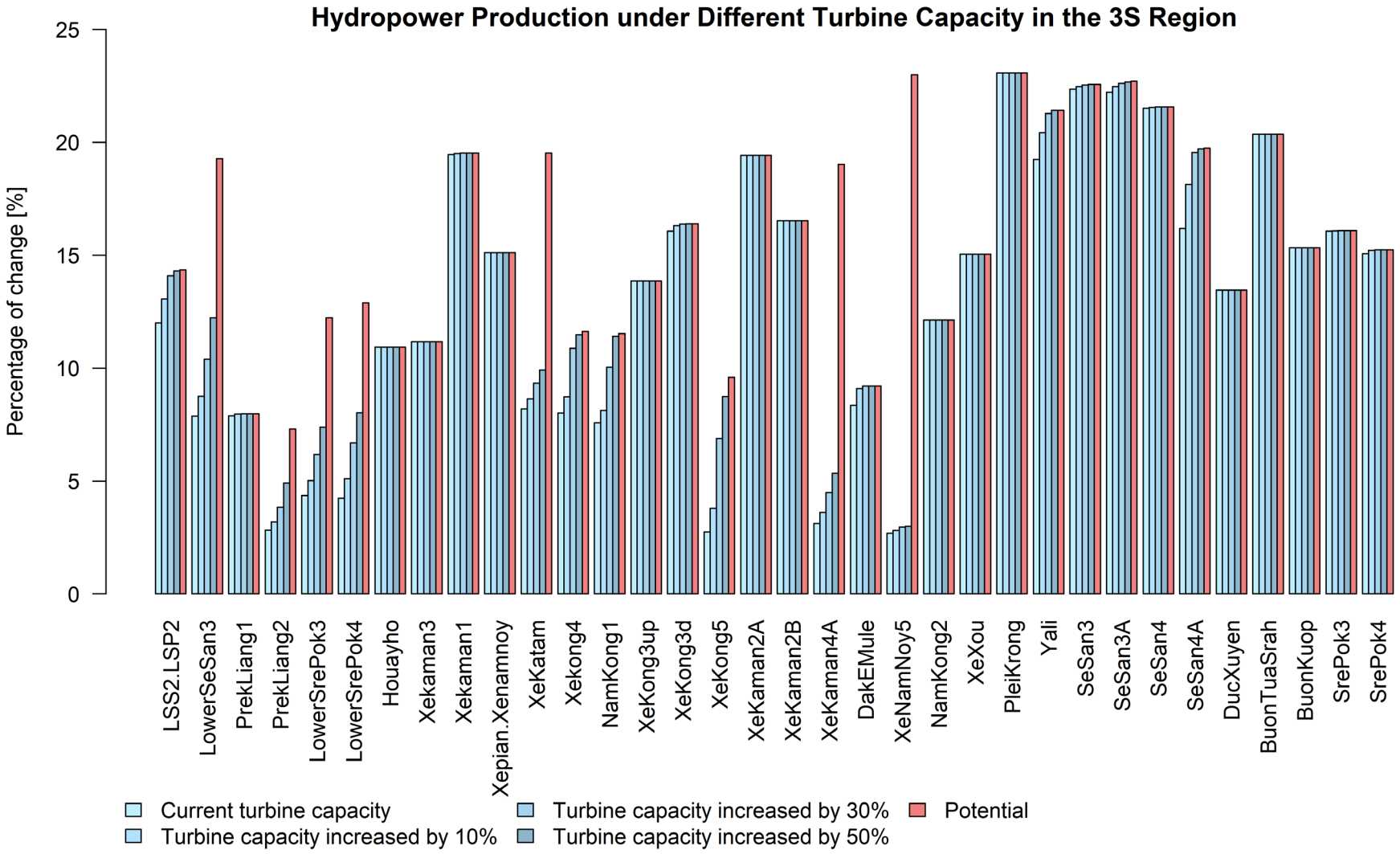

Figure 5.15 Projected hydropower production under different turbine flow capacity of the dams in the 3S region

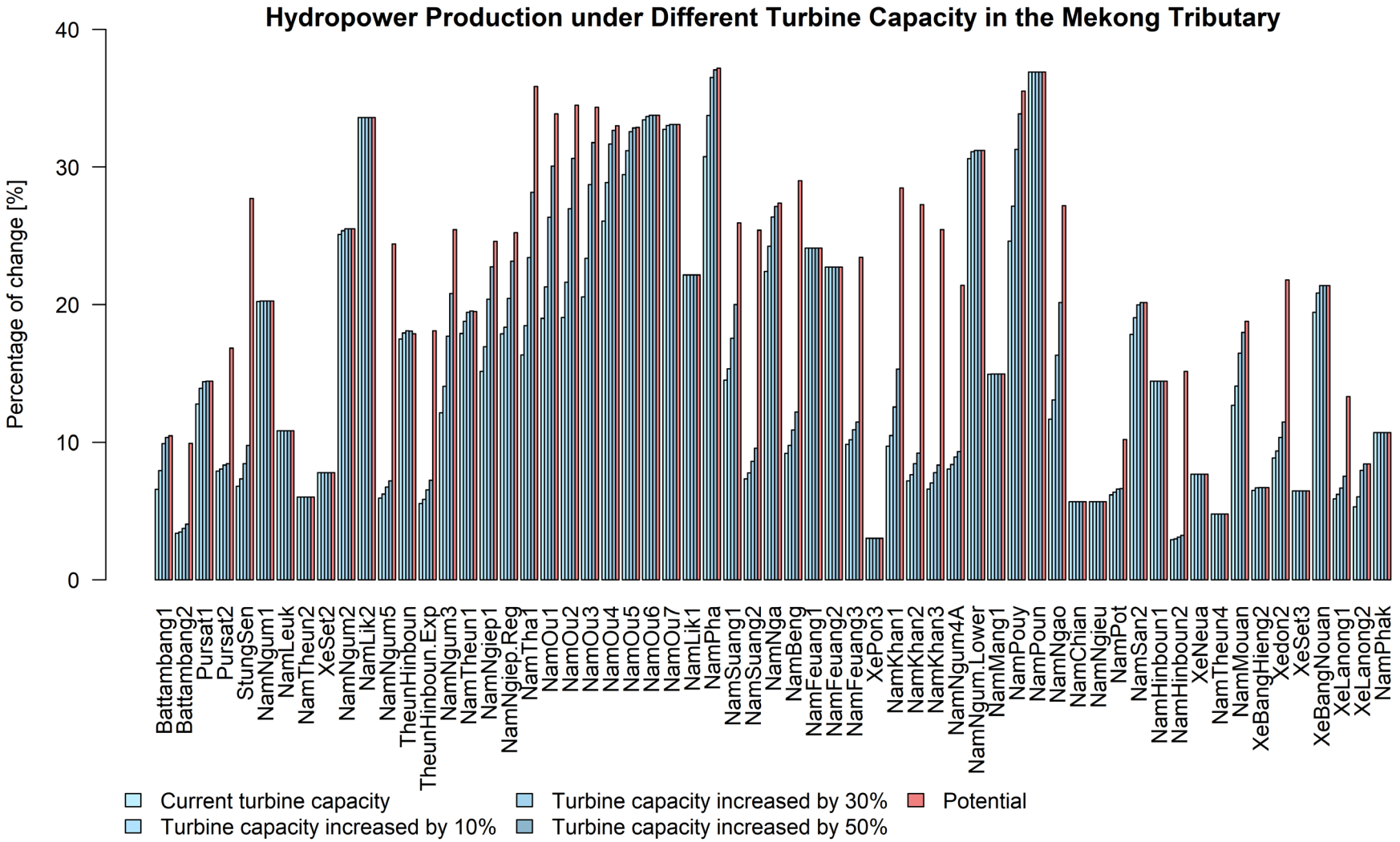

Figure 5.16 Projected hydropower production under different turbine flow capacity of the dams in the Mekong tributary

5.4 Discussion

5.4.1 Main Findings

This study used to most recent CMIP6 GCMs to assess the effects of climate change on hydropower production in the MRB. Results from the RRI simulations suggested that climate change will substantially change the annual discharge and annual total inflow under both SSP2-4.5 and SSP5-8.5 scenarios. Flow alteration can be observed from the upstream at Chiang Saen to the downstream at Kratie. Our findings are consistent to other studies (Hoang et al., 2016; Hoanh et al., 2010; Lauri et al., 2012), although the magnitude of change varies among the studies due to difference in the hydrologic model, climate change scenarios, and the study period. Hoang et al., (2016) predicted an increase in annual discharge of 14% and 15% for RCP4.5 and RCP8.5, respectively, at Chiang Saen. Our study estimated a 14% and 24% increase for SSP2-4.5 and SSP5-8.5, respectively. On the other hand, there was a significant increase in total inflow in both the present hydropower and the future hydropower scenarios, particularly in the far-future period. These increases could be beneficial for energy generation in the MRB.

According to the MRC, (2019b), approximately 200,000 GWh of hydropower can potentially be generated during the historical period in the LMB. Changes in total inflow caused by climate change are expected to have an impact on the hydropower generation in the MRB. Despite a significant increase in annual total inflow, our findings suggested that energy generation of the future hydropower could increase by only 5% as a result of climate change (SSP5-8.5). This constraint was caused by the limited turbine capacity of the hydropower plants, which allowed excessive inflow to pass through the spillway without producing more energy. This limitation in turbine capacity for energy production was also discussed in other studies (Yun et al., 2020; Zhong et al., 2019). According to Zhong et al.,(2019), an increase in streamflow in the mainstream of the UMB in most future climate scenarios corresponded to a potential increase in hydropower production. However, despite the increased inflow, the fixed installed capacity limited additional increases in hydroelectric generation.

Our study classified the hydropower dams into three types according to the turbine flow capacity and future flow increase. The majority of which were Type-A hydropower with future high-flow increases. Results further revealed that the potential increase in hydropower production from dam type-C is typically greater than 50%. However, the energy outputs were very limited due to its characteristics of small turbine capacity with future high-flow increases. Therefore, type-C hydropower was an ideal prospect for future hydropower development in the MRB by modifying

its characteristics by increasing its turbine capacity. Given the expected increase in future total inflow, stakeholders should consider expanding turbine capacity to allow more water to pass through for additional energy generation. Meema et al., (2021) suggested an operation strategy to cope with climate change for hydropower production in the Nam Ngum River in the Mekong basin by increasing the turbine capacity. Their finding found that increasing turbine capacity by 10% could enhance energy output by up to 3.7%. In addition, water loss through the spillway would reduce as the turbine capacity was increased.

This study also identified the potential regions for future hydropower development with the increased turbine capacity. The findings showed that hydropower along the Mekong mainstream in both the UMB and LMB could benefit from the increased turbine capacity more than in other regions. This revealed that their current turbine capacity was not large enough for taking the advantage of the projected future river flow increase. In contrast, increasing turbine capacity would not influence hydropower production in the 3S region because their current capacity is sufficient enough to meet their potential. Most hydropower in the Mekong tributary, on the other hand, has a similar tendency to the 3S region. Thus, the UMB and LMB mainstream should be prioritized for future hydropower development.

5.4.2 Limitations

The study assessed the effect of climate change on hydropower production using a distributed RRI model. However, several factors such as irrigation water withdrawal and future land-use change were not taken into account. Moreover, only one reservoir operation strategy was considered in the reservoir model. Future studies should adopt different reservoir operation scenarios to further understand the changes in hydropower production under different operation strategies on top of climate change. Although this study used the most recent CMIP6 projections, a finer resolution model such as Regional Climate Models (RCM) or downscaled GCMs are recommended for further studies.

5.5 Summary and Conclusion

This chapter investigated the changes in hydropower production in the MRB under future climate projections. The most recent CMIP6 GCMs were adopted in this study to simulate the river discharge under hydropower operation and climate change for the present period (1980–2014) and future period (2026–2100). Our findings revealed an increase in annual discharge as well as total inflow, indicating an increase in energy generation. Significant changes can be observed in

the far-future period under the high-emission scenario (SSP5-8.5). In general, hydropower production showed an increasing trend under future climate change. However, restricted by the current turbine capacity, future hydropower production could increase by only 5% given a 22% increase in total inflow. According to the data analysis, the type-A (large turbine capacity) dam was the most common hydroelectric infrastructure in the MRB, which were mostly located in the LMB, particularly in the Mekong tributaries and 3S river basin. The study further showed that hydropower along the Mekong mainstream are mainly type-C dams. These dams can potentially increase the hydropower production if the total inflow increase, but we found that the increase in high-flow (i.e. discharge $\geq Q_{25}$) was more dominant. As a result, even for the type-A dams, the increase of hydropower production is limited. They also cannot increase the hydropower production as much as the total inflow increase, mainly because of the limited turbine flow capacity. In other words, these dams are more efficient if we increase turbine flow capacity within the MRB by the same amount because they can utilize the increased flow as much as the turbine flow capacity increases. Therefore, future hydropower development should be prioritized in those regions. Stakeholders should consider increasing the turbine capacity of hydropower along the mainstream, as the results suggested that this strategy could significantly increase energy production.

References

ADB. (2008). *Energy Sector in the Greater Mekong Subregion*. Asian Development Bank.

Arias, M. E., Cochrane, T. A., Kummu, M., Lauri, H., Holtgrieve, G. W., Koponen, J., & Piman, T. (2014). Impacts of Hydropower and Climate Change on Drivers of Ecological Productivity of Southeast Asia's Most Important Wetland. *Ecological Modelling*, *272*, 252–263. https://doi.org/10.1016/j.ecolmodel.2013.10.015

Beyene, Tazebe, Dennis, ·, Lettenmaier, P., Kabat, Pavel, Beyene, T, Lettenmaier, · D P, & Kabat, P. (2010). Hydrologic Impacts of Climate Change on the Nile River Basin: Implications of the 2007 IPCC Scenarios. *Climatic Change*, *100*(3), 433–461. https://doi.org/10.1007/S10584-009-9693-0

Bi, D., Dix, M., Marsland, S., O'Farrell, S., Sullivan, A., Bodman, R., Law, R., Harman, I., Srbinovsky, J., Rashid, H. A., Dobrohotoff, P., Mackallah, C., Yan, H., Hirst, A., Savita, A., Dias, F. B., Woodhouse, M., Fiedler, R., Heerdegen, A., … Heerdegen, A. (2020). Configuration and Spin-up of ACCESS-CM2, the New Generation Australian Community Climate and Earth System Simulator Coupled Model. *Journal of Southern Hemisphere Earth Systems Science*, *70*(1), 225–251. https://doi.org/10.1071/ES19040

Boucher, O., Servonnat, J., Albright, A. L., Aumont, O., Balkanski, Y., Bastrikov, V., Bekki, S., Bonnet, R., Bony, S., Bopp, L., Braconnot, P., Brockmann, P., Cadule, P., Caubel, A., Cheruy, F., Codron, F., Cozic, A., Cugnet, D., D'Andrea, F., … Vuichard, N. (2020). Presentation and Evaluation of the IPSL-CM6A-LR Climate Model. *Journal of Advances in Modeling Earth Systems*, *12*(7), e2019MS002010. https://doi.org/10.1029/2019MS002010

Eyring, V., Bony, S., Meehl, G. A., Senior, C. A., Stevens, B., Stouffer, R. J., & Taylor, K. E. (2016). Overview of the Coupled Model Intercomparison Project Phase 6 (CMIP6) Experimental Design and Organization. *Geoscientific Model Development*, *9*(5), 1937–1958. https://doi.org/10.5194/GMD-9-1937-2016

Fan, J. L., Hu, J. W., Zhang, X., Kong, L. S., Li, F., & Mi, Z. (2020). Impacts of Climate Change on Hydropower Generation in China. *Mathematics and Computers in Simulation*, *167*, 4–18. https://doi.org/10.1016/J.MATCOM.2018.01.002

Friedl, M. A., Sulla-Menashe, D., Tan, B., Schneider, A., Ramankutty, N., Sibley, A., & Huang,

X. (2010). MODIS Collection 5 Global Land Cover: Algorithm Refinements and Characterization of New Datasets. *Remote Sensing of Environment*, *114*(1), 168–182. https://doi.org/10.1016/J.RSE.2009.08.016

Hecht, J. S., Lacombe, G., Arias, M. E., Dang, T. D., & Piman, T. (2019). Hydropower Dams of the Mekong River Basin: A Review of Their Hydrological Impacts. *Journal of Hydrology*, *568*, 285–300. https://doi.org/10.1016/j.jhydrol.2018.10.045

Held, I. M., Guo, H., Adcroft, A., Dunne, J. P., Horowitz, L. W., Krasting, J., Shevliakova, E., Winton, M., Zhao, M., Bushuk, M., Wittenberg, A. T., Wyman, B., Xiang, B., Zhang, R., Anderson, W., Balaji, V., Donner, L., Dunne, K., Durachta, J., … Zadeh, N. (2019). Structure and Performance of GFDL's CM4.0 Climate Model. *Journal of Advances in Modeling Earth Systems*, *11*(11), 3691–3727. https://doi.org/10.1029/2019MS001829

Hoang, L. P., Lauri, H., Kummu, M., Koponen, J., van Vliet, M. T. H., Supit, I., Leemans, R., Kabat, P., & Ludwig, F. (2016). Mekong River Flow and Hydrological Extremes under Climate Change. *Hydrology and Earth System Sciences*, *20*(7), 3027–3041. https://doi.org/10.5194/hess-20-3027-2016

Hoanh, C. T., Jirayoot, K., Lacombe, G., & Srinetr, V. (2010). *Impacts of Climate Change and Development on Mekong Flow Regimes First Assessment - 2009. MRC Technical Paper No. 29*. Mekong River Commission.

IPCC. (2014). *Synthesis Report: Contribution of Working Group I, II, and III to the Fifth Assessment Report of the Intergovernmental Panel on Climate Change*. IPCC.

Kobayashi, S., Ota, Y., Harada, Y., Ebita, A., Moriya, M., Onoda, H., Onogi, K., Kamahori, H., Kobayashi, C., Endo, H., Miyaoka, K., & Takahashi, K. (2015). The JRA-55 reanalysis: General Specifications and Basic Characteristics. *Journal of the Meteorological Society of Japan. Ser. II*, *93*(1), 5–48. https://doi.org/10.2151/JMSJ.2015-001

Lauri, H., de Moel, H., Ward, P. J., Räsänen, T. A., Keskinen, M., & Kummu, M. (2012). Future Changes in Mekong River Hydrology: Impact of Climate Change and Reservoir Operation on Discharge. *Hydrology and Earth System Sciences*, *16*(12), 4603–4619. https://doi.org/10.5194/hess-16-4603-2012

Ly, S., Try, S., & Sayama, T. (2021). Hydrological Changes in the Mekong River Basin Under Future Hydropower Developments and Reservoir Operations. *Journal of Japan Society of*

Civil Engineers, Ser. B1 (Hydraulic Engineering), *77*(2), 259–264. https://doi.org/10.2208/jscejhe.77.2_I_259

Mauritsen, T., Bader, J., Becker, T., Behrens, J., Bittner, M., Brokopf, R., Brovkin, V., Claussen, M., Crueger, T., Esch, M., Fast, I., Fiedler, S., Fläschner, D., Gayler, V., Giorgetta, M., Goll, D. S., Haak, H., Hagemann, S., Hedemann, C., … Roeckner, E. (2019). Developments in the MPI-M Earth System Model version 1.2 (MPI-ESM1.2) and Its Response to Increasing CO2. *Journal of Advances in Modeling Earth Systems*, *11*(4), 998–1038. https://doi.org/10.1029/2018MS001400

Meema, T., Tachikawa, Y., Ichikawa, Y., & Yorozu, K. (2021). Uncertainty Assessment of Water Resources and Long-term Hydropower Generation using a Large Ensemble of Future Climate Projections for the Nam Ngum River in the Mekong Basin. *Journal of Hydrology: Regional Studies*, *36*, 100856. https://doi.org/10.1016/J.EJRH.2021.100856

Mohor, G. S., Rodriguez, D. A., Tomasella, J., & Siqueira Júnior, J. L. (2015). Exploratory Analyses for the Assessment of Climate Change Impacts on the Energy Production in an Amazon Run-of-river Hydropower Plant. *Journal of Hydrology: Regional Studies*, *4*(PB), 41–59. https://doi.org/10.1016/J.EJRH.2015.04.003

MRC. (2009). *Database of the Existing, Under Construction and Planning/Proposed Hydropower Projects in the Lower Mekong Basin*. Mekong River Commission.

MRC. (2019a). *Snapshot of the MRC Council Study* Findings and Recommendations*. Mekong River Commission. http://www.mrcmekong.org/

MRC. (2019b). *State of the Basin Report 2018*. Mekong River Commission.

MRC. (2019c). *The MRC Hydropower Mitigation Guidelines Vol. 1*. The Mekong River Commission.

O'Neill, B. C., Tebaldi, C., Van Vuuren, D. P., Eyring, V., Friedlingstein, P., Hurtt, G., Knutti, R., Kriegler, E., Lamarque, J. F., Lowe, J., Meehl, G. A., Moss, R., Riahi, K., & Sanderson, B. M. (2016). The Scenario Model Intercomparison Project (ScenarioMIP) for CMIP6. *Geoscientific Model Development*, *9*(9), 3461–3482. https://doi.org/10.5194/GMD-9-3461-2016

Oeurng, C., Cochrane, T. A., Chung, S., Kondolf, M. G., Piman, T., & Arias, M. E. (2019). Assessing Climate Change Impacts on River Flows in the Tonle Sap Lake Basin, Cambodia.

Water, *11*(3), 618. https://doi.org/10.3390/W11030618

Peter, K., Jeremy, B., & Lawrence, H. (2007). *Environmental Criteria for Hydropower Development in the Mekong Region - Technical Report*. Asian Development Bank.

Piman, T., Cochrane, T. A., & Arias, M. E. (2016). Effect of Proposed Large Dams on Water Flows and Hydropower Production in the Sekong, Sesan and Srepok Rivers of the Mekong Basin. *River Research and Applications*, *32*(10), 2095–2108. https://doi.org/10.1002/rra.3045

Pokhrel, Y., Burbano, M., Roush, J., Kang, H., Sridhar, V., & Hyndman, D. (2018). A Review of the Integrated Effects of Changing Climate, Land Use, and Dams on Mekong River Hydrology. *Water*, *10*(3), 266. https://doi.org/10.3390/w10030266

Räsänen, T. A., Someth, P., Lauri, H., Koponen, J., Sarkkula, J., & Kummu, M. (2017). Observed River Discharge Changes due to Hydropower Operations in the Upper Mekong Basin. *Journal of Hydrology*, *545*, 28–41. https://doi.org/10.1016/j.jhydrol.2016.12.023

Richard, B., & Tran, T. (2014). *Climate Change and Hydropower in the Mekong River Basin: a Synthesis of Research*. Deutsche Gesellschaft für Internationale Zusammenarbeit (giz) GmbH.

Sayama, T., Ozawa, G., Kawakami, T., Nabesaka, S., & Fukami, K. (2012). Rainfall–Runoff–Inundation Analysis of the 2010 Pakistan Flood in the Kabul River Basin. *Hydrological Sciences Journal*, *57*(2), 298–312. https://doi.org/10.1080/02626667.2011.644245

Seland, Ø., Bentsen, M., Olivié, D., Toniazzo, T., Gjermundsen, A., Graff, L. S., Debernard, J. B., Gupta, A. K., He, Y. C., Kirkeväg, A., Schwinger, J., Tjiputra, J., Schanke Aas, K., Bethke, I., Fan, Y., Griesfeller, J., Grini, A., Guo, C., Ilicak, M., … Schulz, M. (2020). Overview of the Norwegian Earth System Model (NorESM2) and Key Climate Response of CMIP6 DECK, Historical, and Scenario Simulations. *Geoscientific Model Development*, *13*(12), 6165–6200. https://doi.org/10.5194/GMD-13-6165-2020

Shrestha, B., Cochrane, T. A., Caruso, B. S., Arias, M. E., & Piman, T. (2016). Uncertainty in Flow and Sediment Projections due to Future Climate Scenarios for the 3S Rivers in the Mekong Basin. *Journal of Hydrology*, *540*, 1088–1104. https://doi.org/10.1016/J.JHYDROL.2016.07.019

Tatebe, H., Ogura, T., Nitta, T., Komuro, Y., Ogochi, K., Takemura, T., Sudo, K., Sekiguchi, M.,

Abe, M., Saito, F., Chikira, M., Watanabe, S., Mori, M., Hirota, N., Kawatani, Y., Mochizuki, T., Yoshimura, K., Takata, K., O'Ishi, R., … Kimoto, M. (2019). Description and Basic Evaluation of Simulated Mean State, Internal Variability, and Climate Sensitivity in MIROC6. *Geoscientific Model Development*, *12*(7), 2727–2765. https://doi.org/10.5194/GMD-12-2727-2019

Try, S., Tanaka, S., Tanaka, K., Sayama, T., Hu, M., Sok, T., & Oeurng, C. (2020a). Projection of Extreme Flood Inundation in the Mekong River Basin under 4K Increasing Scenario using Large Ensemble Climate Data. *Hydrological Processes*, *34*(22), 4350–4364. https://doi.org/10.1002/hyp.13859

Try, S., Tanaka, S., Tanaka, K., Sayama, T., Khujanazarov, T., & Oeurng, C. (2022). Comparison of CMIP5 and CMIP6 GCM Performance for Flood Projections in the Mekong River Basin. *Journal of Hydrology: Regional Studies*, *40*, 101035. https://doi.org/10.1016/J.EJRH.2022.101035

Try, S., Tanaka, S., Tanaka, K., Sayama, T., Lee, G., & Oeurng, C. (2020b). Assessing the Effects of Climate Change on Flood Inundation in the Lower Mekong Basin using High-Resolution AGCM Outputs. *Progress in Earth and Planetary Science*, *7*(1), 1–16. https://doi.org/10.1186/s40645-020-00353-z

Try, S., Tanaka, S., Tanaka, K., Sayama, T., Oeurng, C., Uk, S., Takara, K., Hu, M., & Han, D. (2020c). Comparison of Gridded Precipitation Datasets for Rainfall-Runoff and Inundation Modeling in the Mekong River Basin. *PLoS ONE*, *15*(1), e0226814. https://doi.org/10.1371/journal.pone.0226814

Van Vliet, M. T. H., Wiberg, D., Leduc, S., & Riahi, K. (2016). Power-generation System Vulnerability and Adaptation to Changes in Climate and Water Resources. *Nature Climate Change*, *6*(4), 375–380. https://doi.org/10.1038/nclimate2903

Voldoire, A., Saint-Martin, D., Sénési, S., Decharme, B., Alias, A., Chevallier, M., Colin, J., Guérémy, J. F., Michou, M., Moine, M. P., Nabat, P., Roehrig, R., Salas y Mélia, D., Séférian, R., Valcke, S., Beau, I., Belamari, S., Berthet, S., Cassou, C., … Waldman, R. (2019). Evaluation of CMIP6 DECK Experiments With CNRM-CM6-1. *Journal of Advances in Modeling Earth Systems*, *11*(7), 2177–2213. https://doi.org/10.1029/2019MS001683

Wang, S., Jiao, S., & Xin, H. (2013). Spatio-temporal Characteristics of Temperature and

Precipitation in Sichuan Province, Southwestern China, 1960–2009. *Quaternary International*, *286*, 103–115. https://doi.org/10.1016/J.QUAINT.2012.04.030

Wu, F., Wang, X., Cai, Y., & Li, C. (2016). Spatiotemporal Analysis of Precipitation Trends under Climate Change in the Upper Reach of Mekong River Basin. *Quaternary International*, *392*, 137–146. https://doi.org/10.1016/J.QUAINT.2013.05.049

Yamazaki, D., Ikeshima, D., Tawatari, R., Yamaguchi, T., O'Loughlin, F., Neal, J. C., Sampson, C. C., Kanae, S., & Bates, P. D. (2017). A High-Accuracy Map of Global Terrain Elevations. *Geophysical Research Letters*, *44*(11), 5844–5853. https://doi.org/10.1002/2017GL072874

Yukimoto, S., Kawai, H., Koshiro, T., Oshima, N., Yoshida, K., Urakawa, S., Tsujino, H., Deushi, M., Tanaka, T., Hosaka, M., Yabu, S., Yoshimura, H., Shindo, E., Mizuta, R., Obata, A., Adachi, Y., & Ishii, M. (2019). The Meteorological Research Institute Earth System Model Version 2.0, MRI-ESM2.0: Description and Basic Evaluation of the Physical Component. *Journal of the Meteorological Society of Japan. Ser. II*, *97*(5), 2019–2051. https://doi.org/10.2151/JMSJ.2019-051

Yun, X., Tang, Q., Sun, S., & Wang, J. (2021). Reducing Climate Change Induced Flood at the Cost of Hydropower in the Lancang-Mekong River Basin. *Geophysical Research Letters*, *48*(20), e2021GL094243. https://doi.org/10.1029/2021GL094243

Yun, X., Tang, Q., Wang, J., Liu, X., Zhang, Y., Lu, H., Wang, Y., Zhang, L., & Chen, D. (2020). Impacts of Climate Change and Reservoir Operation on Streamflow and Flood Characteristics in the Lancang-Mekong River Basin. *Journal of Hydrology*, *590*, 125472. https://doi.org/10.1016/J.JHYDROL.2020.125472

Zhong, R., Zhao, T., He, Y., & Chen, X. (2019). Hydropower Change of the Water Tower of Asia in 21st Century: A Case of the Lancang River Hydropower Base, Upper Mekong. *Energy*, *179*, 685–696. https://doi.org/10.1016/J.ENERGY.2019.05.059

CHAPTER 6 Concluding Remarks

6.1 Summary and Conclusion

Temperature rises and changes in precipitation pattern and intensity have posed a serious threat to the river basin around the globe. Future climate change is projected to modify the annual river flow and flood characteristics. On top of climate change, the Mekong River Basin (MRB) is experiencing economic growth through the construction of large infrastructures such as hydropower dams. Such hydropower generally effects alter the natural stage of the river, particularly the seasonal flow. However, it is expected to reduce flood risk, provide additional water for irrigation during the dry season, general energy for domestic usage and foreign export, and improve the navigation system at the same time. Therefore, the purpose of this dissertation was to learn more about the future climate projections and hydropower operations in the MRB. It aimed to provide concrete results and discussions on the impact of those drivers on basin hydrology.

First, the study investigated the impact of future hydropower on river flow in the MRB. A simple storage model for reservoir operation was developed following a non-linear optimization programming with the objective function of maximizing hydropower production. Then it was integrated into the Rainfall-Runoff-Inundation (RRI) model for simulating the river discharge under reservoir operations. The findings indicated the capacity of the RRI model coupled with the reservoir operation model in reproducing the discharge hydrograph in the MRB with the $NSE > 0.8$. On the other hand, monthly and seasonal discharges were expected to alter under reservoir operation. The dry season was expected to increase, while the wet season along with peak discharge was expected to decrease, respectively.

Using eight General Circulation Models (GCM) from the Coupled Model Intercomparison Project Phase 6 (CMIP6), the study assessed the changes in flow regime and flood characteristics in the future, in addition to hydropower operations. Two Share Socioeconomic Pathways (SSP) scenarios, SSP2-4.5 and SSP5-8.5, were considered. All GCMs were bias-corrected with GPCC precipitation by the linear scaling method. The RRI model simulated the daily discharge for the present period (1980–2014) and the future period (2026–2100). Our findings showed significant

seasonal flow alteration and emphasized the crucial function of hydropower in mitigating flood risk in the Lower Mekong Basin (LMB). In general, climate change was expected to increase river discharge in all scenarios; however, hydropower operation was expected to reduce the effect of climate change in the wet season to some degree. Under climate change in the far-future period, average discharge in the wet season at Kratie (i.e., hydrological station in the downstream of LMB) increased by 33%; nonetheless, relative flow changes were potentially decreased to 19% under cumulative impacts (i.e., climate change and hydropower operation). Despite the influence of hydropower operations, climate change remains the key contributor to hydrological changes in the MRB. On the other hand, our results suggested that hydropower, particularly future hydropower dams, could significantly reduce flood magnitude in the LMB's flood-prone areas. The study further evaluated the significance of flood risk by statistical analysis. As a result, the changes in the inundated area were found to be significant in most scenarios.

Given the increase in energy consumption due to population growth, urbanization, economic development, and other factors, renewable energy sources such as hydroelectric dams are getting more and more attention from the riparian countries of the MRB. Climate change, on the other hand, was projected to alter the future river flow, thus affecting hydropower production. Motivated by this, this study also evaluated the energy generation from hydropower dams in the MRB under the future climate projections. Using the CMIP6 GCMs, the study simulated the discharge under hydropower operations and estimated the energy generation from the present period and future period. Annual discharge and total inflow were found to be increased in the future, implying an increase in energy generation from hydropower. Nonetheless, given a 22% increase in total inflow, future hydropower production could only increase by 5% due to the limitation of current turbine capacity. The findings showed that type-A dam (i.e., dam with large turbine capacity compared to inflow) was the most common hydroelectric infrastructure in the MRB, while type-C dam (i.e., dam with small turbine capacity compared to inflow) dam had the most potential for future hydropower production. In order to increase the future energy generation, stakeholders should consider increasing the turbine capacity and give the priority to the mainstream hydropower dams.

6.2 Limitations

The study assessed the impacts of climate change and hydropower operations in the MRB using a hydrologic model, the RRI model, with the most recent CMIP6 climate projections. However, there are three main limitations in this study that need to be addressed.

First of all, there are several limitations to the model simulation adopted in the study. Due to the limited information and data availability, river cross-sections were assumed to be rectangles and approximately estimated as a function of the upstream contributing area. On the other hand, a static land-use was adopted in the whole simulation period for both the present and the future climate projections, although the actual land-use may change due to population growth, urbanization, agricultural expansion, and other factors. Additional, evapotranspiration changes due to climate change was not reflected in the simulations. Besides, groundwater was not considered in the RRI model due to the limited data availability.

Secondly, although the study used the most recent CMIP6 climate projections from the Sixth Assessment Report (AR6) of the Intergovernmental Penal on Climate Change (IPCC), several factors should be considered for future improvements. CMIP6 provides a variety of GCMs selection for future climate change assessment studies; however, the model resolution is still relatively coarse for the basin-scale application such as in the MRB. Therefore, utilization of regional climate models or downscaling the original GCMs should be considered for better accuracy of rainfall patterns, thus improving the simulation of river discharge as well as flood inundation from the hydrologic model.

Lastly, given the unavailability of the reservoir operation rule in the MRB, the study adopted a simple storage model to estimate the released flow of the reservoir with only one objective function of maximizing hydropower production. In actual operation, hydropower may have multiple operation strategies, such as drought relief, ecological conservation, flood control, water supply, and energy production. Therefore, several operation strategies should be considered in future studies in order to reflect the actual operation. Through multiple operating strategies, flow alteration under different scenarios can be understood.

Future research should address all the aforementioned limitations in order to improve the model simulation and the result accuracy.

APPENDIX A: LIST OF PUBLICATIONS

Peer-Reviewed Journals:

Ly, S., Sayama, T. and Try, S. (2022). Integrated Impact of Assessment of Climate Change and Dam Operation on Streamflow and Inundation in the Mekong River Basin. *Journal of Hydrology: Regional Studies*. (under review)

Ly, S., Try, S. and Sayama, T. (2021). Hydrological Changes in the Mekong River Basin Under Future Hydropower Development and Reservoir Operations. *Journal of Japan Society of Civil Engineers Ser B1 (Hydraulic Engineering)*. 77(2), 259–264. doi: 10.2208/jscejhe.77.2_I_259.

Try, S., Sayama, T., Oeurng, C., Sok, T., **Ly, S.** and Uk, S. (2022). Identification of the Spatio-temporal and Fluvial-pluvial Sources of Flood Inundation in the Lower Mekong Basin. *Geosciences Letters*. 9(5). doi: 10.1186/s40562-022-00215-0.

Presentation and Conference Papers:

Ly, S., Try, S. and Sayama, T. (2022). Impacts of Proposed Hydropower Dams and Climate Change on Streamflow and Flood Inundation in the Mekong River Basin. *DPRI Annual Meeting 2022*, February 21–22, 2022. Online Virtual Meeting.

Ly, S., Try, S. and Sayama, T. (2021). Assessing the Impacts of Future Hydropower Developments and Climate Change on the Mekong Flow Regime Using CMIP6 GCMs. *American Geophysical Union (AGU) Conference 2021*. December 6–17, 2021. Online Virtual Meeting.

Ly, S., Sayama, T. and Try, S. (2021). Impacts of Proposed Hydropower Dams on Stream Flow in the Mekong River Basin. *DPRI Annual Meeting 2021*, February 22 & 24, 2021. Online Virtual Meeting.

Ly, S., Sayama, T. and Takara, K. (2020). Hydrologic Characteristics and Modeling of the Tonel Sap Sub-basins. *DPRI Annual Meeting 2020*, February 22–21, 2020. Kyoto University, Japan.

Ly, S., Sayama, T., Try, S. and Takara, K. (2018). Runoff Prediction in Ungauged Basins: A Case Study in Tonle Sap Lake Basin in Cambodia. *The 5th JASTIP SYMPOSIUM,* October 16–19, 2018. Kuala Lumpur, Malaysia.

Try, S., Sayama, T., Oeurng, C., Sok, T., **Ly, S.** and Uk, S. (2021). Investigation of Spatio-temporal Sources of Rainfall of the Historical Large Flood Events in the Lower Mekong Basin. *American Geophysical Union (AGU) Conference 2021*. December 6–17, 2021. Online Virtual Meeting.

Mab, P., **Ly, S.**, Chompuchan, C. and Kositsakulchai, E. (2019). Evaluation of Satellite Precipitation from Google Earth Engine in Tonle Sap Basin, Cambodia. *THA 2019 International Conference on Water Management and Climate Change towards Asia's Water-Energy-Food-Nexus and SDGs*. January 23–25, 2019. Bangkok, Thailand.

APPENDIX B: SHUFFLED COMPLEX EVOLUTION ALGORITHM

SCE-UA method is a global optimization technique for broad class of problems including hydrological optimization trials. It combines the strengths of Controlled Random Search (CRS) algorithms with the concept of competitive evolution and complex shuffling. The steps of the SCE-UA algorithm are as the following.

Step 1: Initialize

Select $p \geq 1$ and $m \geq n + 1$, where $p =$ number of complexes and $m =$ number of points in each complex. Compute the sample size $s = p \times m$.

Step 2: Generate sample

Sample s points $x_1, \cdots, x_s$ in the feasible space $\Omega \subset \mathbb{R}^n$. Compute the function value f_i at each point x_i. In the absence of prior information, use a uniform sampling distribution.

Step 3

Rang points. Sort the s points in the order of increasing function value. Store them in an array $D = \{x_i, f_i, i = 1, \cdots, s\}$, so that $i = 1$ represents the point with the smallest value.

Step 4: Partition into complexes

Partition D into p complexes, $A^1, \cdots, A^p$, each containing m points, such that $A^k = \{x_j^k, f_j^k | x_j^k = x_{k+p(j-1)}, j = 1, \cdots, m\}$.

Step 5: Evolve each complex

Evolve each complex $A^k, k = 1, \cdots, p$ according to the competitive complex evolution algorithm outline as below:

1. Initialize. Select q, α, and β, where $2 \leq q \leq m$, $\alpha \geq 1$, and $\beta \geq 1$.

2. Assign weight. Assign a triangular probability distribution to A^k, i.e.,

$$\rho_i = \frac{2(m + 1 - i)}{m(m + 1)}, i = 1, \cdots, m$$

The point x_1^k has the highest probability, $\rho_1 = 2/(m+1)$. The point x_m^k has the lowest probability, $\rho_m = 2/m(m+1)$.

3. Select parents. Randomly choose q distinct points $u_1, \cdots, u_q$ from A^k according to the probability distribution specified above (the q points define a sub-complex). Store them in array $B = \{u_i, v_i, i = 1, \cdots, q\}$, where v_i is the function value of point u_i. Store in L the locations of A^k which are used to construct B.

4. Generate offspring

   (a) Sort B and L so that the q points are arranged in order of increasing function value. Compute the centroid g using the following equation:

$$g = \left[\frac{1}{q-1}\right]\sum_{j}^{q-1} u_j$$

   (b) Compute the new point $r = 2g - u_q$ (reflection step).

   (c) If r is within Ω, compute the function value f, and go to step (d); else, compute the smallest hypercube H $\subset \mathbb{R}^n$ that contains A^k, randomly generate a point z within H, compute f_z, set $f_r = f_z$ (mutation step).

   (d) If $f_r < f_z$, replace u_q by r go to Step (f); else, compute $c = (q + u_q)/2$ and f_c (contraction step).

5. Replace parents by offspring. Replace B into A^k using the original locations stored in L. Sort A^k in order of increasing function value.

6. Iterate. Repeat Steps 1) through 4) β times, where $\beta \geq 1$ is a user-specified parameter which determines how many offspring should be generate.

Step 6: Shuffle complexes

Replace $A^1, \cdots, A^p$ into D, such that $D = \{A^k, k = 1, \cdots, p\}$. Sort D in order of increasing function value.

Step 7: Check convergence

If the convergence criteria are satisfied, stop; otherwise, return to Step 4.